ENOS
Enabling Onshore CO2 Storage

A CO_2GeoNet Initiative

ENOS D3.2 | final

Assessing risks presented by boreholes: Recommendations on a risk assessment framework for CO_2 storage

Date	28.12.2018
Author(s)	Eric Patrick Ford, NORCE Aruoture V Omekeh, NORCE *Roman Berenblyum, NORCE Lars Kollbotn, NORCE Vit Hladik, CGS Juraj Francu, CGS Miroslav Pereszlenyi, CGS Vladimir Kolejka, CGS Petr Jirman, CGS * - corresponding author contact: robe@norceresearch.no
Number of pages	76 (without appendices)
Number of appendices	2
Project name	ENOS
Project website	http://www.enos-project.eu
Project number	Grant Agreement No 653718

This project has received funding from the European Union's Horizon 2020 research and innovation programme under grant agreement No 653718

Public

Contents

1 Executive summary

The ENOS (ENabling Onshore CO_2 Storage) project (www.enos-project.eu), addresses the challenges to apply the Carbon-dioxide Capture and Storage (CCS) technology onshore in Europe, with its unique geological and socio-economic context. The advantages of local onshore storage include empowering communities to steer the process, supporting local jobs and industries and enabling sustainable development. Onshore storage is needed to meet climate targets and offer opportunities for EU Member States that do not have easy access to storage potential in the North Sea (where CO_2 storage has been demonstrated for over two decades). In addition, the costs for transport and storage onshore are much lower than offshore.

The ENOS consortium includes more than 100 professionals (scientists and engineers, experts in geology, monitoring and social sciences and many others) from 29 organisations based in 17 European countries.
The main objective of the project is to enable the development of CO_2 storage onshore in Europe by:

- Developing, testing and demonstrating in the field, under “real-life conditions”, key technologies specifically adapted to onshore contexts (for example tools to monitor CO_2 storage sites);
- Involving local communities in CO_2 geological storage development (e.g. establishing dialogue groups with researchers, citizens and civil society representatives);
- Sharing experience and knowledge across Europe to contribute to the creation of a favourable environment for onshore storage.

One of the key elements in CO_2 storage is to ensure the process is safe and avoid any leakage. Around the world, 23 large scale CCS facilities have been safely operated, including the Val Verde CO_2-EOR operation in the US since 1972 and the Sleipner CO_2 storage operation offshore Norway since 1996 (GCCSI report, 2018). Nevertheless, the task of properly assessing leakage risk, even if very low, is vital for safety of operation, permitting, and public awareness and acceptance of the CCS technology.

The first part of this report provides recommendations on how to perform a risk assessment for a CO_2 storage project, focusing, in particular, on the potential risk of leakage from abandoned wells. The risk assessment methodology comprises three main steps; 1) risk identification, 2) risk analysis, and 3) risk evaluation. The main body of the work in the first part of this report is concerned with the risk analysis, specifically assessment of leakage rates.

Providing a complete and extensive risk assessment of a specific site is beyond the current scope of this work. The risk assessment in this report provides recommendations based on ENOS project work and experience from previous work on the REPP-CO_2 project, drawing on generic lessons learned that should prove useful for similar projects.

The first step, risk identification, utilises a bow tie methodology as the overall conceptual model for compartmentalizing the assessment into causes (hazards), preventive and mitigating measures, and effects (consequences). A combination of barrier analysis and Features, Events and Processes (FEP) analysis is used to identify potential leakage pathways and scenarios, supported by documentation and information collection from the sites used as case examples.

The second step, risk analysis, is used to recommend tools for quantifying leakage risk, based on experience from example wells from the LBr-1 and Getica fields. Following on from the work carried out

for this report, it is recommended that risk analysis is started by coarsely assessing probabilities and consequences, using probability and consequence classification tables, to narrow the scope of the analysis and focus on the risks of importance, having either a high probability of occurrence, a high consequence, or both.

The findings of the third step, risk evaluation, are that the potential leakage rates are strongly dependent on both the chosen leakage scenario, as well as the main governing parameters, such as reservoir and well characteristics, plugging & abandonment (P&A) design, and, especially, the degree of failure. The report focuses on a micro-annuli scenario, in which there is a gap between the casing cement and the formation, potentially allowing for movement of CO_2. One of the reasons for focusing on this scenario is that it expands upon work from risk assessment of the REPP-CO_2 project (Ford et. al., 2016), where the leakage assessments therein were limited to leakage through bulk cement.

While it is challenging to provide an accurate text description of this scenario, the report shows the importance of the assumptions that are made, and how factors such as assumed cement integrity can have a large impact on the resulting model leakage rates. It is clear from the example model outcomes shown, that a combination of a large, vertically continuous, micro-annuli gap and a driving pressure are required to reach elevated levels (~100 t/year) of CO_2 leakage. The size of such gaps is related to the effective wellbore permeability, which in turn relates to the bond between borehole completion materials, e.g. casing cement, and rock formation. As such, the quality of the cement barrier is crucial, and the information that exists determining its state and quality directly impacts the level of confidence in the leakage rate analysis.

The report also presents results of a near wellbore simulator model where the reactivity of cement is considered in a possible CO_2 leakage scenario through an already existing micro-annuli opening between the cement and the formation. The result of the simulation shows that CO_2 leakage rate through such an opening is reduced with time, as CO_2 reacts with the cements and forms new cement phases that gradually seals the openings.

Beyond leakage rates, other measures of risk provided in the report include examples of potential impact on human health when considering rapid accumulation of CO_2 into a confined space, using simulated leakage rates and CO_2 exposure levels, and the dispersion levels of CO_2 for varying distance from the leakage point under different wind conditions.

The risk evaluation discusses, in particular, the aspect of acceptable risk, and how such levels can be established and used in conjunction with the results from the risk analysis.

The overall contribution of the risk assessment is a general framework where certain aspects are detailed, providing means to identify, quantify, and evaluate the risks related to abandoned wells. The framework does not provide *all* the answers, and should rather be viewed as a collection of tools and techniques that together provide *one* set of answers, and a starting point for risk analysis in similar projects.

Finally, a feasibility study into the possibility of early leakage detection using downhole well pressure gauges was carried out. The study concluded that downhole pressure monitoring is a viable tool that should be used alongside other monitoring methods.

2 Introduction

The need to reverse the trend of increasing CO_2 in the atmosphere is urgent. A vital part of the effort to reduce the amount CO_2 in the atmosphere is the storage of CO_2 in saline aquifers or abandoned oil and gas fields. The prospect of safe underground storage of CO_2 is appealing as underground formations can potentially store large quantities of CO_2 in the same way that water, oil, and gas were trapped for millions of years. Exhausted and near depleted oil and gas fields are of interest as they already have a proven ability to securely store fluids for millions of years. In addition, their volumes are generally known, the removal of oil or gas generates a lower pressure reservoir in which CO_2 can be stored, and there is generally a wealth of information and a good understanding of the geology of the site, including response to fluid flow through the rocks. While current operating facilities have proven that operations can be carried out in a safe manner, the risk of possible CO_2 leakage from such sites needs to be evaluated on a site-by-site basis.

ENOS will study both faults and wells, to determine their capability to act as barriers or conduits to CO_2 movement. As CO_2 tends to move toward the surface, most risks related to CO_2 storage are the result of the unforeseen migration of the injected CO_2 along faults or abandoned wells. The potential for CO_2 migration along a fault will be tested during injection of CO_2 at the Sotacarbo Fault Lab in Sulcis, Italy. Data from this experiment will be used in computer models to estimate long-term, large-scale processes at different types of sites. In addition, faults with leaking, naturally-produced CO_2 at Latera, San Vittorino and Ailano (Italy) will be examined to compare natural and experimental migration processes, to further improve monitoring strategies. Regarding wells, studies will be based on existing datasets from abandoned wells in the Czech Republic and Romania.

This report presents some of the main findings of ENOS task 3.2.4: “Assessing risks presented by boreholes”. The main objective is a risk assessment of leakage from abandoned wells and recompletion procedures using the LBr-1 field as case study. The outcomes will provide input to technical guidelines and recommendations for best practice that will be integrated into other ENOS activities (WP7) and disseminated via this report. These are relevant for performing similar assessments for other CO_2 storage projects.

This assessment builds on work previously performed in the REPP-CO_2 project (Ford et. al., 2016), where a risk assessment framework for quantifying well-specific leakage risk was established. The leakage rate assessments in that project were limited to leakage through cement plugs, which produced very low leakage rates. However, to account for the more realistic scenario of leakage through micro-annuli, the work performed here focuses on this. The current assessment covers the three basic elements of the risk assessment process, i.e.: 1) risk identification; 2) Risk analysis; and, 3) Risk evaluation; as the main steps outlined in the ISO 31000:2018 standard (Figure 1).

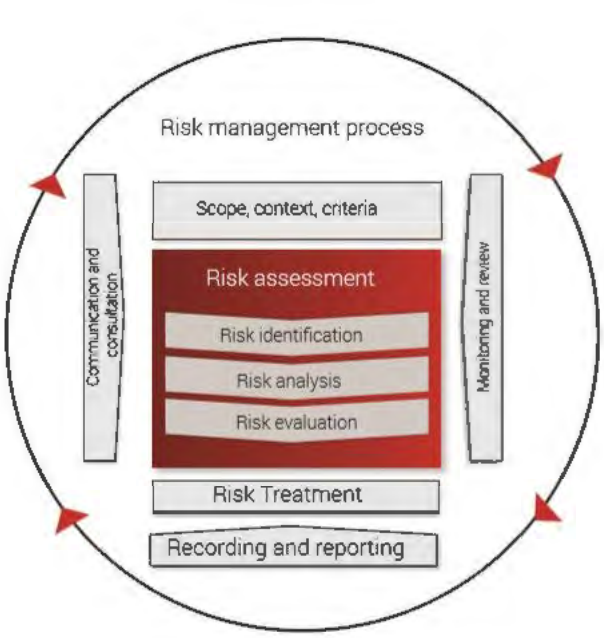

Figure 1 Risk management process (as per ISO 31000:2018)

The “Risk identification” stage, as the first step of the process, is influenced by the scope, context and criteria set out as the starting point for the assessment. This stage provides the foundation for the subsequent activities by outlining sources of risks and their causes, preventive and mitigating measures/barriers, and potential consequences of the risks. In the following “risk analysis”, the most important risks are then analyzed with respect to probability of occurrence (uncertainty) and impact of the consequences, considering also measures/barriers to each risk. Finally, in the “risk evaluation” step, the identified and analyzed risks are compared with the relevant criteria set in the initial stage, to judge the acceptability, and to provide input to the decision-making process.

For the risk assessment process, a bow-tie analysis was chosen as the over-arching system model. A bow-tie is a simple diagrammatic way of describing and analyzing the pathways of a risk from hazards to outcomes and to review controls. It can be considered as a combination of the logic of a fault tree in terms of analyzing the cause of an event (represented by the knot of a bow tie) and the pathways of an event tree in terms of analyzing the consequences (ISO, 2009). The elements of the of the bow-tie diagram are defined as follows:

- Causes – The underlying cause of a CO_2 leakage event. A cause is related to a threat in that a cause is a manifestation of a threat. A cause may represent a single or multiple sequential events occurring.
- Preventive (proactive) barriers – A function or features of the system, which if it/they function as intended, will prevent a potential CO_2 leakage event from occurring
- Leak – Loss of containment of CO_2 from the storage facility. A leak is any release of CO_2 from the storage complex, which includes all the physical preventive barriers, but not necessarily a release to the atmosphere.
- Mitigating (reactive) barriers – A function or features of the system, which if it/they function as intended, will reduce the severity of the consequences of a leak.
- Effects – Synonymous with consequences. Three consequence aspects will be considered; operational, human, and environmental.

Figure 2 shows a bow-tie diagram, where “Leak” is the risk event under consideration, marked with a circle in the center of the diagram. The left side of the diagram focuses on potential causes of leakage and

preventive barriers established to prevent leakage from occurring, while the right side of the diagram focuses on remedial barriers, aimed at reducing the impact of leakage, and corresponding consequences, should the leakage materialize.

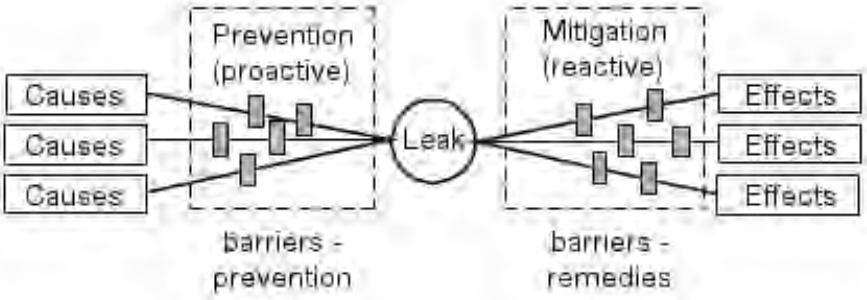

Figure 2 Conceptual bow-tie diagram showing the main components. The diagram is read from left to right.

3 Terms and definitions

This section lists some of the most important definitions and key terminology used throughout this report. The definitions are adopted from ISO 31000:2018 and ISO Guide 73:2009.

- Risk – Effect of uncertainty on objectives.
    - Note 1: An Effect is a deviation from the expected. It can be positive, negative, or both, and can address, create, or result in Opportunities and Threats.
    - Note 2: Objectives can have different aspects and categories, and can be applied at different levels.
    - Note 3: Risk is usually expressed in terms of risk sources, potential events, their consequences, and their likelihood.
- Risk assessment – Overall process of risk identification, risk analysis, and risk evaluation.
- Risk identification – Process of finding, recognizing, and describing risks.
    - Note 1: Risk identification involves the identification of risk sources, events, their causes, and their potential consequences.
    - Note 2: Risk identification can involve historical data, theoretical analysis, informed and expert opinions, and stakeholder's needs.
- Risk analysis – Process to comprehend the nature of risk and to determine the level of risk.
- Risk evaluation – Process of comparing the results of risk analysis with risk criteria to determine whether the risk and/or its magnitude is acceptable or tolerable
- Event – Occurrence of or change in a particular set of circumstances.
    - Note 1: An Event can be one or more Occurrences, and can have several causes. An event can consist of something not happening. An event can sometimes be referred to as an "incident" or "accident". An event without consequences can also be referred to as a "near miss", "incident", "near hit", or "close call".
- Consequence – Outcome of an event affecting objectives.
    - Note 1: An event can lead to a range of consequences. A Consequence can be certain or uncertain and can have positive or negative effects on objectives.
    - Note 2: Consequences can be expressed qualitatively or quantitatively. Initial consequences can escalate through knock-on effects.
- Likelihood – Chance of something happening.
    - Note 1: In risk management terminology, the word "likelihood" is used to refer to the chance of something happening, whether defined, measured or determined objectively or subjectively, qualitatively or quantitatively, and described using general terms or mathematically (such as probability or a frequency over a given time period).
    - Note 2: The English term "likelihood" does not have a direct equivalent in some languages; instead, the equivalent of the term "probability" is often used. However, in English, "probability" is often narrowly interpreted as a mathematical term. Therefore, in risk management terminology, "likelihood" is used with the intent that it should have the same broad interpretation as the term "probability" has in many languages other than English.
- Risk source – Element which alone or in combination has the intrinsic potential to give rise to risk.
- Risk criteria – Terms of reference which the significance of a risk is evaluated.

Note 1: Risk criteria are based on organizational objectives, and external or internal context.
Note 2: Risk criteria can be derived from standards, laws, policies and other requirements.

4 Risk identification

4.1 General framework

A starting point of the risk assessment is to identify so-called 'leakage paths'. We may define a leakage path as a particular traversal of the bow-tie diagram from the left side to the right, as illustrated in Figure 4. More specifically, from a failure mode on one or more preventive barriers initiated by one or more causes, leading to a leakage event, and eventually to final effects (consequences).

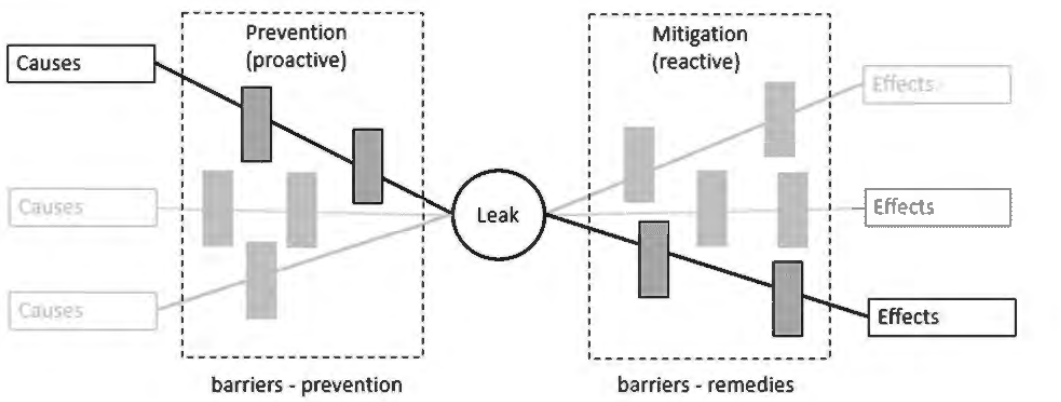

Figure 3 Illustration of a leakage path, i.e. a particular traversal of the bow-tie from left to right, where a cause has led to a breach in one or more preventive barriers, resulting in a leak. The magnitude of the leak may be reduced by mitigating barriers before materializing in a particular set of effects (consequences).

There are various techniques or methodologies that can be used to identify leakage paths. Two examples are the FEP (Features, Events and Processes) approach and the 'barrier' approach. Choosing an appropriate risk identification technique will rely on the competencies of the analysis team, available information, project constraints, etc. A thorough discussion of the pros and cons of the two aforementioned methods is presented in Arild et. al., 2017. Sources of support for an FEP process include the Quintessa database (Savage et. al., 2004), and for a barrier approach, standards such as NORSOK D-010:2013 can be used.

In addition to structured methodologies for risk identification, conducting literature reviews and semi-structured brainstorming sessions drawing on expertise within the project teams is recommended, to ensure that all relevant causes and barriers are covered

The resulting identification process should yield specific lists of causes (and optionally risk sources), preventive measures, mitigating measures and consequences, thus expanding the conceptual bow-tie, as shown in Figure 5. This expanded bow-tie diagram, along with underlying documentation, serves as the starting point for the screening phase of the risk analysis.

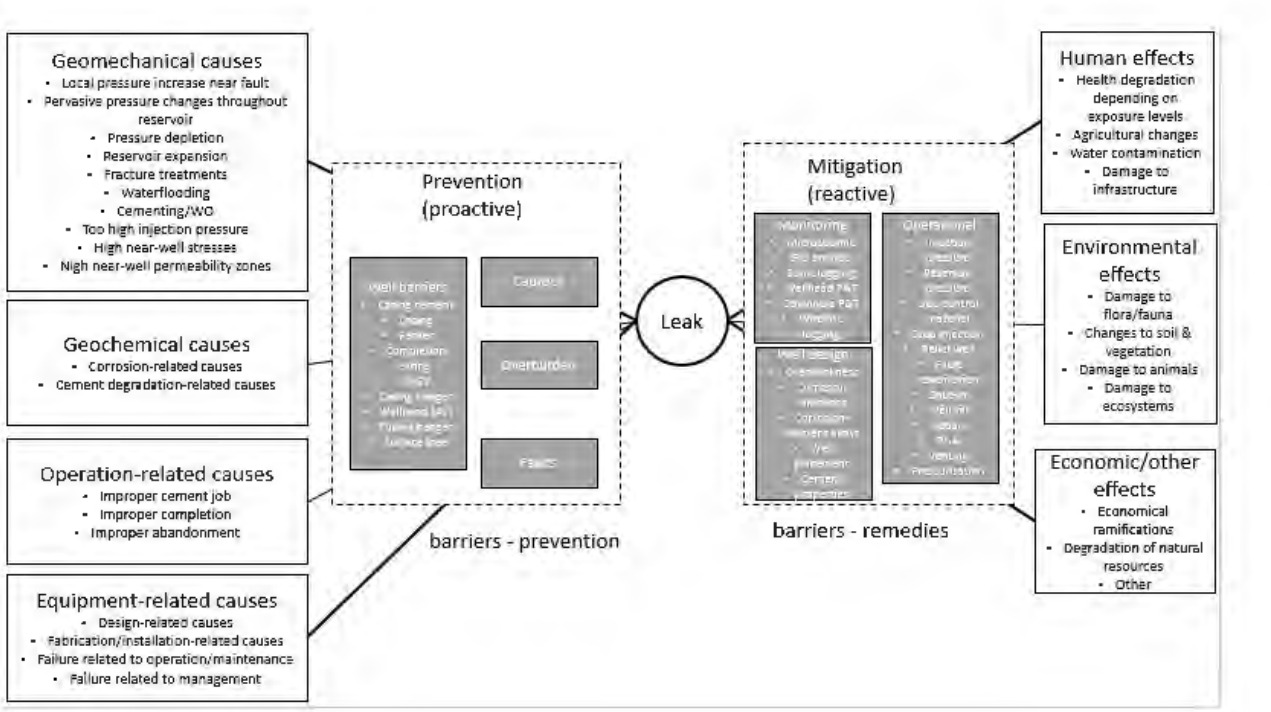

Figure 4 An example of the populated Bow-tie diagram (to simplify the illustration, the links between causes/barriers and barriers/effects are not shown) (Ford et. al., 2016) (Abbreviations: AV = Annulus valve, DHSV = Downhole Safety Valve, WO = Workover, P&T = Pressure & Temperature, P&A = Plug & Abandonment).

4.2 Abandoned wells and well abandonment procedures at LBr-1

General description of LBr-1 field

The LBr-1 hydrocarbon field is situated in the Czech part of the Vienna Basin, near the town of Lanžhot and close to the border of the Slovak Republic (Fig. 6). It represents the northern part of the Brodské complex –several small hydrocarbon accumulations located at both sides of the Czech-Slovak border. Originally, the whole complex was called the Brodské field. After the splitting of Czechoslovakia in 1993, the northern part of the complex was re-named to “Lanžhot-Brodské” (field No. 3241900 according to the ČGS-Geofond evidence), and its area was covered by the exploration licence 40010 “Lanžhot I”.

The main volumes of oil and gas were produced in 1959-1969, but sporadic production continued until 2000 (registered production 200 t of oil). The site operator was the state company “Moravské naftové doly” (nowadays MND a.s.). In 2004 the site operator asked for a write-off of the remaining reserves, by which the field was declared abandoned. In 2016 the Czech Mining Authority decided to cancel the production licence. Nevertheless, the whole area is still covered by the oil and gas exploration licence “Vienna Basin VIII” held by MND a.s.

The main stratigraphic oil-bearing horizon of the field comprises the Middle-Badenian sands, known as the Láb horizon. It is situated at a depth of ca. 1,000 m below surface and has outstanding collector properties (porosity up to 25 %, permeability up to 500 mD). This fact, in combination with relatively good geological knowledge and the presence of good-quality caprock – the Middle-Badenian claystones, is the main reason why LBr-1 is considered a good candidate for a pilot reservoir for geological storage of CO_2. The Láb horizon can be divided into four partial collector bodies (L1, L2, L3 and L4) that are separated by less permeable clayey intercalations with occasional interconnection.

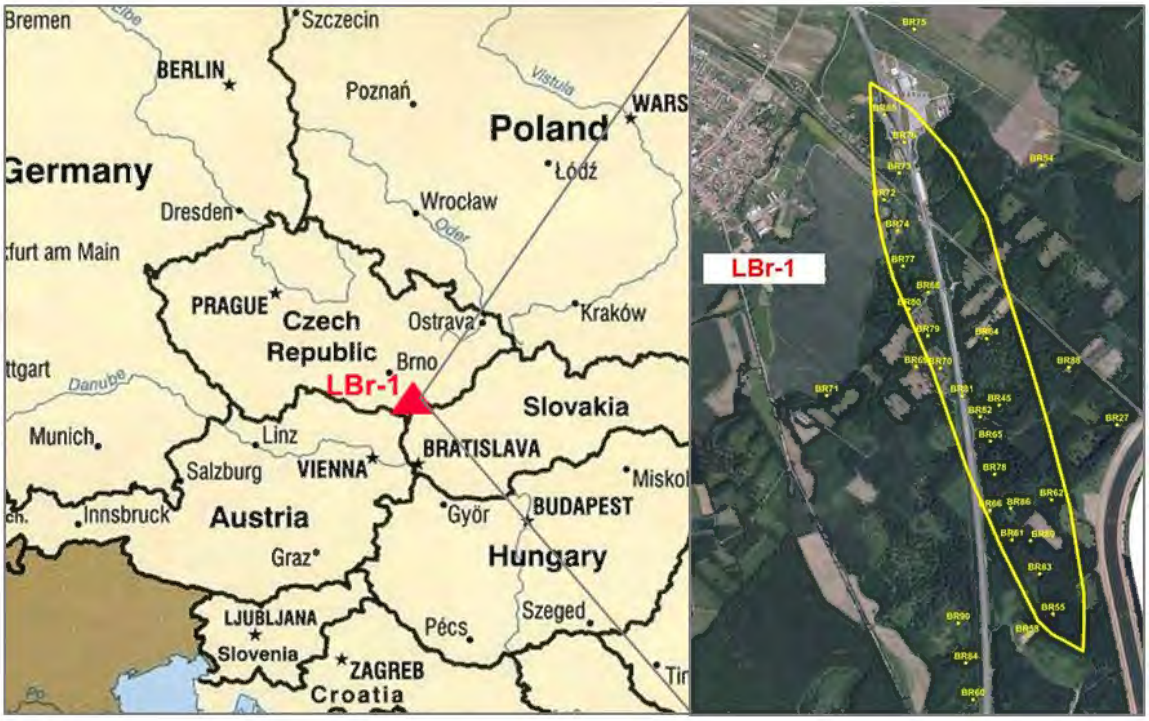

Figure 6 Situation of the LBr-1 site (left) and satellite image of the site (right) with outline of the reservoir area (yellow polygon) and legacy wells (yellow dots). The reservoir is ca. 3 km long and max. 600 m wide.

LBr-1 is now subject of continued detailed site assessment, with the vision to turn the abandoned oilfield into a research CO_2 storage pilot site. The work was started in the previous REPP-CO_2 project (Hladik et al., 2017) and is now continuing within ENOS.

The detailed position of the LBr-1 field within the Brodské complex area is shown in Fig. 7. LBr-1 represents the northern hydrocarbon-bearing part of the complex. Brodské-South is tectonically bound by the extensional Brodské fault on the East and due to subsidence forms the hanging wall-block situated deeper than the other structures. Brodské-Middle is a relatively independent hydrocarbon lens, primarily connected with Brodské-South through the adjacent aquifer. The shallower Brodské-Upper Block is situated on the eastern side of the Brodské fault, with a throw of around 120 m.

Wells at LBr-1 and in the Brodské complex area

The exploration of the Brodské complex started already in 1917, at the end of World War I, when the first exploration well, Br-1, was drilled in its southern part (today on the territory of Slovakia). Exploration continued in 1927-1928 by the drilling of two more wells – Br-2 and Br-3, and then during World War II when a number of shallow exploration wells were drilled, together with gravity and seismic surveys. The well Br-4 encountered an oil-bearing horizon in Middle Badenian strata in 1949-1950, and exploration and production development activities in the Brodské-South area continued until 1964.

In the northern part, i.e. in the LBr-1 area, the first positive well was Br-45 drilled in 1957. The drilling of twenty-four more exploration and production wells penetrating the reservoir followed in this area up to 1960. The cumulative production (until 2000 when the production was stopped) amounted to 61,900 m^3 of oil and 68.7 mil. m^3 of gas.

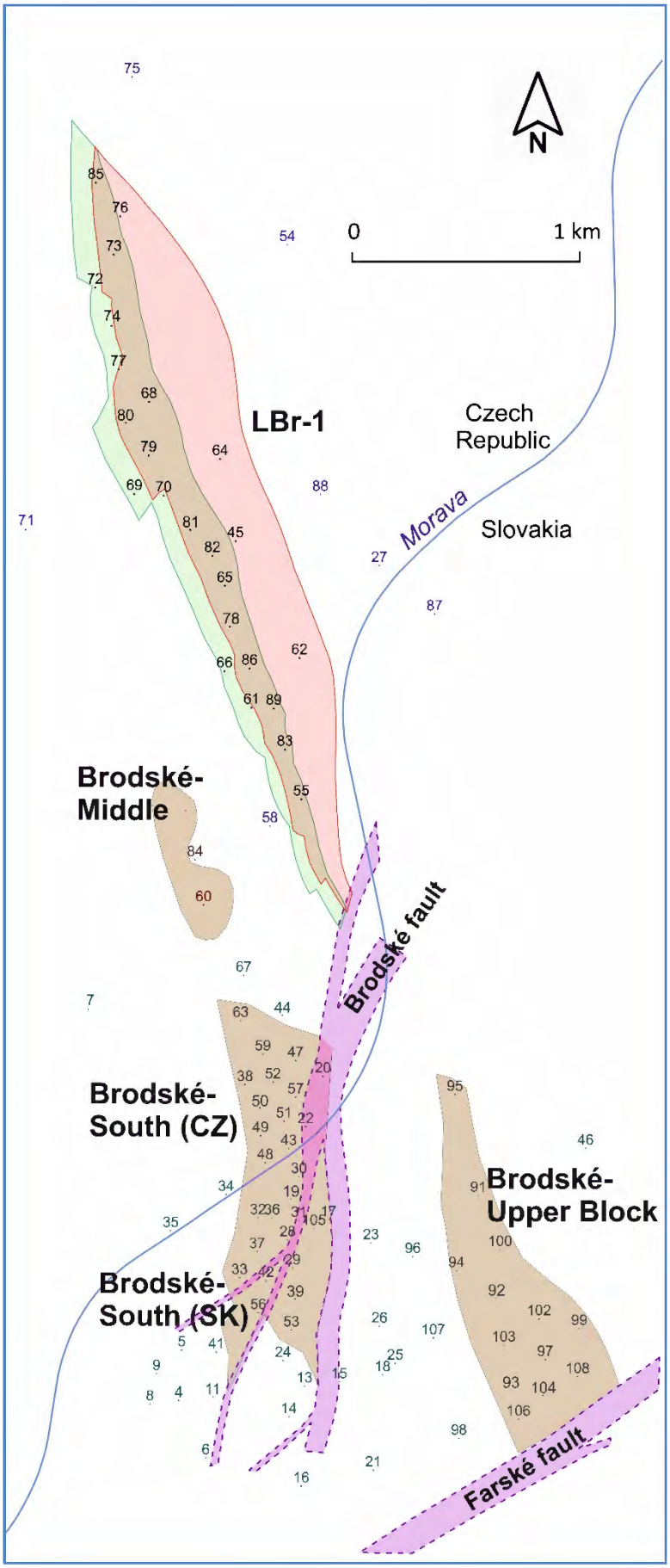

Figure 7

Map of the Brodské hydrocarbon complex. The numbered dots depict the positions of wells (the "Br-" part of the well names was left out; e.g., 85 corresponds to well Br-85). The Morava river also represents the state boundary between the Czech Republic and Slovakia. The initial gas zone at LBr-1 is marked in pink and the initial oil zone in green. Extent of other hydrocarbon zones at Brodské-Middle, Brodské-South and Brodské-Upper Block is marked in brown. Main faults are drawn in violet.

In total, more than 100 wells were drilled in the area of the Brodské complex. Regarding their location, they can be divided as follows (see Fig. 7):

- Lbr-1 – reservoir area – 25 wells
- Dry wells outside LBr-1 – 6 wells
- Brodské–Middle (independent production lens) – 3 wells
- Brodské-South – Czech part – reservoir area – 15 wells
- Dry wells outside Brodské-South – Czech territory – 3 wells
- Brodské-South – Slovak part – reservoir area – 27 wells

More than 20 wells were drilled in the Brodské-Upper Block area.

All wells are currently abandoned. The dates of abandonment of the wells on the Czech territory vary from 1957 to 2004, and there is not a clear dependence of the abandonment dates on the termination of production. Within a project “remediation of old environmental damages”, 22 wells in the Czech part of the complex were selected for re-abandonment, which was carried out in 2012–2015. Six of these wells penetrate the LBr-1 reservoir, four are dry wells around LBr-1, nine penetrate Brodské-South and three are located around Brodské-South, outside of the field itself.

All the above-mentioned wells represent potential leakage pathways for fluids from the reservoir (or deep structures in general) and towards the surface. For this reason, much attention is being paid to the assessment of the status of these wells and their abandonment. The wells penetrating the LBr-1 reservoir are of highest priority because they will be in direct contact with the CO_2 plume after CO_2 injection into the reservoir begins.

The wells penetrating LBr-1 and dry wells around the field were subject of a thorough assessment in the previous project REPP-CO_2 (Ford et al., 2016). Brodské-Middle wells were also covered. In the ENOS project, the focus area has been extended to Brodské-South, specifically as part of a follow-up study on possible trans-boundary effects of CO_2 storage at LBr-1 that is the subject of ENOS Task 4.2.3.

Data on abandonment and re-abandonment of wells were collected from MND a.s. (former LBr-1 field operator), PKÚ, s.p. (company responsible for re-abandonment campaign in the 2010s) and NAFTA a.s. (Slovak national oil company managing the archives of Slovak oilfield data).

In addition to wells from the Brodské-South area, a new assessment, based on newly uncovered data, was made for the two wells at LBr-1 that experienced accidents during exploration – Br-62 and Br-64. New well diagrams were drawn, focusing on possible leakage pathways for CO_2 and natural gas originally in place. (Fig. 8 & 9).

The Br-62 well was chosen for detailed assessment, modelling, and simulation (see Chapter 5.4.2).

The archival well data in the Brodské-South area were compiled in tables and schemes. They comprise the dates of drilling and abandonment, depth intervals of casings, cement jobs, and perforations. Repeated abandonment reports were processed in a similar way. Finally, the well schemes were integrated – together with well logs, stratigraphy and lithological interpretation - into the well diagrams (see Fig. 8 & 9 and Appendix 2).

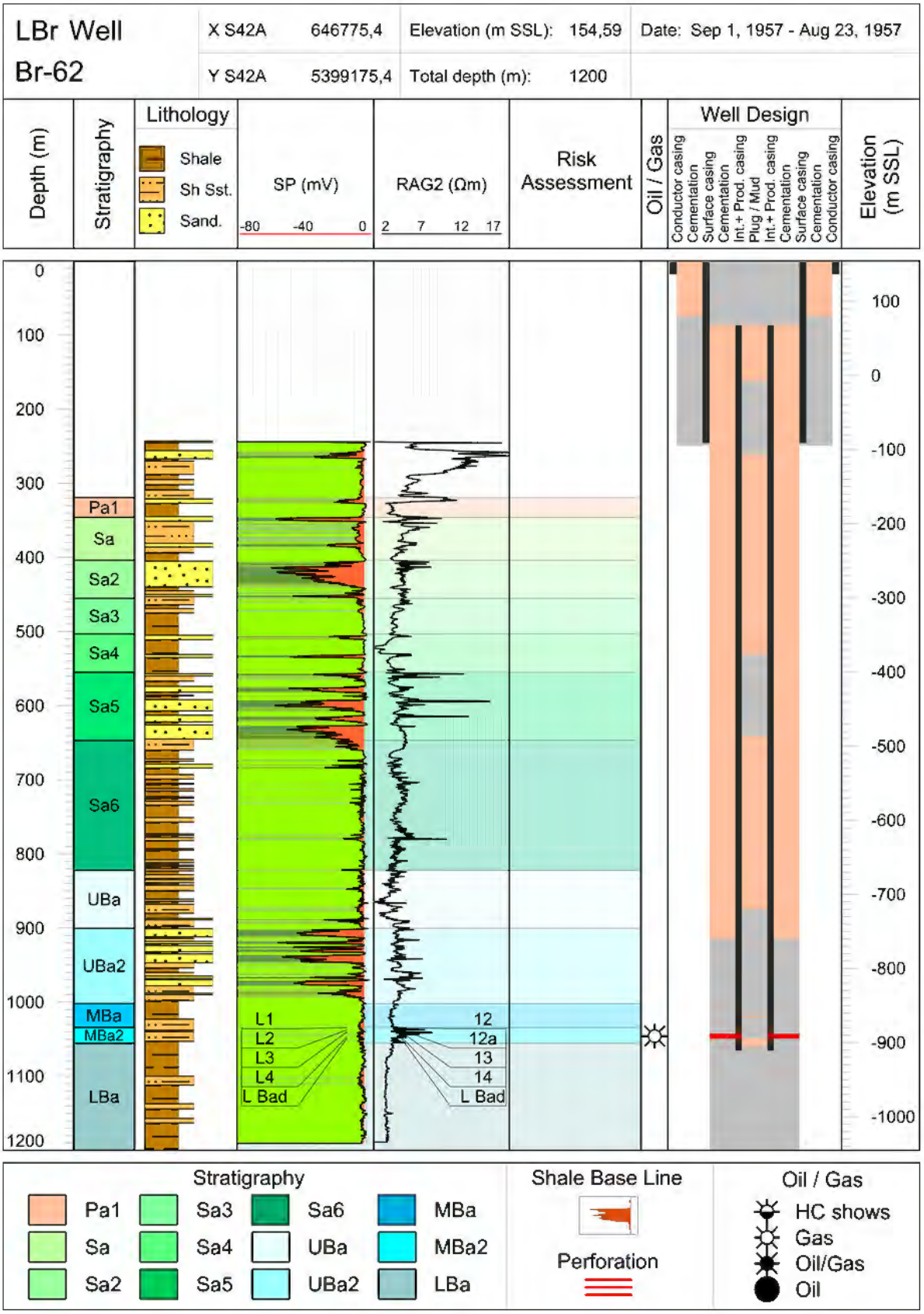

Figure 8 New well diagram for well Br-62 with well logs and lithological interpretation

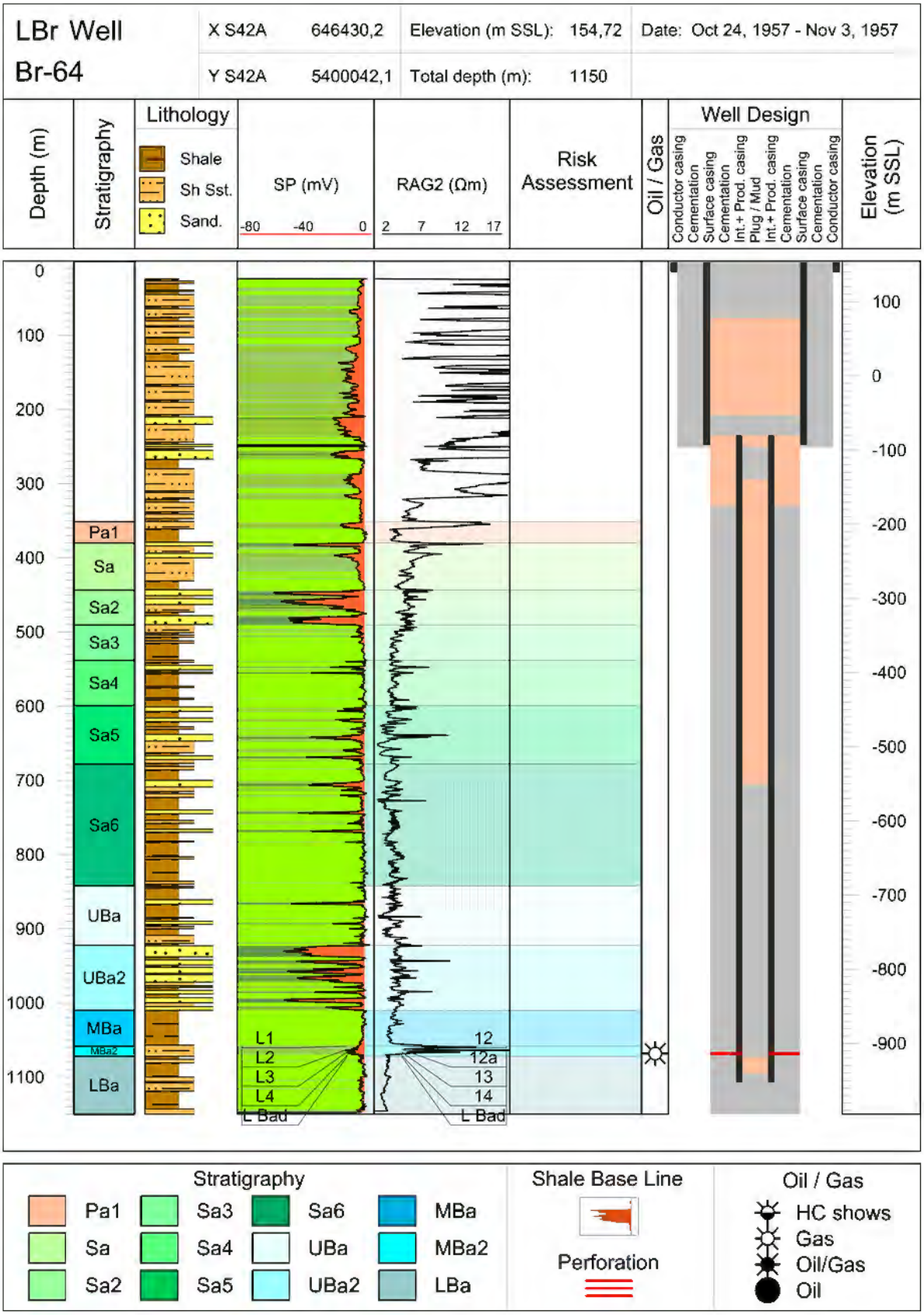

Figure 9 New well diagram for well Br-64 with well logs and lithological interpretation

The newly processed well diagrams of wells situated in the Czech part of the Brodské-South field and its surroundings are attached to this report in Appendix 2.

The dataset describing the status of abandonment of all wells in the Brodské complex on the Czech territory was used to compare this status with the currently valid regulatory requirements for the abandonment of wells (see Chapter 5.3).

5 Risk analysis

5.1 Screening

Once the risk identification process is finished, the number of different leakage scenarios may be considerable, and processing all of these cases in-depth is probably not feasible. A screening process, to identify the most critical risks, should therefore be conducted in the preliminary stages of the risk analysis.

Screening for the most important risks can be performed using a HAZID (Hazard Identification)-style approach, gathering opinions from experts from different disciplines. The information obtained can be used to identify the primary concerns and to help focus the risk assessment. Typically, specific assessments of probabilities and consequences are, to a large extent, based on a combination of expert judgments of the personnel involved in the project, available historic failure rates and available project documents.

5.2 Probability assessment

To give a structured framework the assessment of the probability of an event occurring can be based on a coarse probability scale, in which each probability class is mapped to a frequency of occurrence range and a general interpretation of that range. The ranges and number of classes, and their interpretation, should be adapted to the specific context of the assessment. As an example, the interpretation and understanding of what constitutes a “probable” event will depend on the point of reference and the timeframe of consideration. An example of a probability frequency classification scheme is shown in Table 1.

Table 1 Example of a probability classification table

Class	Frequency of occurrence (per year)	Description
1 - Improbable	$< 10^{-6}$	Virtually improbable and unrealistic
2 - Remote	$10^{-6} – 10^{-4}$	Not expected nor anticipated to occur
3 - Rare	$10^{-4} – 10^{-3}$	Occurrence considered rare
4 - Probable	$10^{-3} – 10^{-1}$	Expected to occur at least once in 10 years
5 - Frequent	$> 10^{-1}$	Likely to occur several times a year

While Table 1 may be considered the primary tool for quantifying probabilities of occurrence, statistical frequencies may be included, where available. Regardless of whether such data exist, the assessed probabilities should be viewed as subjective, best-knowledge judgments, and not as an attempt to approach some “true objective frequency”, as this does not exist.

Each leakage scenario, constructed based on reviews and evaluation of the findings from the risk identification task, as well expert judgments and other information that can support the probability classification process, should lead to a coarse probability assessment similar to that shown in Table 2.

Table 2 Example of a coarse probability assessment for identified leakage scenarios (Ford et. al., 2016)

Leakage scenario	Frequency of occurrence (per year)	Classification
Leakage through wells		
Leakage from an injection well to atmosphere	$8.08*10^{-5}$	Not expected nor anticipated to occur
Blowout from an injection well during drilling	$7.2*10^{-5}$	Not expected nor anticipated to occur
Leakage from an abandoned well to the atmosphere	$4.49*10^{-3}$ – $4.40*10^{-2}$	Occurrence considered rare / Expected to occur at least once in 10 years
Reservoir leakage		
Leakage through the caprock due to gradual failure	$< 10^{-6}$	Improbable and unrealistic
Leakage through the caprock due to rapid, catastrophic failure	$< 10^{-6}$	Improbable and unrealistic
Leakage through existing faults due to increased pressure	$< 10^{-6}$	Improbable and unrealistic
Leakage through induced faults due to increase pressure	$< 10^{-6}$	Improbable and unrealistic
Leakage through spill points	$< 10^{-6}$	Improbable and unrealistic

Table 2 serves as a basis for prioritizing those risks that are of most concern. Which risks are deemed most relevant for further in-depth analyses will depend on the acceptance criteria set forth in the early stages of the risk assessment process.

5.3 Assessment of well abandonment status in the area of LBr-1 and the Brodské HC complex

The consolidated dataset describing the status of abandonment of all wells in the Brodské complex on the Czech territory was used to compare this status with the currently valid regulatory requirements for the abandonment of wells. In addition, a sample of six wells in the Slovak part of the Brodské complex was assessed for comparison.

The regulatory requirements in the Czech Republic are described in amendment 52/2011 Coll. to Decree 239/1998 of 21/02/2011, effective from 01/06/2011. It updates the original decree of 1998 with changes to many of the paragraphs, and by adding appendices 5 and 6 which concern the principles and minimum technical requirements for securing abandoned wells.

The abandonment is defined as putting the well into a state were natural barriers removed during drilling activities have been replaced by artificial barriers that prevent possible communication between the various

formations, or between the formations and the surface. §42 defines cement plugs and the verification of cement plugs. More details on abandonment techniques and plug parameters are defined in appendices 5 and 6 of the decree.

Fig. 10 shows the abandonment requirements for three typical cases. In principle, a well-cemented, unperforated casing is sufficient to prevent flow between formations and between formations and the surface (Case 0). If the casing is perforated, the regulation requires plugging of the perforated interval, a plug inside the casing of at least 30 m length above the uppermost perforation, as well as good annular cement at and above the perforations (Case 2). If there is no annular cement for some part of the casing, the casing should be cut and pulled, and a cement plug set at the cuts (Case 5).

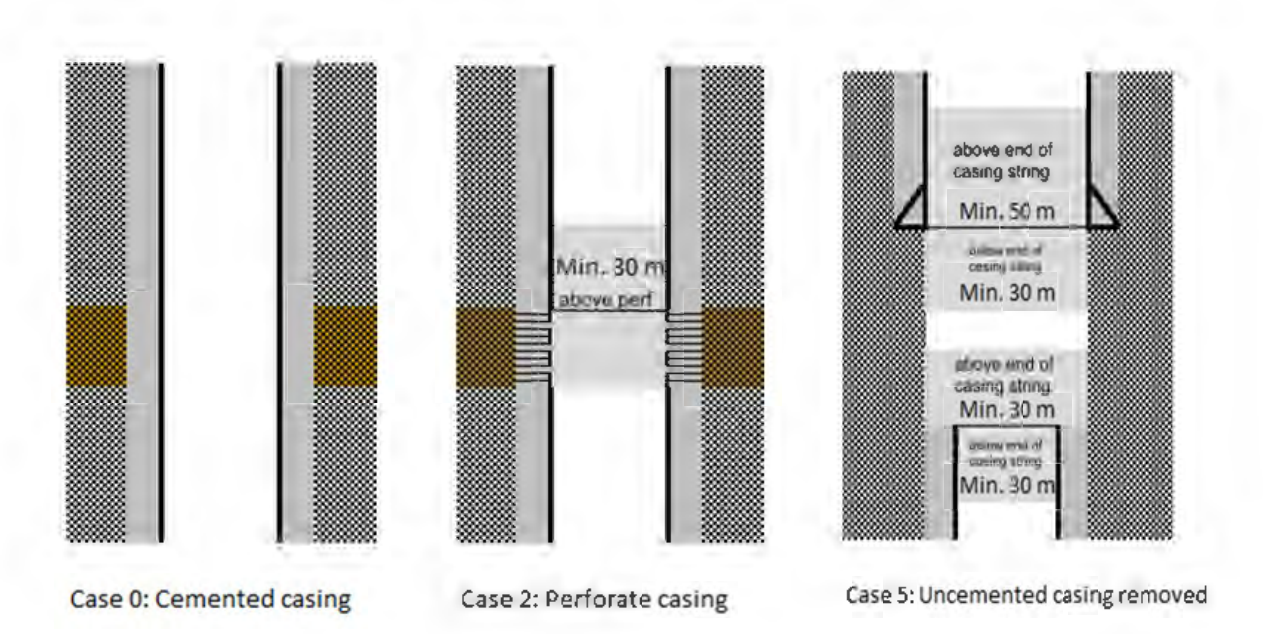

Fig. 10 Isolation requirements for cemented casing (good annular cement), perforated casing (plug extending 30 meters above perforations), and uncemented casing, which has been cut and removed (modified after Ford et al., 2016).

The results of comparison of the well abandonment status with the currently valid legislation are shown in Tables 3 – 8. It should be noted that all the original abandonments were performed before the validity of the amendment of the regulatory decree (June 2011) when no exact rules for cement plug length were in place. Only the re-abandonment campaign in 2012–2015 was regulated by the new rules.

A traffic-light system was used to assess the status of individual wells. It is also used in the tables. Green indicates that the abandonment status is compliant with the current regulations, while red indicates clear discrepancy. Orange indicates only marginal deviations from the prescribed status.

Table 3 Overview of the status of well abandonment – wells penetrating the LBr-1 reservoir

LBr-1 reservoir	perforated interval from	perforated interval to	cement plugs from	cement plugs to	perforat. plugged	plug length above top	plug length below	compliance	whole well	comment
Br-45	1 910,5	1 920,0	1 879,0	1 920,0	Yes	31,5		YES	NO	Length OK, perforations entirely plugged
	1 863,5	1 870,5	1 794,0	1 863,0	No	69,0		NO		Length OK, but perforations are not plugged
	1 779,0	1 781,0	1 767,0	1 780,0	Partially	12,0		NO		Length < 30 m, perforations only partially plugged
	1 740,0	1 742,0	1 666,0	1 737,0	No	71,0		NO		Length OK, but perforations are not plugged
	1 648,0	1 652,0	1 617,0	1 660,0	Yes	31,0		YES		Length OK, perforations entirely plugged
	1 605,5	1 612,5	1 605,0	1 660,0	Yes	0,5		NO		Perforations plugged, but length < 30 m
	1 531,5	1 533,0	1 505,0	1 530,0	No	25,0		NO		Length < 30 m, perforations not plugged
	1 482,0	1 484,0	1 420,0	1 496,0	Yes	62,0		YES		Length OK, perforations entirely plugged
	1 216,0	1 219,0	1 200,0	1 214,5	No	14,5		NO		Length < 30 m, perforations not plugged
	1 171,5	1 173,5	1 146,5	1 169,5	No	23,0		NO		Length < 30 m, perforations not plugged
	1 073,0	1 080,0	1 049,0	1 083,0	Yes	24,0		NO		Perforations plugged, but length < 30 m
Br-55	1 195,0	1 197,0	1 145,0	1 177,0	No	32,0		NO	NO	Length OK, but perforations are not plugged (plug bottom 18 m above perforation top)
	1 129,0	1 130,5	1 015,9	1 145,0	Yes	113,1		YES		Length OK, perforations entirely plugged
	1 086,0	1 100,0	1 015,9	1 145,0	Yes	70,1		YES		Length OK, perforations entirely plugged
Br-58 (re-aban)	1 108,5	1 110,0	1,6	1 143,0	Yes	1 106,9		YES	YES	Length OK, perforations entirely plugged
	1 009,0	1 010,0	1,6	1 143,0	Yes	1 007,4		YES		Length OK, perforations entirely plugged
	957,0	958,5	1,6	1 143,0	Yes	955,4		YES		Length OK, perforations entirely plugged
	593,4	594,0	1,6	1 143,0	Yes	591,8		YES		Length OK, perforations entirely plugged
	591,3	592,2	1,6	1 143,0	Yes	589,7		YES		Length OK, perforations entirely plugged
	557,3	558,9	1,6	1 143,0	Yes	555,7		YES		Length OK, perforations entirely plugged
	554,0	555,0	1,6	1 143,0	Yes	552,4		YES		Length OK, perforations entirely plugged
Br-61	1 144,0	1 145,2	1 068,0	1 145,0	Partially	76,0		Partially	PARTIALLY	Length OK, but perforations only partially plugged (-20 cm!)
	1 095,0	1 099,5	1 068,0	1 145,0	Yes	27,0		Partially		Perforations plugged, but length < 30 m (-3 m)
Br-62	1 043,0	1 049,0	1 021,7	1 049,0	Yes	21,3		NO	NO	Perforations plugged, but length < 30 m (next plug 875,5 - 1019,6 m)
Br-64	1 066,5	1 070,0	704,7	1 072,8	Yes	361,8		YES	YES	Length OK, perforations entirely plugged
Br-65	1 099,0	1 101,0	1 097,0	1 150,0	Yes	2,0		NO	NO	Perforations plugged, but length < 30 m
	1 092,0	1 093,0	717,2	775,2	No	58,0		NO		Length OK, but perforations are not plugged (plug bottom 317 m above perf top)
	1 083,0	1 090,0	717,2	775,2	No	58,0		NO		Length OK, but perforations are not plugged (plug bottom 308 m above perf top)
Br-66 (re-aban)	1 107,5	1 108,5	774,8	1 140,0	Yes	332,7		YES	YES	Length OK, perforations entirely plugged
	1 104,0	1 106,5	774,8	1 140,0	Yes	329,2		YES		Length OK, perforations entirely plugged
	1 098,5	1 100,0	774,8	1 140,0	Yes	323,7		YES		Length OK, perforations entirely plugged
Br-68 (re-aban)	1 091,0	1 095,0	957,3	1 104,5	Yes	133,7		YES	YES	Length OK, perforations entirely plugged
	1 087,0	1 088,0	957,3	1 104,5	Yes	129,7		YES		Length OK, perforations entirely plugged
	1 079,5	1 083,5	957,3	1 104,5	Yes	122,2		YES		Length OK, perforations entirely plugged
	1 004,5	1 006,5	957,3	1 104,5	Yes	47,2		YES		Length OK, perforations entirely plugged
	744,0	746,5	672,8	957,0	Yes	71,2		YES		Length OK, perforations entirely plugged
Br-69 (re-aban)	No perforations		2,0	320,6			33,8	YES	YES	No production (intermediate) casing, conductor and surface casing entirely plugged (33,8 m below end of surface casing)
Br-70	1 101,0	1 108,0	1 041,0	1 230,0	Yes	60,0		YES	YES	Length OK, perforations entirely plugged
Br-72 (re-aban)	1 115,0	1 116,0	2,0	1 175,0	Yes	1 113,0		YES	YES	Length OK, perforations entirely plugged
	1 112,0	1 113,0	2,0	1 175,0	Yes	1 110,0		YES		Length OK, perforations entirely plugged
	1 107,0	1 108,5	2,0	1 175,0	Yes	1 105,0		YES		Length OK, perforations entirely plugged
	1 102,0	1 105,0	2,0	1 175,0	Yes	1 100,0		YES		Length OK, perforations entirely plugged
Br-73	1 100,0	1 105,0	1 098,0	1 130,0	Yes	2,0		NO	NO	Perforations plugged, but length < 30 m
	1 091,5	1 094,5	1 028,3	1 094,5	Yes	63,2		YES		Length OK, perforations entirely plugged
Br-74 (re-aban)	1 101,5	1 103,0	2,0	1 118,6	Yes	1 099,5		YES	YES	Length OK, perforations entirely plugged
	1 099,5	1 101,0	2,0	1 118,6	Yes	1 097,5		YES		Length OK, perforations entirely plugged
	1 095,5	1 097,0	2,0	1 118,6	Yes	1 093,5		YES		Length OK, perforations entirely plugged
	295,5	296,5	2,0	1 118,6	Yes	293,5		YES		Length OK, perforations entirely plugged
Br-76	1 096,0	1 097,5	1 060,0	1 180,0	Yes	36,0		YES	YES	Length OK, perforations entirely plugged
Br-77	1 102,0	1 104,0	1 044,0	1 104,3	Yes	58,1		YES	YES	Length OK, perforations entirely plugged
Br-78	1 096,0	1 102,0	982,0	1 057,0	No	75,0		NO	NO	Length OK, but perforations are not plugged (plug bottom 39 m above perf top)

LBr-1 reservoir	perforated interval from	perforated interval to	cement plugs from	cement plugs to	perforat. plugged	plug length above top	plug length below	compliance	whole well	comment
Br-79	1 102,5	1 105,0	980,0	1 180,0	Yes	122,5		YES	YES	Length OK, perforations entirely plugged
	1 090,5	1 094,0	980,0	1 180,0	Yes	110,5		YES		Length OK, perforations entirely plugged
	1 013,0	1 015,0	980,0	1 180,0	Yes	33,0		YES		Length OK, perforations entirely plugged
Br-80	1 105,0	1 106,0	1 022,0	1 126,0	Yes	83,0		YES	YES	Length OK, perforations entirely plugged
	1 104,0	1 105,0	1 022,0	1 126,0	Yes	83,0		YES		Length OK, perforations entirely plugged
	1 096,0	1 098,5	915,7	1 022,0	Yes	180,4		YES		Length OK, perforations entirely plugged
	1 021,0	1 022,5	915,7	1 180,0	Yes	105,4		YES		Length OK, perforations entirely plugged
Br-81	1 116,5	1 125,0	1 084,9	1 124,0	Partially	31.6		Partially	NO (re-abandon impossible motorway)	Length < 30 m, perforations only partially plugged (1 m is not plugged)
	1 107,5	1 113,0	1 084,9	1 124,0	Yes	22,6		NO		Perforations plugged, but length < 30 m
	1 106,0	1 107,0	1 084,9	1 124,0	Yes	21,1		NO		Perforations plugged, but length < 30 m
	1 100,5	1 104,0	1 084,9	1 124,0	Yes	15,6		NO		Perforations plugged, but length < 30 m
	1 098,5	1 100,0	1 084,9	1 124,0	Yes	13,6		NO		Perforations plugged, but length < 30 m
	1 095,5	1 098,0	1 084,9	1 124,0	Yes	10,6		NO		Perforations plugged, but length < 30 m
	1 090,0	1 094,5	1 084,9	1 124,0	Yes	5,1		NO		Perforations plugged, but length < 30 m
	1 089,0	1 092,5	1 084,9	1 124,0	Yes	4,1		NO		Perforations plugged, but length < 30 m
Br-82	1 105,0	1 106,0	1 039,2	1 126,0	Yes	65,8		YES	YES	Length OK, perforations entirely plugged
	1 104,5	1 105,0	1 039,2	1 126,0	Yes	65,3		YES		Length OK, perforations entirely plugged
	1 099,0	1 100,0	1 039,2	1 126,0	Yes	59,8		YES		Length OK, perforations entirely plugged
	1 093,5	1 095,5	1 039,2	1 126,0	Yes	54,3		YES		Length OK, perforations entirely plugged
Br-83	1 105,0	1 106,0	1 037,0	1 115,0	Yes	68,0		YES	YES	Length OK, perforations entirely plugged
	1 104,5	1 105,5	1 037,0	1 115,0	Yes	67,5		YES		Length OK, perforations entirely plugged
	1 097,0	1 098,0	1 037,0	1 115,0	Yes	60,0		YES		Length OK, perforations entirely plugged
Br-85	1 104,0	1 107,0	1 085,0	1 115,0	Yes	19,0		NO	NO (re-abandon impossible motorway)	Perforations plugged, but length < 30 m (partially unknown)
	1 098,0	1 099,5	1 085,0	1 115,0	Yes	13,0		NO		Perforations plugged, but length < 30 m (partially unknown)
Br-86	1 103,5	1 104,5	998,0	1 070,7	No	72,7		NO	NO	Length OK (plag bottom 32.8 m above top perf.) but perforations are not plugged
Br-89	1 101,0	1 102,0	1 090,0	1 106,0	Yes	11,0		NO	NO	Perforations plugged but length < 30 m
	1 097,0	1 098,0	1 090,0	1 106,0	Yes	7,0		NO		Perforations plugged but length < 30 m
	1 093,0	1 094,0	1 090,0	1 106,0	Yes	3,0		NO		Perforations plugged but length < 30 m
	1 090,0	1 091,0	1 090,0	1 106,0	Yes	0,0		NO		Perforations plugged but length < 30 m
	1 084,0	1 087,5	1 057,9	1 087,3	Partially	26,1		NO		Perforations plugged partially (-20 cm!), length < 30 m

Table 3 shows the status of the wells penetrating the LBr-1 reservoir. Of the 25 wells, 14 meet the regulation requirements, one is almost compliant with them, and 10 do not satisfy the criteria (three due to unplugged perforations, five due to insufficient length of plugs, and two due to both reasons). To evaluate the risk these wells represent for CO_2 storage operations and possible CO_2 leakage from the reservoir, it is necessary to compare their position with the results of CO_2 injection simulations, especially with the development of the CO_2 plume extent with time and with the predicted changes (increase) of the reservoir pressure.

The status of the five dry wells outside of the LBr-1 reservoir (Table 4) is not very satisfactory – two of them do not meet regulatory requirements, two have slight deficiencies and only one is in good shape. On the other hand, due to their positon outside of the reservoir, they do not represent significant risk for the storage site integrity.

Of the three wells at Brodské-Middle (Table 5), only one is compliant with current legislation. However, due to its geological position, this partial reservoir will not be affected by the CO_2 storage operations.

The status of wells penetrating the Czech part of the Brodské-South reservoir is shown in Table 6. Ten wells (out of 15) are compliant with the regulation, two are almost satisfactory, and only three do not meet the criteria. The status of these wells is important for the assessment of possible cross-border issues related to CO_2 storage at LBr-1, especially in case of CO_2 migration below the southern LBr-1 spill point to the South.

All three dry wells outside of the Brodské-South reservoir on the Czech territory have been re-abandoned in the 2010s and are in accord with the valid decree (Table 7).

Table 4 Overview of the status of well abandonment – dry wells around the LBr-1 reservoir

Outside LBr-1	perforated interval from	perforated interval to	cement plugs from	cement plugs to	perforat. plugged	plug length above top	plug length below	compliance	whole well	comment
Br-27	1 141,5	1 145,0	1 090,2	1 140,0	No	49,8		NO	NO	Length OK, but perforations are not plugged
	555,5	585,5	525,0	558,0	No	30,5		NO		Length OK, but perforations are not plugged
Br-54 (re-aban)	1 452,0	1 454,0			No	0,0		NO	NO	Length < 30 m, perforations not plugged
	1 358,0	1 378,0	1 332,0	1 349,0	No	17,0		NO		Length < 30 m, perforations not plugged
	1 347,0	1 354,0	1 332,0	1 349,0	Partially	15,0		NO		Length < 30 m, perforations only partially plugged
	1 320,0	1 329,0	1 310,0	1 322,0	Partially	10,0		NO		Length < 30 m, perforations only partially plugged
	1 301,5	1 303,0	1 282,0	1 304,0	Yes	19,5		NO		Perforations plugged, but length < 30 m
	1 292,5	1 297,0	1 282,0	1 304,0	Yes	10,5		NO		Perforations plugged, but length < 30 m
	1 273,5	1 279,0	1 267,0	1 279,0	Yes	6,5		NO		Perforations plugged, but length < 30 m
	1 239,0	1 263,0	1 028,5	1 265,2	Yes	210,5		YES		Length OK, perforations entirely plugged
Br-71 (re-aban)	1 933,5	1 937,5	1 910,0	1 935,0	Partially	23,5		NO	PARTIALLY	Length < 30 m, perforations only partially plugged
	1 904,0	1 906,0	1 837,0	1 877,0	No	40,0		NO		Length OK, but perforations are not plugged
	1 771,0	1 776,0	927,5	1 726,0	No	798,5		NO		Length OK, but perforations are not plugged
	1 701,0	1 706,0	927,5	1 726,0	Yes	773,5		YES		Length OK, perforations entirely plugged
	1 658,0	1 661,0	927,5	1 726,0	Yes	730,5		YES		Length OK, perforations entirely plugged
	1 649,0	1 655,0	927,5	1 726,0	Yes	721,5		YES		Length OK, perforations entirely plugged
	1 644,5	1 647,5	927,5	1 726,0	Yes	717,0		YES		Length OK, perforations entirely plugged
	1 640,0	1 643,0	927,5	1 726,0	Yes	712,5		YES		Length OK, perforations entirely plugged
	1 520,0	1 520,5	927,5	1 726,0	Yes	592,5		YES		Length OK, perforations entirely plugged
	1 483,0	1 485,0	927,5	1 726,0	Yes	555,5		YES		Length OK, perforations entirely plugged
	1 402,0	1 404,0	927,5	1 726,0	Yes	474,5		YES		Length OK, perforations entirely plugged
	1 362,0	1 366,0	927,5	1 726,0	Yes	434,5		YES		Length OK, perforations entirely plugged
	1 169,0	1 172,0	927,5	1 726,0	Yes	241,5		YES		Length OK, perforations entirely plugged
	1 163,0	1 164,5	927,5	1 726,0	Yes	235,5		YES		Length OK, perforations entirely plugged
	1 159,0	1 161,0	927,5	1 726,0	Yes	231,5		YES		Length OK, perforations entirely plugged
	1 067,0	1 069,0	927,5	1 726,0	Yes	139,5		YES		Length OK, perforations entirely plugged
Br-75 (re-aban)	No perforations		1,6	330,0			23,0	Partially	PARTIALLY	No production (intermediate) casing, conductor and surface casing entirely plugged but only 23 m (-7 m) below end of surface casing
Br-88 (re-aban)	No perforations		2,0	274,4			31,1	YES	YES	No production (intermediate) casing, conductor and surface casing entirely plugged (31,1 m below end of surface casing)

Table 5 Overview of the status of well abandonment – wells penetrating the Brodské-Middle hydrocarbon lens

Brodské-Middle	perforated interval from	perforated interval to	cement plugs from	cement plugs to	perforat. plugged	plug length above top	compliance	whole well	comment
Br-60	1 659,0	1 662,0	1 653,0	1 691,0	Yes	6,0	YES	NO	Perforations plugged, but length < 30 m
	1 645,0	1 650,0	1 628,0	1 643,0	No	15,0	NO		Length < 30 m, perforations not plugged
	1 612,0	1 613,0	1 611,0	1 615,0	Yes	1,0	YES		Perforations plugged, but length < 30 m
	1 607,0	1 609,0	1 600,0	1 604,0	No	4,0	NO		Length < 30 m, perforations not plugged
	1 461,0	1 462,0	1 178,0	1 200,5	No	22,5	NO		Length < 30 m, perforations not plugged
	1 150,0	1 153,0	1 147,0	1 150,0	No	3,0	NO		Length < 30 m, perforations not plugged
	1 139,0	1 142,0	1 104,0	1 143,0	Yes	35,0	YES		Length OK, perforations entirely plugged
Br-84	1 150,0	1 152,5	???	???				NO	Unknown plug interval
Br-90	1 147,0	1 151,0	1 097,0	1 155,0	Yes	50,0	YES	YES	Length OK, perforations entirely plugged

Table 6 Overview of the status of well abandonment – wells penetrating the Brodské-South reservoir / Czech part

Brodské-South	perforated interval		cement plugs		perforat. plugged	plug length above top	compliance	whole well	comment
	from	to	from	to					
Br-20 (re-aban)	1 164,5	1 167,5	986,0	1 168,0	Yes	178,5	YES	YES	Length OK, perforations entirely plugged
Br-22 (re-aban)	1 141,0	1 143,0	1,6	1 155,0	Yes	1 139,4	YES	YES	Length OK, perforations entirely plugged
	1 130,0	1 133,5	1,6	1 155,0	Yes	1 128,4	YES		Length OK, perforations entirely plugged
	1 122,0	1 124,0	1,6	1 155,0	Yes	1 120,4	YES		Length OK, perforations entirely plugged
Br-34	1 187,0	1 188,0	1 109,0	1 217,6	Yes	78,0	YES	YES (re-aban impossible, barrage)	Length OK, perforations entirely plugged
	1 178,0	1 179,0	1 109,0	1 217,6	Yes	69,0	YES		Length OK, perforations entirely plugged
	1 138,5	1 141,0	1 109,0	1 217,6	Yes	29,5	YES		Perforations plugged, but length < 30 m (only 0,5 m difference!)
Br-35	1 749,0	1 752,0	1 760,0	1 800,0	No	0,0	NO	NO (re-aban impossible, barrage)	Length < 30 m, perforations not plugged
	1 148,0	1 150,0	-	-	No	0,0	NO		Length < 30 m, perforations not plugged
Br-38 (re-aban)	1 180,0	1 182,5	1 173,0	1 195,0	Yes	7,0	NO	PARTIALLY	Perforations plugged, but length < 30 m (between bottom of the new plug and top of the old plug is 2,6 m of something?)
	1 163,0	1 164,0	942,1	1 170,4	Yes	220,9	NO		Length OK, perforations entirely plugged
	1 158,0	1 160,0	942,1	1 170,4	Yes	215,9	NO		Length OK, perforations entirely plugged
	1 140,5	1 142,0	942,1	1 170,4	Yes	198,4	NO		Length OK, perforations entirely plugged
	1 139,5	1 143,0	942,1	1 170,4	Yes	197,4	NO		Length OK, perforations entirely plugged
Br-43	1 139,0	1 143,0	1 160,0	1 200,0	No	0,0	NO	NO (re-aban impossible, barrage)	Length < 30 m, perforations not plugged
Br-47	1 131,5	1 134,0	1 093,0	1 157,0	Yes	38,5	YES	YES	Length OK, perforations entirely plugged
	1 131,5	1 132,5	1 093,0	1 157,0	Yes	38,5	YES		Length OK, perforations entirely plugged (Re-perfor)
Br-48	1 152,0	1 154,0	1 151,0	1 120,0	Yes	1,0	NO	NO (re-aban impossible, barrage)	Perforations plugged, but length < 30 m
	1 139,5	1 141,5	1 135,4	1 151,0	Yes	4,1	NO		Perforations plugged, but length < 30 m
	1 130,0	1 133,5	1 082,0	1 135,4	Yes	48,0	YES		Length OK, perforations entirely plugged
Br-49 (re-aban)	1 183,5	1 193,5	959,7	1 199,4	Yes	223,8	YES	YES	Length OK, perforations entirely plugged
	1 177,0	1 181,0	959,7	1 199,4	Yes	217,3	YES		Length OK, perforations entirely plugged
	1 160,0	1 163,0	959,7	1 199,4	Yes	200,3	YES		Length OK, perforations entirely plugged
	1 156,5	1 159,0	959,7	1 199,4	Yes	196,8	YES		Length OK, perforations entirely plugged
	1 135,5	1 138,0	959,7	1 199,4	Yes	175,8	YES		Length OK, perforations entirely plugged
Br-50 (re-aban)	1 154,5	1 156,0	1,6	1 204,8	Yes	1 152,9	YES	YES	Length OK, perforations entirely plugged
	1 152,2	1 153,4	1,6	1 204,8	Yes	1 150,6	YES		Length OK, perforations entirely plugged
	1 134,0	1 135,5	1,6	1 204,8	Yes	1 132,4	YES		Length OK, perforations entirely plugged
Br-51 (re-aba)	1 149,5	1 151,0	957,0	1 175,1	Yes	192,5	YES	YES	Length OK, perforations entirely plugged
	1 145,0	1 148,0	957,0	1 175,1	Yes	188,0	YES		Length OK, perforations entirely plugged
Br-52 (re-aban)	1 150,5	1 151,5	936,5	1 159,6	Yes	214,0	YES	YES	Length OK, perforations entirely plugged
	1 147,5	1 149,5	936,5	1 159,6	Yes	211,0	YES		Length OK, perforations entirely plugged
	1 129,5	1 131,5	936,5	1 159,6	Yes	193,0	YES		Length OK, perforations entirely plugged
	1 129,0	1 132,5	936,5	1 159,6	Yes	192,5	YES		Length OK, perforations entirely plugged
Br-57 (re-aban)	1 136,8	1 143,0	886,8	1 148,6	Yes	250,0	YES	YES	Length OK, perforations entirely plugged
	1 120,0	1 125,5	886,8	1 148,6	Yes	233,2	YES		Length OK, perforations entirely plugged
Br-59 (re-aban)	1 148,0	1 150,0	975,5	1 160,2	Yes	172,5	YES	YES	Length OK, perforations entirely plugged

Table 7 Overview of the status of well abandonment – dry wells around the Brodské-South reservoir / Czech part

Outside Brodské-S.	perforated interval		cement plugs		perforat. plugged	plug length above top	plug length below	compliance	whole well	comment
	from	to	from	to						
Br-7 (re-aban)	1 571,0	1 574,0	1 301,0	1 599,1	Yes	270,0		YES	YES	Length OK, perforations entirely plugged
	1 571,0	1 577,0	1 301,0	1 599,1	Yes	270,0		YES		Length OK, perforations entirely plugged
	1 566,0	1 566,5	1 301,0	1 599,1	Yes	265,0		YES		Length OK, perforations entirely plugged
	1 555,0	1 561,0	1 301,0	1 599,1	Yes	254,0		YES		Length OK, perforations entirely plugged
	621,5	625,0	359,0	650,0	Yes	262,5		YES		Length OK, perforations entirely plugged
	592,0	595,0	359,0	650,0	Yes	233,0		YES		Length OK, perforations entirely plugged
Br-44 (re-aban)	1 184,0	1 186,0	632,4	1 187,2	Yes	551,6		YES	YES	Length OK, perforations entirely plugged
	1 145,0	1 148,0	632,4	1 187,2	Yes	512,6		YES		Length OK, perforations entirely plugged
	1 134,0	1 135,0	632,4	1 187,2	Yes	501,6		YES		Length OK, perforations entirely plugged
	1 130,0	1 131,0	632,4	1 187,2	Yes	497,6		YES		Length OK, perforations entirely plugged
	1 128,5	1 129,5	632,4	1 187,2	Yes	496,1		YES		Length OK, perforations entirely plugged
	1 116,5	1 118,5	632,4	1 187,2	Yes	484,1		YES		Length OK, perforations entirely plugged
	700,0	702,0	632,4	1 187,2	Yes	67,6		YES		Length OK, perforations entirely plugged
Br-67 (re-aban)	No perforations		1,6	274,1			31,1	YES	YES	No production (intermediate) casing, conductor and surface casing entirely plugged (31,1 m below end of surface casing)

Figures 11 and 12 summarize the results described in Tables 3–8. The charts show percentage representations of individual well categories, based on the status of well abandonment compared with the currently valid national legislation. Fig. 11 illustrates the situation at LBr-1; only wells penetrating the reservoir selected for CO_2 storage are considered. 56% of these wells were abandoned in a way that complies with current legislation while 40% demonstrate various kinds of deficiencies.

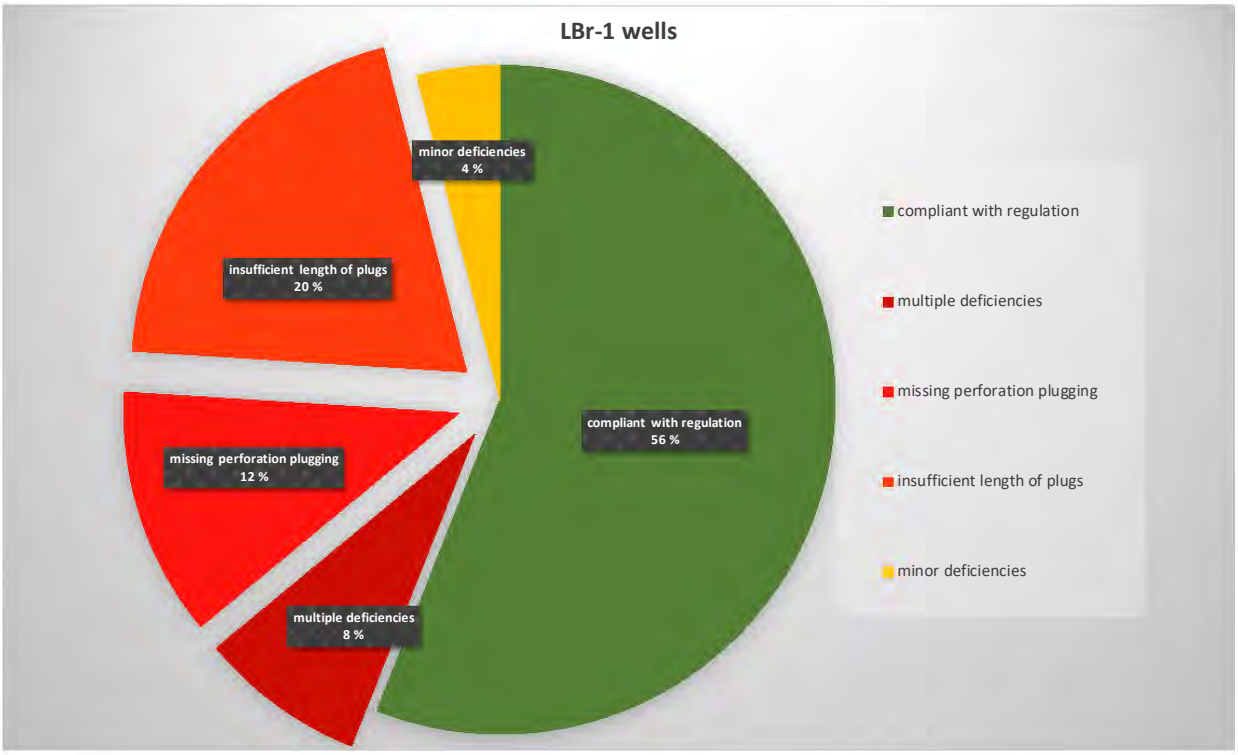

Fig. 11 Summary of well abandonment status for wells penetrating the LBr-1 reservoir

Figure 12 shows the situation for the set of all wells in the Czech part of the Brodské complex. The percentage representations are similar to the set of LBr-1 wells with 57% of wells compliant with regulation and 33% showing deficiencies.

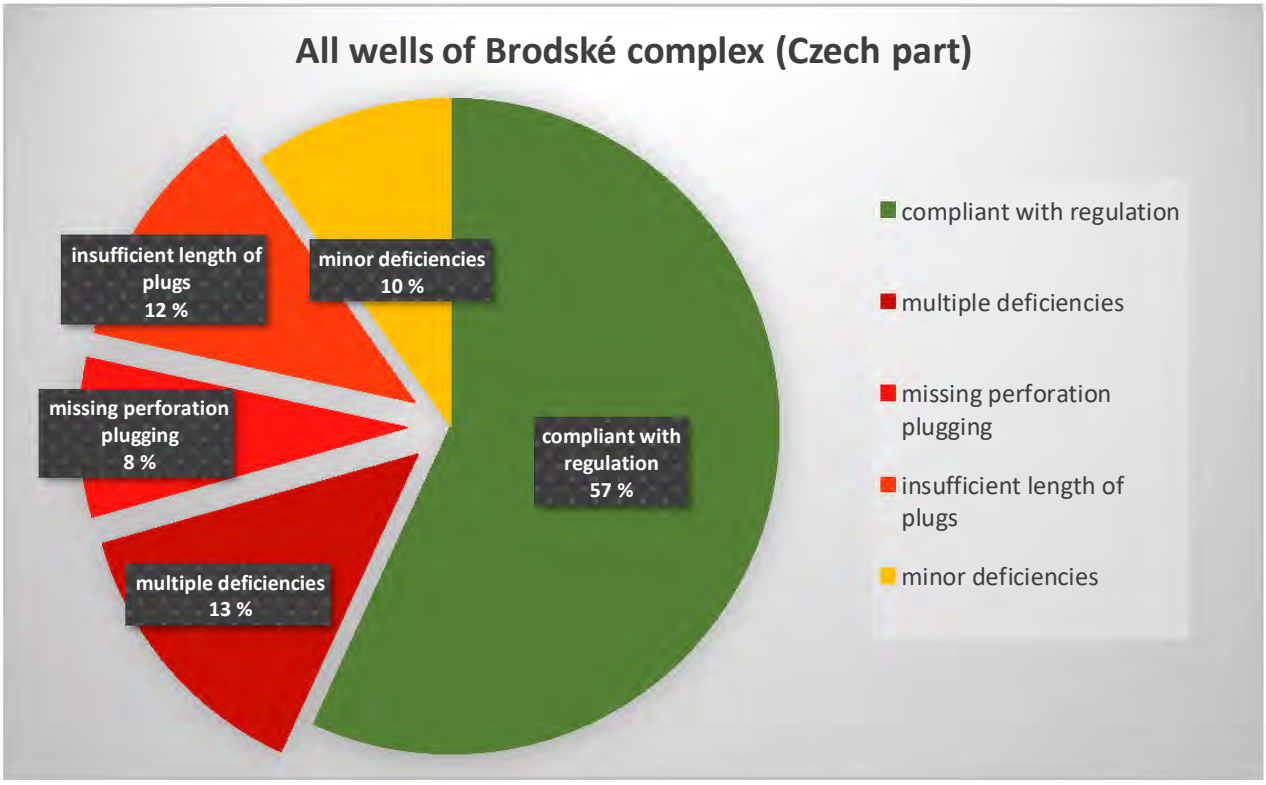

Fig. 12 Summary of well abandonment status for all wells in the Czech part of the Brodské hydrocarbon complex

In addition to the wells on the Czech territory, a sample of six wells in the Slovak part of the Brodské complex was assessed for comparison. Five of them are located in the Slovak part of the Brodské-South field and one (Br-87) close to the edge of LBr-1, just across the Morava river.

There is not any regulation available in the Slovak Republic that would concretely define the well abandonment requirements as comparable to the Czech decree No 52/2011. The currently valid Slovak decree No 7/1981 (amended by decree No 88/1985) provides only some general guidelines. For this reason, the status of the selected wells from the Slovak part of Brodské-South was compared with the requirements set by the Czech legislation, which enabled a same basis comparison.

The results of comparison of the well status with the Czech legislation is shown in Table 8. All six wells are marked in red, i.e. they are not compliant with the requirements. It can be stated that the status of well abandonment in the Slovak part of the Brodské complex is worse than that in the Czech part. This reflects the general situation that will be examined more in detail in the Czech-Slovak trans-boundary study in ENOS Task 4.2.3.

Table 8 Overview of the status of well abandonment – sample wells on the Slovak territory

Brodské-South (SK)	perforated interval from	perforated interval to	cement plugs from	cement plugs to	perforat. plugged	plug length above top	plug length below	compliance	whole well	comment
Br-4	1 293,0	1 390,0	1 240,0	?	?	53,0		?	NO	Length OK, perforations unknown
	1 214,0	1 216,5	1 188,0	1 216,0	Yes	26,0		NO		Perforations plugged, but length < 30 m
	1 176,0	1 183,0	1 170,5	1 183,0	Yes	5,5		NO		Perforations plugged, but length < 30 m
	1 160,0	1 161,0	1 106,0	1 169,0	Yes	54,0		YES		Length OK, perforations entirely plugged
	1 139,5	1 144,0			No	0,0		NO		Length < 30 m, perforations not plugged
	1 038,0	1 048,0			No	0,0		NO		Length < 30 m, perforations not plugged
	1 029,0	1 034,0			No	0,0		NO		Length < 30 m, perforations not plugged
	1 023,0	1 027,0			No	0,0		NO		Length < 30 m, perforations not plugged
Br-5	No perforations		2,0	20,0			0,0	NO	NO	No production (intermediade) casing. Blowout in the depth 1560 m, the drilling tools are left in depth interval 1421- 1560 m.
Br-6	No perforations		2,0	450,0			0,0	NO	NO	No production (intermediate) casing, conductor and surface casing strigs plugged but no plug below end of surface casing
Br-8	1 204,3	1 206,1	1 150,0	1 200,0	No	54,3		NO	NO	Length OK, but perforations are not plugged (plug bottom 4 m above perfor top)
	1 203,0	1 205,5	1 150,0	1 200,0	No	53,0		NO		Length OK, but perforations are not plugged (plug bottom 3 m above perfor top)
Br-9	1182,0	1185,0			No	0,0		NO	NO	Length < 30 m, perforations not plugged
	1181,5	1186,0			No	0,0		NO		Length < 30 m, perforations not plugged
Br-87	558,5	560,5	536,0	564,0	Yes	22,5		NO	NO	Perforations plugged, but length < 30 m
	544,5	545,5	536,0	564,0	Yes	8,5		NO		Perforations plugged, but length < 30 m
	526,0	528,0	508,0	524,0	No	18,0		NO		Length < 30 m, perforations not plugged
	497,5	499,0	460,0	498,0	Partly	37,5		Partly		Perforations partly (0,5 from 1,5 m) plugged, length O.K.
	290,5	292,0	285,0	295,0	Yes	5,5		NO		Perforations plugged, but length < 30 m
	290,5	296,0	285,0	295,0	Partly	5,5		NO		Perforations partly (5 from 6 m) plugged, but length < 30 m

The results of the well status assessment and comparison with legislation have been summarised and graphically displayed in a “traffic-light” map (Fig. 13). The map shows the positions of individual wells and the colours depict their status as evaluated in Tables 3–8.

From the risk assessment point of view, interesting information can be drawn from the comparison of the simulated extent of the CO_2 plume in the LBr-1 reservoir with the position of individual wells and their status, as shown in maps in Figure 14. The maps clearly indicate which wells are likely to contact the plume of stored CO_2 and – in case of bad condition – may represent leakage pathways for the CO_2 stored in the reservoir.

Both maps in Fig. 14 show simulation results of CO_2 injection for the basic storage pilot scenario, which assumes injection of 70,000 t of CO2 over six years. The map on the left depicts the extent of CO2 plume after injection of 35,000 t CO_2 over 3 years. Six wells are clearly situated in the plume area and three wells are at the plume edge. Of these nine wells, in only two cases (Br-82 and Br-83) does the status of abandonment satisfy the regulation criteria. One well (Br-61) shows only minor deficiencies in this respect. In two wells (Br-78 and Br-86) the perforations have not been sufficiently plugged, and one well (Br-62) has insufficient lengths of plugs above perforations. The Br-62 well has been chosen for a further modelling and simulation study (see chapter 5.4.2). In three cases (Br-45, Br-65 and Br-89), the status of well abandonment demonstrates multiple deficiencies in comparison with the regulation requirements.

The map in the right part of Fig. 14 shows the simulated extent of CO2 plume after the planned full amount of CO_2 (70,000 t) is injected. Compared to the situation after three years, only two additional wells are clearly affected by the CO_2 plume: Br 55 (showing multiple abandonment deficiencies) and Br-64

(compliant with regulation). Four other wells are situated just outside the plume: Br-68, Br-70, Br-79 (all compliant with regulation) and Br-81 (with multiple deficiencies)

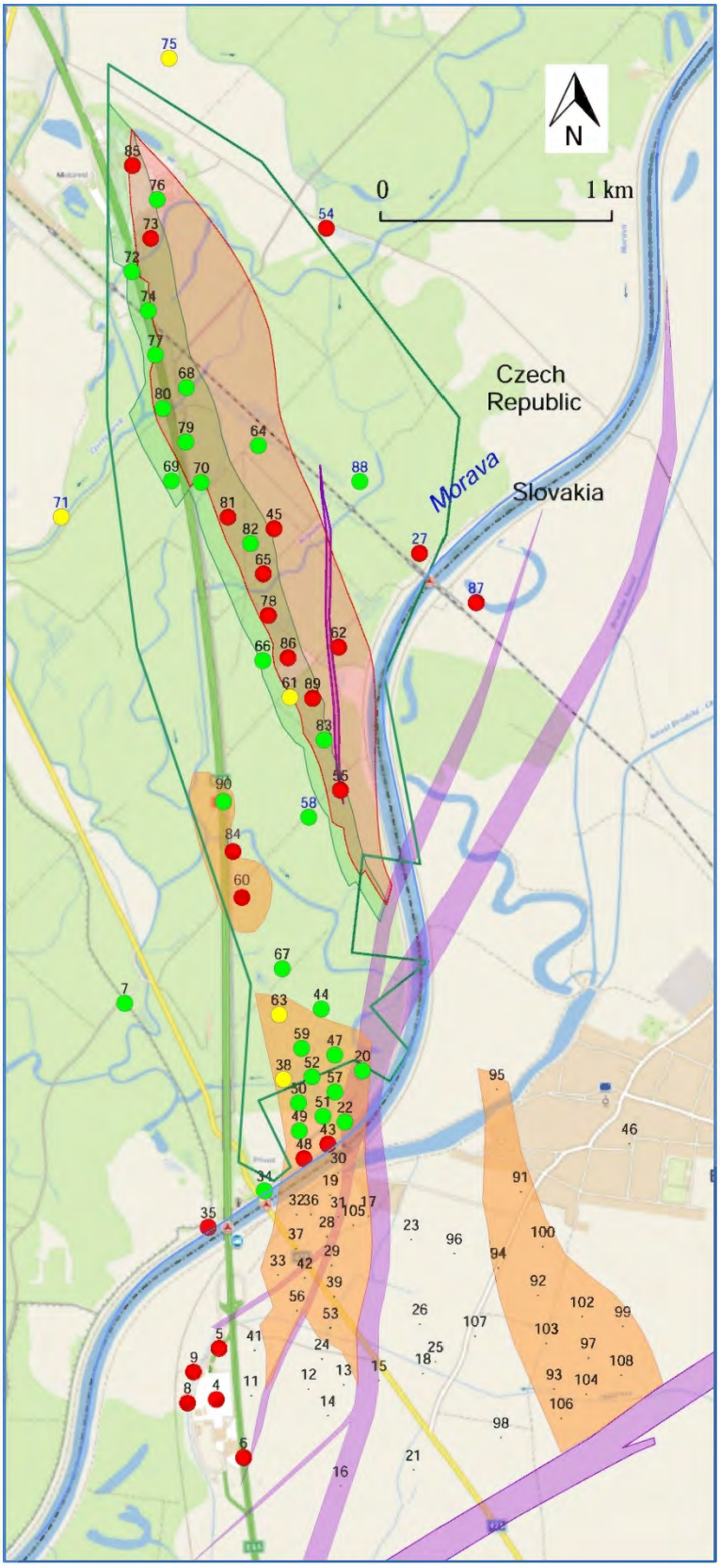

Figure 13
"Traffic-light" map of wells in the Czech part of the Brodské hydrocarbon complex. Green circles indicate wells for which the current status of abandonment meets the requirements of valid legislation. Abandonment status of wells indicated by red circles does not meet these requirements. Orange circles indicate only marginal deviations from the prescribed status.
Coloured polygons indicate the position of original hydrocarbon-bearing zones. Main faults are drawn in violet.
The Morava river also represents the Czech-Slovak state boundary.

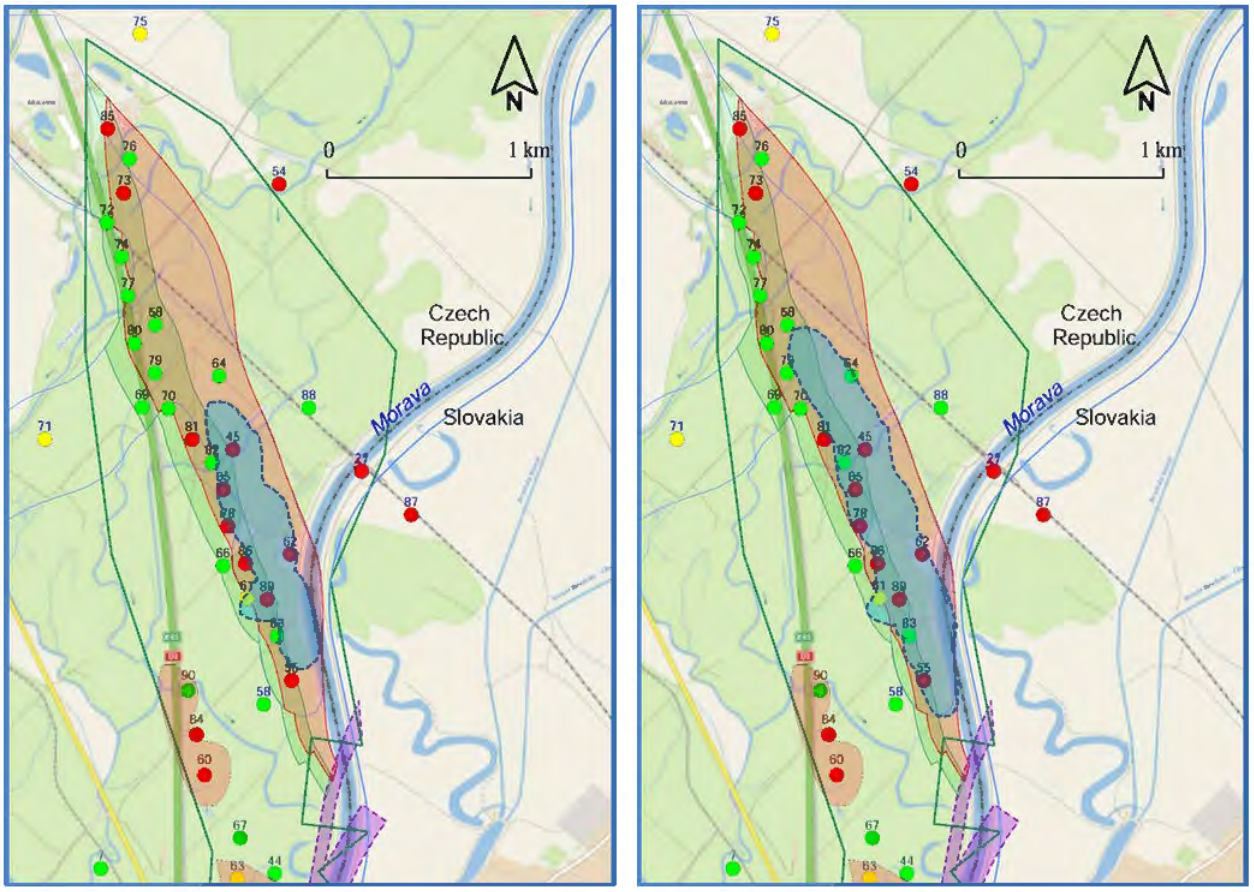

Fig. 14 Maps of LBr-1 showing the simulated extent of CO_2 plume in the basic pilot project scenario (injection of 70,000 t CO_2), superimposed on the "traffic-lights" map from Fig. 13. Left – plume extent after injection of 35,000 t CO_2 (three years); right – plume extent after injection of 70,000 t CO_2 (six years).

It should be noted that the fact that a well abandonment is not in compliance with currently valid regulation in itself does not mean that the well will leak. In most cases, the abandonment was carried out before the current decree took effect. From this point of view, each of the wells needs to be assessed separately to evaluate the risk of leakage its status represents. The "traffic-lights" system used here only indicates the wells that warrant increased attention.

In conclusion, this chapter describes an approach toward qualification of a depleted oil field as a CO_2 storage site, with respect to potential for leakage from abandoned wells, using the LBr-1 reservoir in the Czech Republic as an example. It illustrates an outcome where the leakage risk is manageable, but several of the old wells must be further evaluated, and potentially secured, before CO2 injection can start.

5.4 Leakage rate assessments

Whenever the CO_2 is planned to be injected into an abandoned oil and gas field, the risk of leakage through existing boreholes constitutes one of the main concerns, and is therefore subject to in-depth risk analysis. As a first step, information should be gathered that provides an overview of the specific wells and their immediate location, well schematics showing casing programme and Plugging and Abandonment (P&A) design, history of the wells, and any information that could be used to make judgments on their integrity, such as pressure integrity tests, cement bond logs (CBL), etc.

Leakage from abandoned wells can occur due to the failure of barriers such as cement plugs, giving rise to leakage pathways through which fluids and gas may escape into the environment. In SPE 185890, three main pathways are addressed, namely 1) leakage through bulk cement, 2) leakage through cracks and 3) leakage through micro-annuli. This paper also provides a framework for quantitatively assessing leakage rates and uncertainty in these rates. This chapter outlines the main steps of such an approach, using an example well for illustrative purposes. It is however stressed that the main purpose here is not to provide exact results for this well, but to show how an assessment is performed. More information on the integrity of the well barriers would be required in order to provide reliable results, and the results provided here should therefore be viewed in light of this.

The following sections present an example case from the Czech LBr-1 field and associated leakage rate calculations under the given assumptions.

5.4.1 A framework for assessing leakage rates

A framework for quantitatively assessing leakage rates for plugged and abandoned wells is briefly presented here. For further details, please refer to SPE 185890 and the references therein.

The main components required to perform leakage rate assessments are shown in Figure 6.

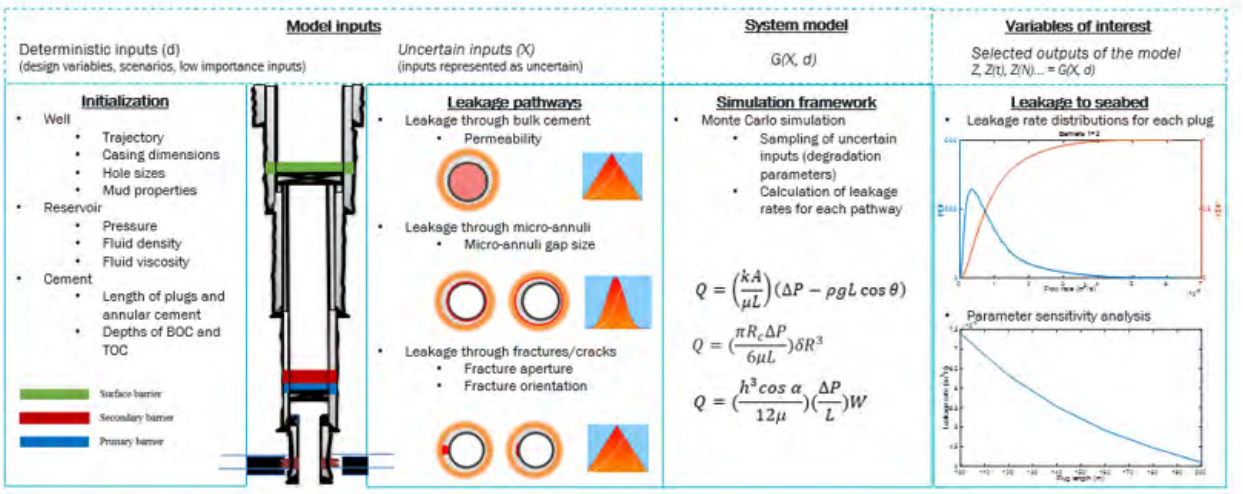

Figure 5 Main components of the leakage rate calculator (Ford et. al., 2017) (Abbreviations BOC = Bottom of Cement, TOC = Top of Cement).

The main input parameters consist of deterministic input, such as well and P&A design and reservoir characteristics, as well as uncertain inputs that typically relate to the size of fractures, micro-annuli and permeability of cement. Assuming that the uncertain input parameters can somehow be established, the underlying models for leakage rates (bulk, fractures, micro-annuli) are run in a Monte Carlo framework to produce leakage rate distributions. In the model outcomes, as the storage complex pressures evolve over time, so too does the resulting leakage rate. In this framework, parameter uncertainties are represented as probability distributions.

5.4.2 LBr-1 Well Br-62

5.4.2.1 Background

Wells Br-62 and Br-64 were affected by methane blowouts during the exploration phase of the LBr-1 field The Br-62 blowout occurred in 1957 and was stopped in ca. 12 days. According to verbal evidence from people familiar with the locality, surface gas shows were observed for the next 40 years, until well plugging and abandonment in 2000. The abandonment procedure from 2000 does not comply with the requirements of the current Czech legislation (valid from 2011 onwards) – the thickness of the plug above the top of perforation (21.3 m) is less than that required by the decree (30 m). The potential risk associated with any gaps in the behind-casing cementation over the depth interval 246 – 915 m requires more detailed investigation.

This site and wells are used as a case study for the purposes of improving the ENOS project modelling exercise by building scenarios using input from a real world reservoir and wells. The results of this modelling exercise do not in any way infer that leakage would occur at these wells.

5.4.2.2 Well design and leakage pathways

The well design, including cement plugs, is shown in Figure 7.

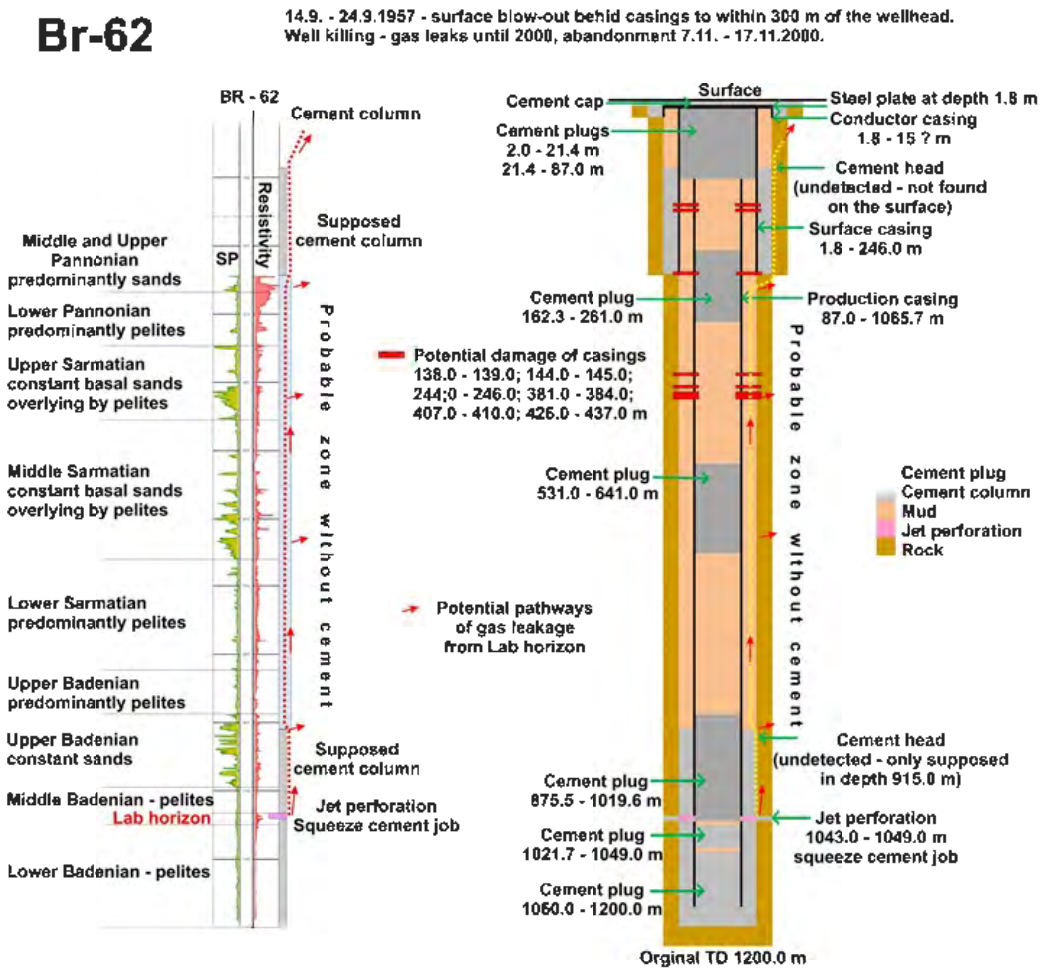

Figure 6 Well design for Br-62 in the LBr-1 field and potential leakage pathways if plugging and abandonment procedures did not result in isolation of the reservoir from the surface. Well design for Br-62 with well logs (left). Probable zone without cement is outside casing, as the cement head was undetected, but believed to be at 915 m.

Figure 7 also shows the potential pathway for a gas leak from the well, in which micro-annuli between the outer cement and the formation, both in the low and upper section of the well, could lead to gas migration to the surface. There are, as already mentioned, other possible migration paths, but the remainder of this section will only consider the illustrated leakage pathway.

5.4.2.3 Establishing input parameters

Besides the well design, the reservoir properties are relatively straightforward to establish. The values of some of the properties have been assumed for simplification. A summary is shown in Table 3.

Table 3 Summary of some of the basic reservoir properties for Br-62. Note that assumptions and/or simplifications have been made. Triangular distributions are denoted T(min., mean, max. values of the parameter).

Parameter	Value	Unit
Top depth (MD)	1043	m
Porosity	15	%
Average permeability	100	mD
Oil density	904.7	kg/m^3
Gas gravity	T(0.69, 0.71, 0.72)	-
Gas/oil ratio	35.3	Sm^3/Sm^3
Virgin reservoir pressure	102	bar
Initial pressure (time=0)	T(122,127,132)	bar
Initial temperature (time=0)	T(30,43,45)	°C
Initial oil in place	5.010^5	m^3
Initial gas in place	5.010^6	m^3
Initial water in place	5.010^5	m^3

The initial pressure (i.e. the pressure in the reservoir immediately following CO_2 injection) is an important factor affecting the potential leakage rates. The maximum pressure, according to regulations, should not exceed 30% above hydrostatic pressure. In our scenarios it is therefore 20 to 30 bar above hydrostatic with a mean value of 25 bar over.

The most important factor, however, is the micro-annuli gap size. The leakage rates are extremely sensitive to the value of this parameter. In practice, this parameter is unknown and potentially subject to large uncertainty, in particular where there is concern regarding the overall integrity of cement. While cement bond logs (CBL) or Sustained Casing Pressure (SCP) can sometimes be used to make inference on the integrity of cement barriers, these still don't translate into any meaningful expression for micro-annuli size.

Establishing a highly reliable expression for the micro-annuli gap size for a specific well, such as Br-62, is beyond the scope of this project. However, various scenarios can be established to illustrate how the expected leakage rate would vary with changing micro-annuli size. There are two approaches that can be applied to generate such scenarios:

1. Provide an explicit distribution for the micro-annuli gap size, based on some limiting range
2. Generate distributions for the micro-annuli gap size based on assumptions on effective wellbore permeability.

There is much available literature concerning micro-annuli in plugged and abandoned wells, some of which relates the micro-annuli size to an effective wellbore permeability. The effective wellbore permeability relates to the ability of the confining barriers (in this context, the outer cement and the formation wall) to allow gas migration. In Stormont et. al. (2018) such a relationship is used, assuming all wellbore permeability can be attributed to the microannulus, for particular wellbore and casing dimensions.

The relation between effective wellbore permeability and micro-annuli size is given as:

$$h = \left(12k\frac{{d_o}^2 - {d_i}^2}{4d_i}\right)^{\overline{3}} \quad [1]$$

where h is the micro-annuli size [m], k is effective wellbore permeability [m^2], d_o is the outer (wellbore) diameter [m] and d_i is the inner (casing) diameter [m].

If a further assumption is made that the relationship between cement integrity (in terms of permeability) and effective wellbore permeability are equivalent, a distribution for the micro-annuli size could be established based on expert judgment on the quality of the cement barriers. Literature, such as Fabbri et. al., 2011 and Celia et. al., 2005, can be used to state ranges for “good” and “degraded” cement (e.g. ≤10^{-20} m^2 and ≥10^{-16} m^2, respectively). The challenge would then instead be to select an appropriate probability distribution. For example, if no information at all exists on the well integrity, a uniform distribution could be assumed: For recently abandoned wells, the distribution could be weighted towards the “good” cement range, and, conversely, for older wells with questionable well integrity, towards degraded cement quality.

The process of constructing probability distributions for effective wellbore permeability has been addressed in published literature (NRAP, 2017). This approach generates bi-modal, log-normal distributions for the effective wellbore permeability, based on mean permeability and variance for a “good” and a “bad” case, and also shows example cases using “good”, “medium”, and “bad” scenarios. Once the permeability distribution is established, the micro-annuli size may be computed.

In the following subsections, a wellbore diameter of 8.6 in and a casing diameter of 6.63 in has been used as input to generate the micro-annuli size distributions. The different scenarios illustrate how the leakage rates change with varying degrees of knowledge, conditioned on specified assumptions. Note here that pressure evolution over time has not been considered, and the results are thus *initial leakage rates (time=0)*.

5.4.2.4 Microannular scenario 1

In the simplest case, an assumption is made that the effective wellbore permeability is unknown and could be anywhere in the range <10^{-20}, 10^{-12}> m^2, and that this can be assumed to follow a uniform distribution. Sampling from such a distribution and using Equation 1 to equate effective wellbore permeability into micro-annuli size, would yield a distribution as shown in Figure 9.

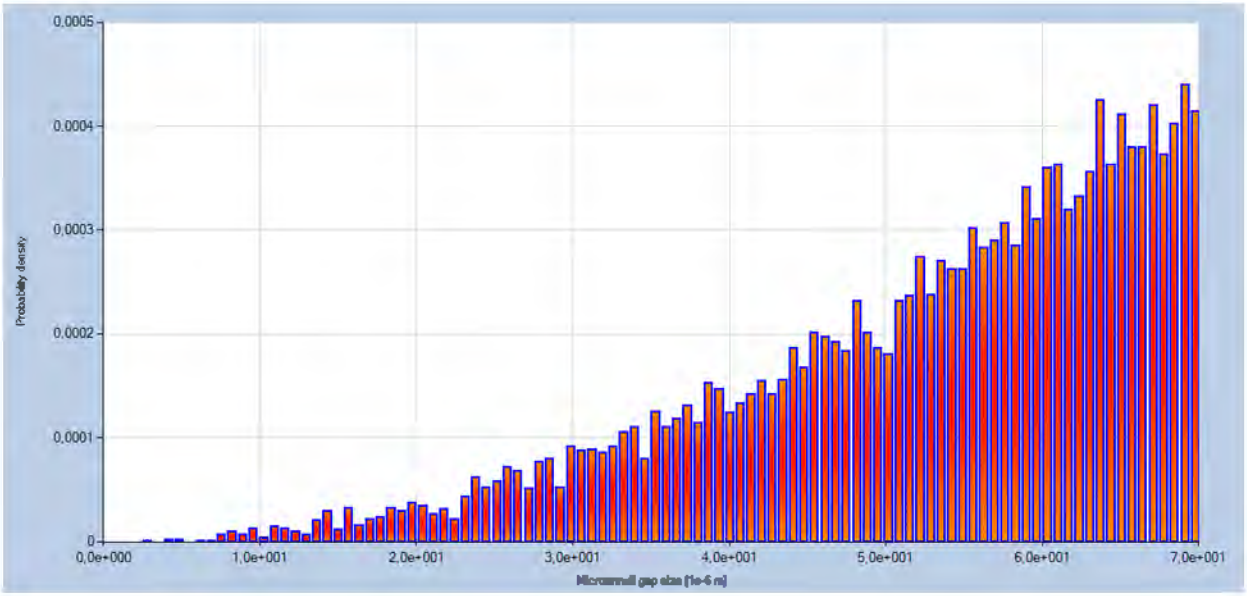

Figure 7 Generated micro-annuli size distribution, using n = 10 000, and permeability = U(1.0E-20, 1.0E-12) m^2.

As can be observed from Figure 9, a relatively large portion of the distribution would consist of relatively large (>20 µm) micro-annuli. The mean value for this particular distribution is 52.7 µm.

Using this generated distribution as a basis for modelling the leakage path shown in Figure 7, results in a leakage rate distribution as shown in Figure 10.

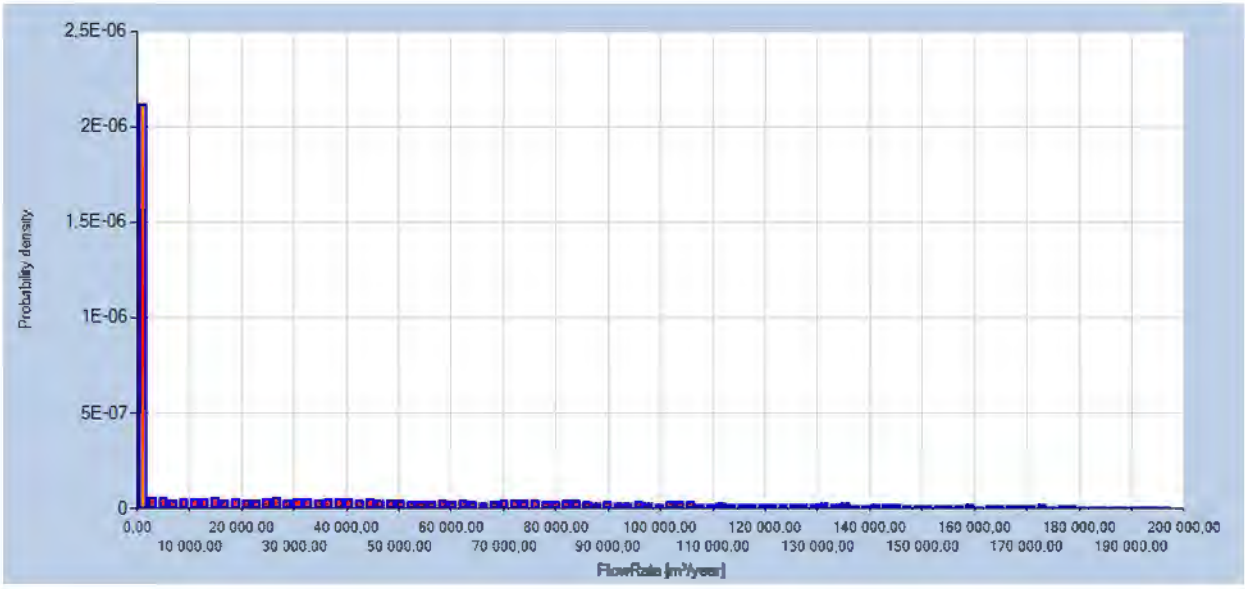

Figure 8 Simulated initial leakage rate, at surface, for Microannular scenario 1 (n = 1000). Mean = 41 867 m^3/year, P10 = 42 m^3/year, P90 = 125 747 m^3/year.

Unsurprisingly, the lack of knowledge in relation to effective permeability translates into a wide range of possible leakage rates for this scenario. At surface temperature and pressure conditions (20°C, 1 atm) this would correspond to a mean CO_2 mass flow rate of approximately 77 t/year (41 867 m^3/year), with corresponding P10 and P90 of 0.08 t/year(42 m^3/year) and 230 t/year (125 747 m^3/year), respectively.

5.4.2.5 Microannular scenario 2

In contrast to scenario 1, if it is assumed that there is some knowledge about the distribution of the effective wellbore permeability, in terms of an expert opinion about the most likely value, and likely maximum and minimum values, we could instead use a triangular distribution. For example, if, based on interpretation of data such as CBL, it is inferred that “good” quality cement is expected, but the information is still insufficient to exclude both the possibility that it may still be degraded as well as the possibility of it being better than expected. Therefore, the cement permeability distribution is based on literature data for both “good” and degraded cement (Fabbri et. al., 2011), (Celia et. al., 2005), a distribution T(1E-20, 1E-18, 1E-14) m^2 could be established. In this case, the resulting micro-annuli size distribution is as shown in Figure 11.

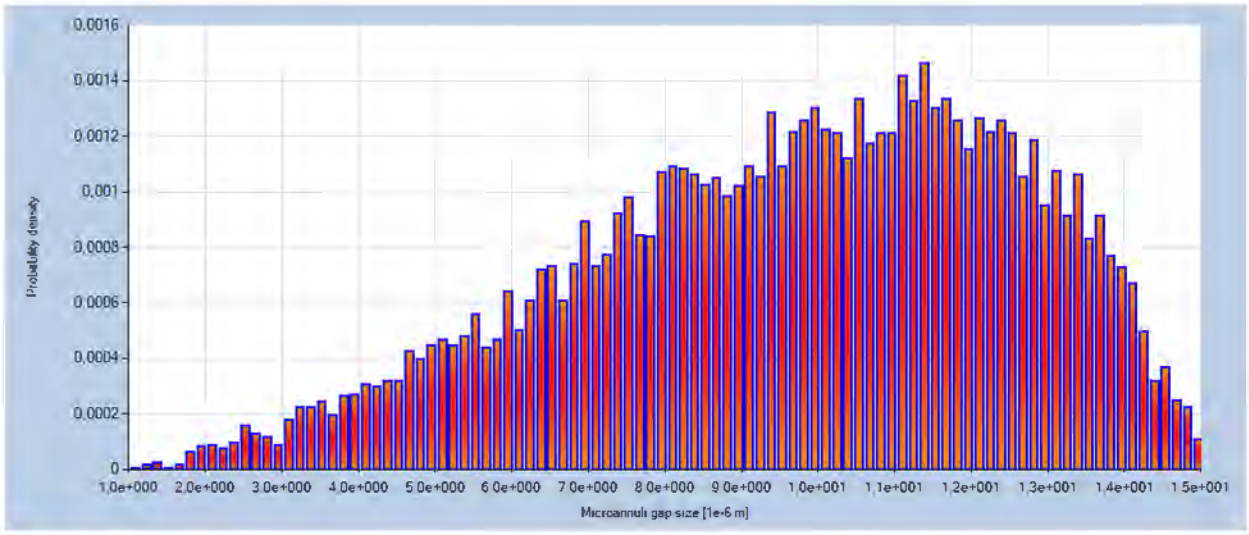

Figure 9 Generated micro-annuli size distribution, using n = 10 000, and permeability = T(1.0E-20, 1.0E-18, 1.0E-14) m^2.

Compared to Figure 9, this distribution has a significantly lower mean value, due both to the non-normal distribution biased towards lower micro-annuli values, and the lower maximum value.

Using this generated distribution as a basis for modelling the leakage path shown in Figure 7 results in a leakage rate distribution as shown in Figure 12.

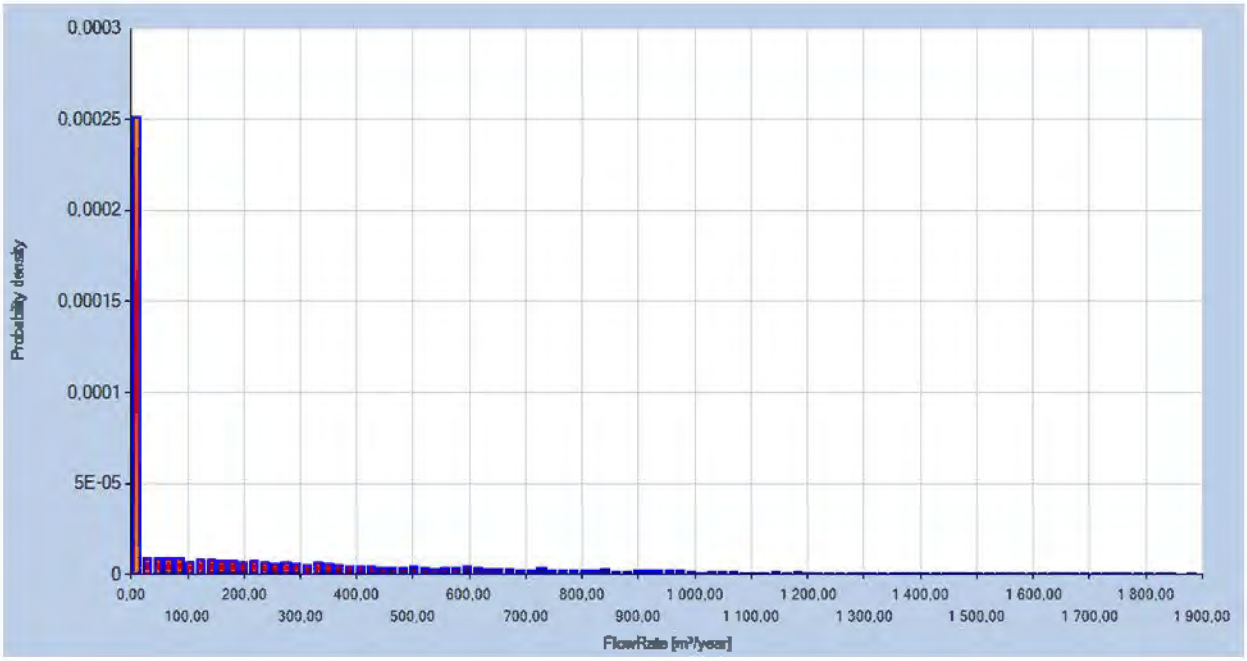

Figure 10 Simulated initial leakage rate, at surface, for Micro-annular scenario 2 (n = 1000). Mean = 247 m^3/year, P10 = 0.2 m^3/year, P90 = 799 m^3/year.

Compared with scenario 1, the range is far narrower and it can also be observed that the distribution is weighted to the left, owing to the non-normal distribution of the micro-annular size distribution for size > 7.5 µm. At surface temperature and pressure conditions (20 °C, 1 atm) the flow rates produced by this simulation would correspond to a mean CO_2 mass flow rate of approximately 0.5 t/year (247 m^3/year), with corresponding P10 and P90 of 0.0004 t/year (0.2 m^3/year) and 1.5 t/year (799 m^3/year), respectively.

5.4.2.6 Micro-annular scenario 3

In the previous two scenarios, it was assumed that one distribution could represent the effective wellbore permeability. In some cases, if sufficient data were available to distinguish wells into two or more categories based on judged well integrity (for example recently abandoned wells complying to modern P&A regulations, and older abandoned wells with questionable integrity that would not necessarily comply with modern P&A regulations), a better approach would be to have two separate distributions. These could be aggregated into one bi-modal distribution if we could assign a probability of P(recent abandonment) and P(older abandonment) based on the frequency of each category. Such an approach was performed by National Risk Assessment Partnership (NRAP, 2017), and the same approach is used for scenario 3.

In this case, it was assumed that there is a 90% chance that the well integrity is good. A lognormal distribution, with mean = -20 and variance = 2, is used to represent the case of “good” well integrity, and a lognormal distribution with mean = -15 and variance = 2 is used to represent the case of “degraded” well integrity. Under these conditions the equivalent sampled distribution becomes as shown in Figure 13.

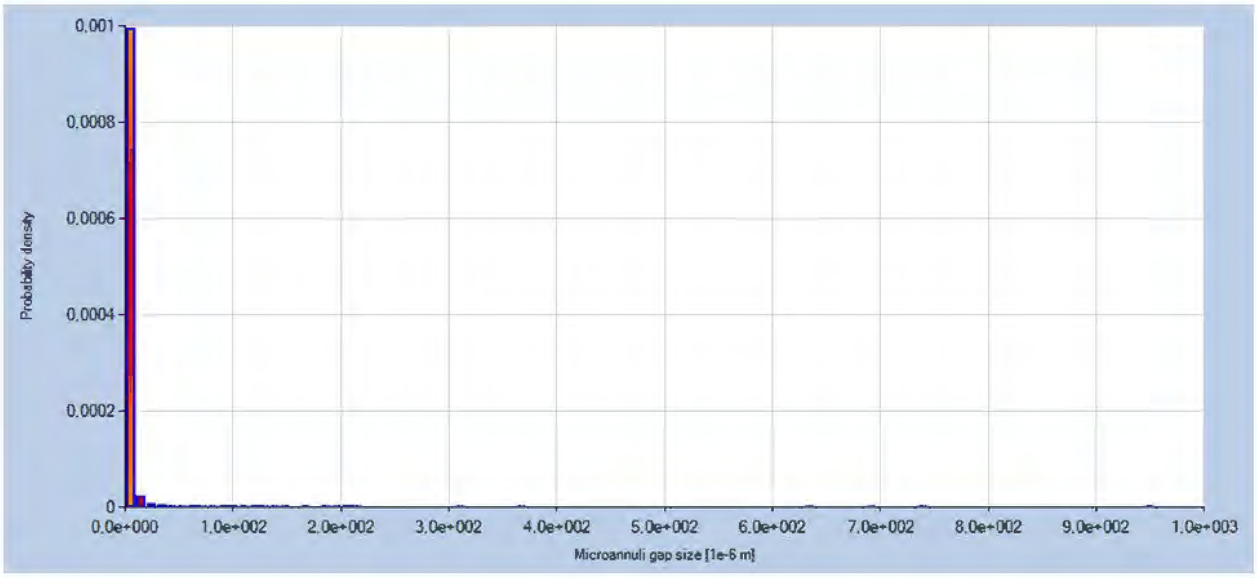

Figure 11 Generated micro-annuli size distribution based on 10,000 samples from a bimodal log-normal permeability distribution created by summing 10% of one distribution with mean -15 and variance 2, and 90% of another distribution with mean -20 and variance 2. The mean value of this distribution is 2.7 µm.

Using this generated distribution as a basis for modelling the leakage path shown in Figure 7, results in a leakage rate distribution as shown in Figure 14.

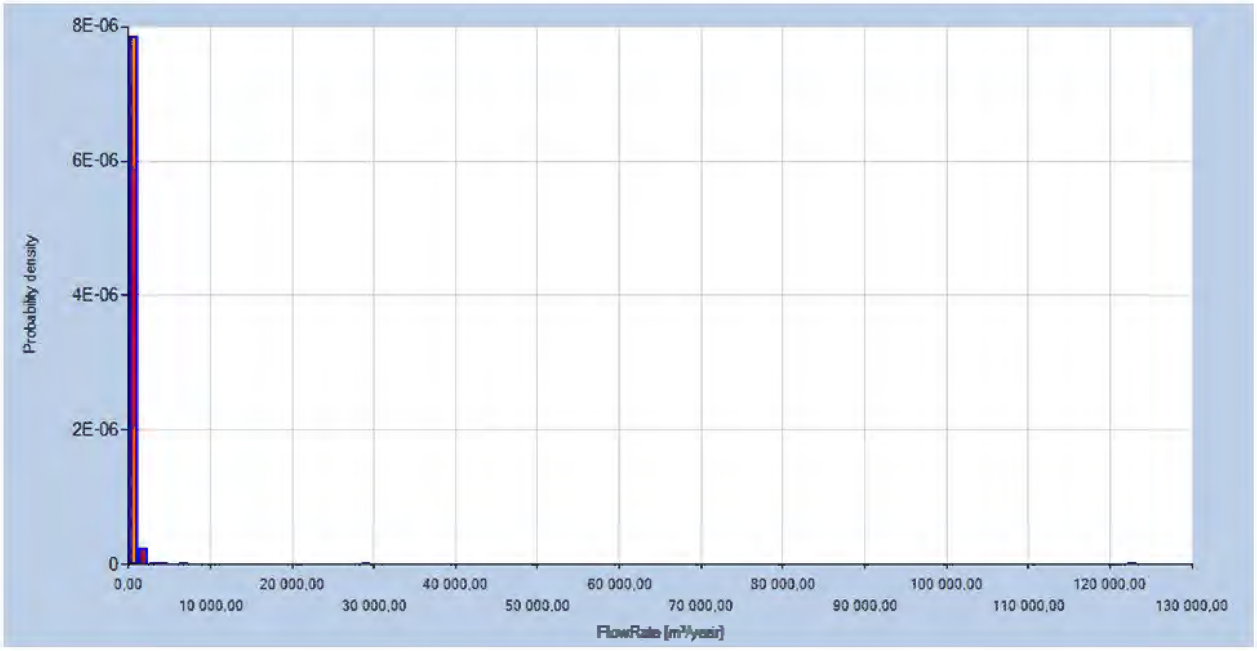

Figure 12 Simulated initial leakage rate, at surface, for Microannular scenario 3 (n = 1000). Mean = 233 m^3/year, P10 = 0.1 m^3/year, P90 = 674 m^3/year.

At surface temperature and pressure conditions (20°C, 1 atm) this simulation would correspond to a mean CO_2 mass flow rate of approximately 0.4 t/year (233 m^3/year), with corresponding P10 and P90 of 0.0002(0.1 m^3/year) t/year and 1.2 t/year (674 m^3/year), respectively. Compared with scenario 2, the interval <P10, P90> is quite similar, the difference being that due to the 10% “bad cases” distributed with a long right-side “tail” corresponding to large micro-annuli, the maximum values in the scenario are considerably larger than in scenario 2 (but still with a very low probability).

5.4.2.7 Micro-annuli scenario 4

In the final scenario for Lbr-1 well Br-62, it was assumed that information concerning the compliance with current P&A regulations of all wells on the field is known, and allows us to infer a grouping into categories “good”, “medium”, and “bad”, where “good” constitutes wells that comply with current regulatory standards that have been recently re-abandoned, “medium” are wells that have an unknown status, and “bad” consist of wells that are confirmed to not comply with regulatory standards and have not been recently re-abandoned.

The basis for the classification could be as shown in Figure 15.

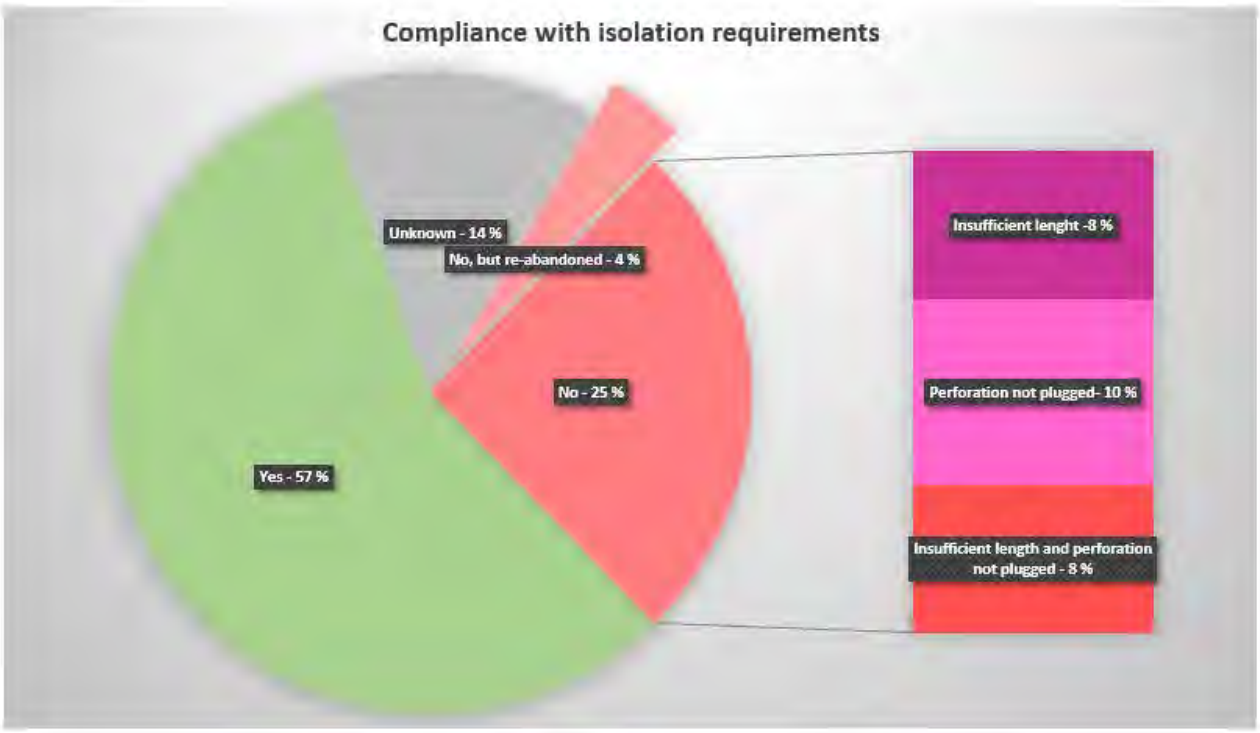

Figure 13 Example of distribution of wells in relation to compliance with regulatory P&A (isolation) standards (Ford et. al., 2016)

Using the assumption that a lognormal distribution with mean = -20 and variance = 1 represents cases with “good” well integrity, that the “medium” case is represented using a lognormal distribution with mean = -18 and variance = 1, and a lognormal distribution with mean = -16 and variance = 1 to represent the “bad” cases, and where the probability for cases “good”, “medium” and “bad” are 57%, 18% and 25% (based on Figure 15), respectively, the distribution shown in Figure 16 is produced.

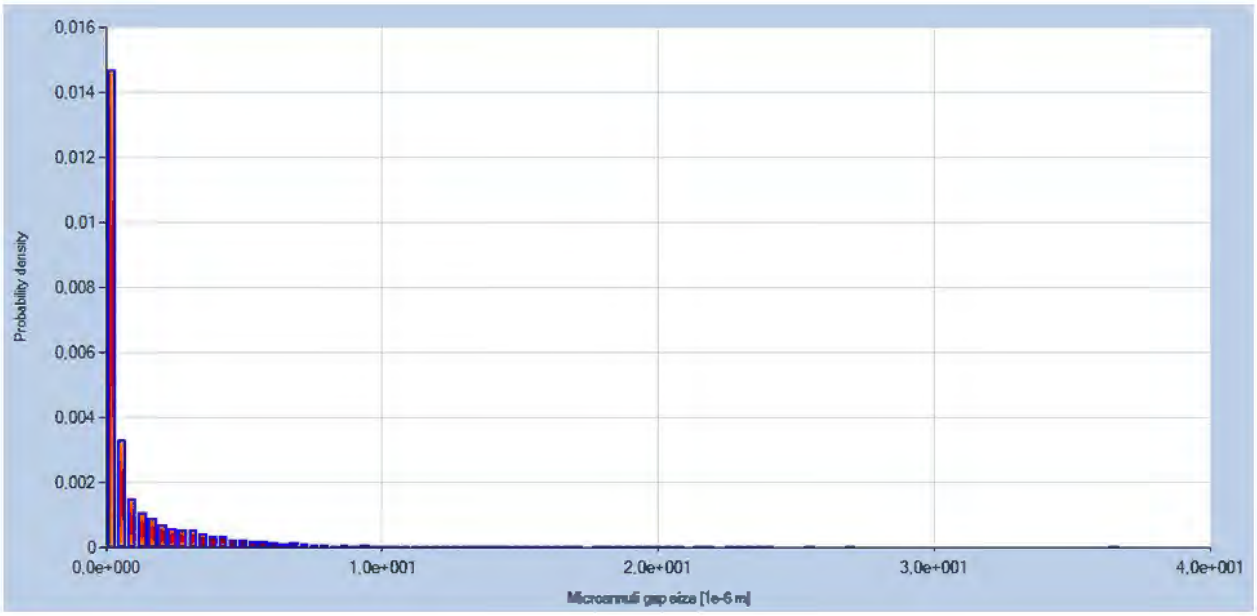

Figure 14 Generated micro-annuli size distribution based on 10,000 samples from a trimodal log-normal permeability distribution created by summing 25% of one distribution with mean -16 and variance 1, 18% of one distribution with mean = -18 and variance 1, and 57% of another distribution with mean -20 and variance 1. The mean value of this distribution is 1.4 µm.

Using this generated distribution as a basis for modelling the leakage path shown in Figure 7, results in a leakage rate distribution as shown in Figure 17.

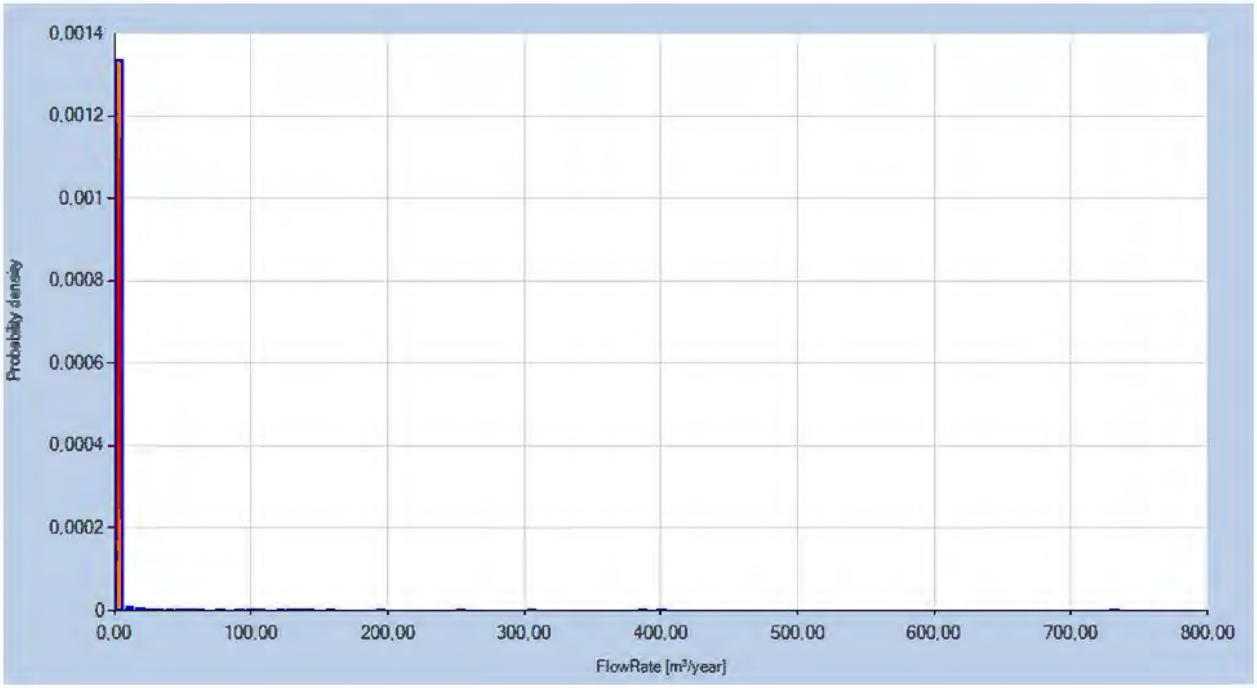

Figure 15 Simulated initial leakage rate, at surface, for Microannular scenario 4 (n = 1000). Mean = 0.2 m^3/year, P10 = 0.00001 m^3/year, P90 = 0.9 m^3/year.

At surface temperature and pressure conditions (20 °C, 1 atm) this simulation would correspond to a mean CO_2 mass flow rate of approximately 0.0004 t/year (0.2 m^3/year), with corresponding P10 and P90 of 1.8e-8 t/year (0.0004 m^3/year) and 0.002 t/yea (0.9 m^3/year)r, respectively.

5.4.2.8 Summary of LBr-1 model findings

In summary, the micro-annuli scenarios provided here indicate the sensitivity of the modelling to the assumptions made about the integrity of the P&A procedures and therefore the effective wellbore permeability. Where no or few data were available, the outcomes show a relatively high potential leakage rate (230 t/year at P90). Where it was assumed that expert opinion indicated good cement integrity, then ranges for potential leakage rates were significantly reduced as was the calculated leakage rate (0.0002 t/y at P90). It must however be stressed that the model findings are primarily meant to serve as illustrations of the importance of knowledge of barrier integrity, and that the leakage rates are strongly dependent on the assumptions in model parameters and the models themselves.

5.4.3 Getica example well

5.4.3.1 Background

The Getica CCS Demo Project was proposed for Gorj county, in Romania's South West Development Region. The South West Development Region comprises five counties: Dolj, Olt, Valcea, Mehedinti and Gorj (Global CCS Institute, 2018).

This site and wells are used as a case study for the purposes of improving the ENOS project modelling exercise by building scenarios using input from a real-world geological reservoir and wells. The results of this modelling exercise do not in any way infer that leakage would occur at these wells.

5.4.3.2 Example well and input parameters

There are far fewer data for the Getica field compared with LBr-1. The latter was the subject of a large project that aimed to establish significant amounts of data necessary for assessments (REPP-CO_2). As the objective of this report is not to perform precise risk assessments for both fields, but to provide some guidance on how risk assessments for abandoned oil & gas fields should be performed using case studies, Getica was considered as a second case study since some data were available and it is hoped that CO_2 storage will be carried out in this region. As there were fewer data, the case study for a Getica well is in large part, a synthetic case study, where well design is constructed, and some P&A design was available, but where no information was available on reservoir characteristics, nor the current status of well barriers.

The reservoir fluid parameters are therefore assumed to be similar to the LBr-1 field, although the point of inflow is for Getica set to 1207 m TVD (ca. 200 meters deeper than Br-62). A virgin reservoir pressure of 118 bar is assumed, and the initial reservoir pressure is set to T(138, 148, 154) bar. Temperature is set to 50°C, and a gas gravity of T(0.67, 0.69, 0.71) s.g. is used. The remaining differences are related to well design and P&A design. A conceptual schematic for the Getica example well is shown in Figure 18.

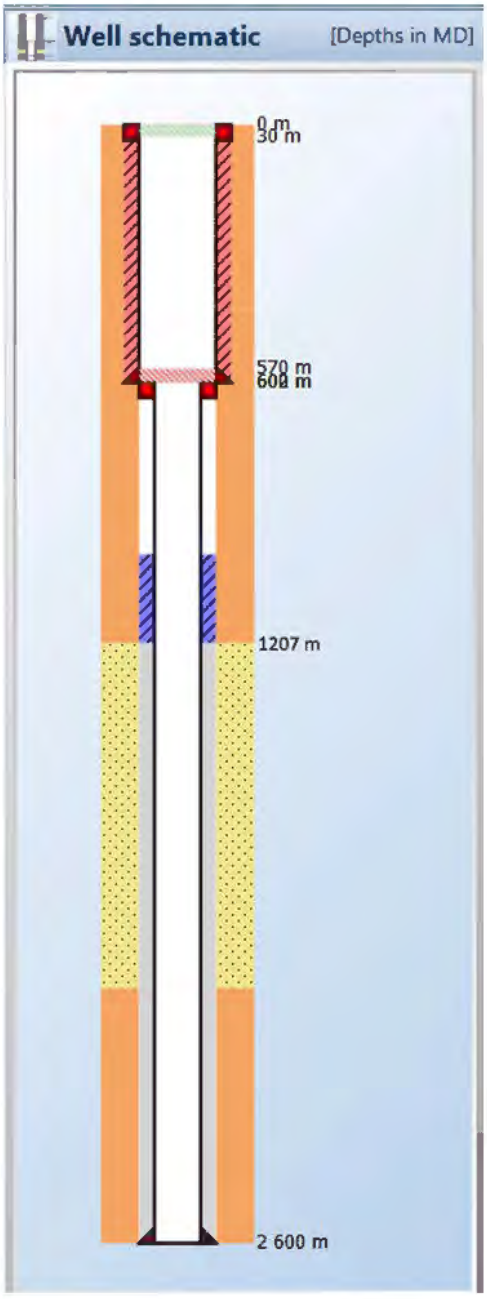

Figure 16 Conceptual schematic for a Getica example well. Potential leakage pathways are equivalent to those of Br-62, see Figure 7.

The well consists of two casings, a conductor casing with outer diameter = 10 ¾ in with casing shoe at 602 m, and a surface casing with outer diameter = 5 ¾ in with casing shoe at 2600 m. The well is assumed to be vertical, and the respective hole sizes are assumed to be 12 ¼ in and 6 ½ in. There are two cement plugs in the well, a 30 m plug at surface, and a 30 m plug with cement head at 570 m. Top of cement (TOC) for the annulus cement of the surface casing section is 1000 m.

5.4.3.3 Leakage simulations

Equivalent simulations as for LBr-1 were performed, i.e. the leakage pathways have been assumed, and the same micro-annuli size distributions have been used, see Chapters 5.4.2.4 - 5.4.2.7. The results for the Getica example well are summarized here, see Table 4.

Table 4 Summary of surface leakage rate simulations for the Getica example well. Micro-annuli scenarios are equivalent to those for LBr-1 Br-62, see Chapters 5.4.2.4 - 5.4.2.7.

Micro-annuli scenario	Leakage rates, m^3/year (t/year) P10	Mean	P90
1	0	9 662	27 995
	(0)	(17.7)	(51.3)
2	216	784	1 575
	(0.4)	(1.4)	(2.9)
3	0	131	395
	(0)	(0.2)	(0.7)
4	0	0.3	0.05
	(0)	(0.001)	(0.0001)

5.5 Monitoring wellbore leakage using pressure gauges

Installation of Permanent Downhole Gauges (PDGs) measuring pressure and temperature in real-time is one of the options for well and reservoir monitoring after the CO_2 injectors are closed. Such gauges can be installed inside the wells, close to reservoir injection point, with continuous data readout at surface through cable connections.

We studied the feasibility of leakage monitoring based on well and reservoir parameters of the LBr-1 site and capabilities of the modern PDGs provided by service companies. The main question studied here is: 'what leakage rates may be detected'?

The study was performed by simulating a single well injecting into a virtually infinite reservoir for some time, followed by well shut-in, causing pressure fall-off (Figure 19). The wellbore leakage was simulated by back producing the injected fluid at various rates, starting 500 hours after the well shut-in. The results were interpreted using Pressure Transient Analysis (PTA, Bourdet, 2002).

The simulation results show that leakage rates of two to four orders of magnitude lower than the injection rate (e.g. 0.01 to 10 cubic meter per day at in-situ conditions), will cause only minor deviations from the base-line pressure fall-off of a 'no-leakage' case (Figure 19) and may therefore be difficult to detect from conventional pressure monitoring. However, the pressure derivative (i.e. variation in pressure trend vs time - conventionally used in PTA), showed strong sensitivity to the onset of the leakage, exhibiting a clear jump in the derivative curve when the leakage starts (Figure 19). The derivative responded significantly even at a relatively small leakage rate of 0.1 m^3/D, while deviation in the absolute pressure curve is difficult to observe at the chosen scale. Therefore, analysis of pressure derivative in log-log scale may be used for leakage diagnostics.

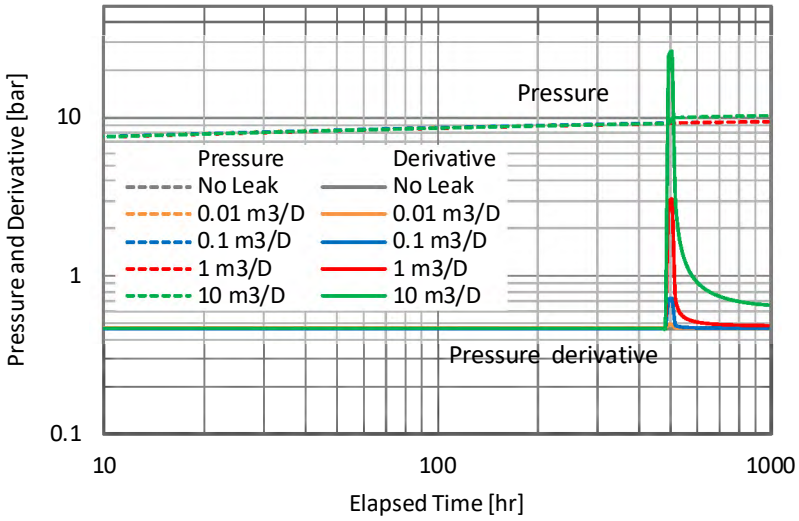

Figure 17 Log-log plot of pressure fall-off (and pressure derivative) after injection period and response to leakage of different rates (0.01 – 10 m^3/D) initiated at 500 hours after the well shut-in.

When leakage is detected from the pressure derivative monitoring, small scale deviations in pressure for the leakage period may be analysed (Figure 20). Feasibility of the leakage detection using PDGs available on the market may be further elaborated based on the pressure drawdown plot (Figure 20). The leakage initiates deviation of pressure if compared to the base-line ('No Leak') pressure fall-off response. According to specifications of PDGs (Downhole Pressure Gauges, Schlumberger, 2018), accuracy and resolution of modern PDGs are about 0.1 and 0.0002 bar correspondingly. We can see from Figure 20, that the pressure deviation caused by all the rates simulated is larger than the gauge resolution, which limits the sensitivity of pressure measurements. Taking into account the potential presence of noise in actual pressure measurements (complicating the detection of the lowest leakage rate of 0.01 m^3/D), detection of leakage with rate of 0.1 cubic meters per day and larger is certainly possible with modern gauges in the simulated case.

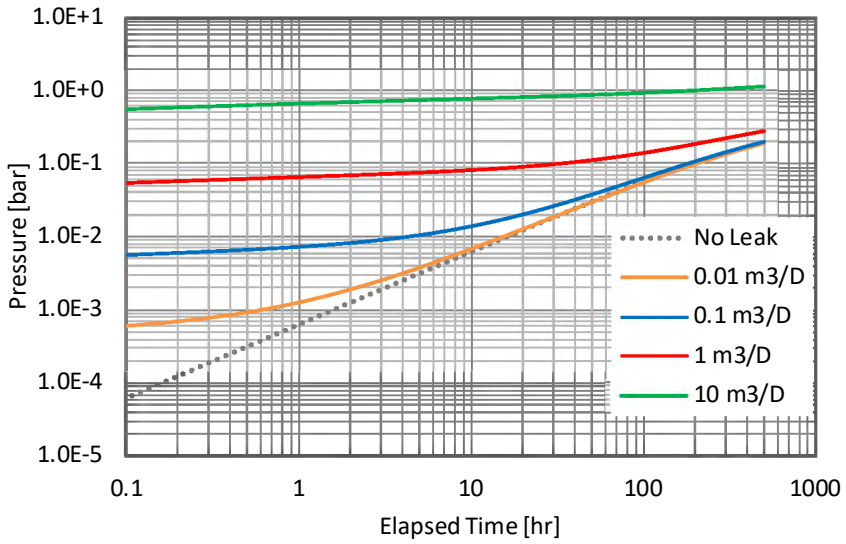

Figure 18 Log-log plot of pressure drawdown due to the leakage of different rates (0.01-10 m^3/D) and base-line pressure drawdown governed by pressure fall-off for the same period ('No leak').

The feasibility study has confirmed the capability of wellbore leakage detection with modern PDGs. Taking LBr-1 wellbore and reservoir parameters as reference, we can conclude that PDGs are capable of measuring pressure deviations due to leakage with rates starting from 0.1 cubic meters per day. Efficient leakage monitoring and leakage rate assessment may be guaranteed with proper design of well monitoring surveys (in particular monitoring of pressure derivative) and application of dedicated tools such as PTA.

5.6 Blowout assessment (injection wells)

Performing quantitative assessments of blowout potential for injection wells may also be required as part of the overall risk assessment. Such assessments are, however, more straight-forward than the assessment of leakage potential from abandoned wells, as more of the required information will be available, and there is less uncertainty related to the most important parameters. Essentially, the required input needed for a blowout analysis is the well design (specifically casing programme, tubing, trajectory), basic reservoir information (depths, fluid properties, flow potential), and probabilistic weighting related to different blowout leakage paths. The latter category proves the most challenging in terms of assessment, but can be aided by the use of databases for blowout statistics (e.g. Sintef Offshore Blowout Database (Sintef, 2018)). Software tools exist for performing blowout assessments, such as OLGA (Schlumberger, 2018) and Prosper (Petroleum Experts, 2018) (deterministic) or BlowFlow (Karlsen & Ford, 2014) (stochastic). Blowout volumes can also be derived from such calculations assuming that information concerning the kill process and reservoir evolution can be determined.

5.7 Consequence assessment

A CO_2 leak could result in emissions at surface, or into groundwater aquifers, and contamination of the surface environment and groundwater. CO_2 is denser than air at near surface conditions and tends to migrate downwards. In areas with low air flows, atmospheric CO_2 could not only build up in the atmosphere, but also in soils, particularly in hollows in the land or in deep lake water, and can potentially create higher concentrations inside buildings or confined spaces. CO_2 leakage could present differently depending on the migration mechanisms, e.g. a CO_2 leak could be fast and direct, localized or diffuse, and could be over in a few days or last for long periods of time.

At any site, a site-specific risk assessment would have identified the main vulnerable elements to be considered, i.e. the receptors of the relevant risks. General categories will include humans, animals, vegetation, water sources, ecosystems, etc. The measures by which consequences are assessed typically include impact on human health, environmental consequences and economic consequences. Similar to assessment of probabilities, a useful preliminary approach for coarsely assessing consequences is using a consequence classification scheme, an example format is shown in Table 5.

Table 5 Example of a consequence classification table

Class	Safety consequences	Operational consequences	Environmental consequences
1 - Insignificant	Medical treatment, minor health effects, first aid case, or less	0-10M USD	Small scale and short recovery time
2 - Minor	Medical treatment with restricted duty or medium health effects	10-100M USD	Large scale and short recovery time
3 - Moderate	One or more lost time workday cases or	100M-1MM USD	Short scale and long recovery time

Class	Safety consequences	Operational consequences	Environmental consequences
	significant medical treatment		
4 - Major	Permanent disability, multiple hospitalizations, or major health effects	1-10MM USD	Large scale and long recovery time
5 - Catastrophic	Fatality, Public hospitalization, or severe health effects	> 10MM USD	Large scale and long-lasting effect or permanent damage

The table can be used in conjunction with the identified leakage scenarios to highlight which consequences require further assessment. Typically, these consequences will be the risks with high probability, high consequence or both, although this selection depends on the risk acceptability within the context of the risk assessment.

5.7.1 Consequences – human health

The main risk to human health stems from a sudden and abrupt leakage of CO_2 or CH_4, resulting in serious injury or death of personnel at the injection site. For any non-abrupt leakage scenarios to pose a health threat, this would require the trapping of the CO_2 or CH_4 in a closed space to which humans were then exposed. One way to quantitatively assess the latter case, is to consider CO_2 exposure levels to humans using the calculated leakage rates as a basis and to assume that CO_2 is somehow trapped in a confined space. An example of such calculations, using a confined space of 1 m^3 and micro-annulus scenarios 1 and 4 (high and low cases) is shown in Table 6.

Table 6 Example of time to reach various CO_2 exposure levels, assuming trapping inside 1 m^3 space, for selected leakage scenarios for LBr-1 Well Br-62 (using mean leakage rates for micro-annuli scenarios 1 and 4 of 77 and 0.0004 t/year, respectively).

CO_2 exposure level [%]	Effect of exposure to human	Leakage rate [t/year]	Duration until 1 m^3 reaches exposure level
0.5	Maximum allowable concentration at workplaces	77	4 seconds
		0.0004	8.2 days
1.5	Breathing rate increases to 40% above the normal level	77	11 seconds
		0.0004	25 days
5	Breathing increases to approximately four times the normal rate, symptoms of intoxication become evident, vertigo, slight feeling of choking	77	37 seconds
		0.0004	82.5 days
10	Unconsciousness occurs more rapidly;	77	1.2 minutes
		0.0004	165 days

CO_2 exposure level [%]	Effect of exposure to human	Leakage rate [t/year]	Duration until 1 m^3 reaches exposure level
	prolonged exposure may result in death from asphyxiation		

The purpose of Table 6 is to give an indication of the relationship between the modelled leakage rates and critical CO_2/CH_4 exposure levels, for a case where the leaking CO_2 becomes trapped in a confined space. In reality, it would be unlikely for leakage from a wellbore to become trapped in a confined space in which humans were present, and would most likely escape directly to the atmosphere and be diffused by wind.

Another possible way to view the consequence of a leakage, is by considering the CO_2 dispersion. An example is provided in Figure 19, based on the high leakage rate of 77 t/year (mean value from micro-annuli scenario 1), and using using a Gaussian Plume Equation (Abdel-Rahman, 2008).

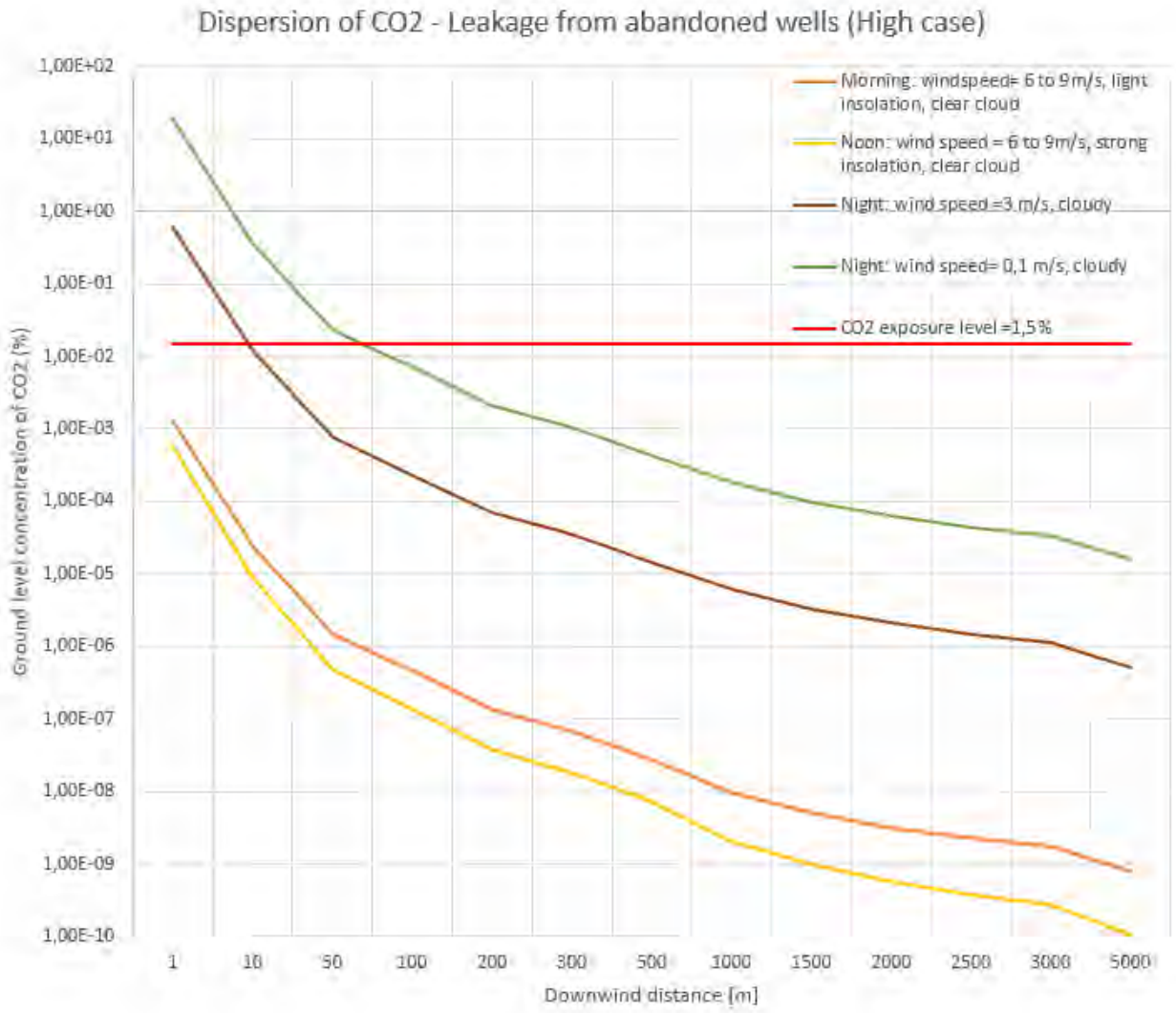

Figure 19 Example of CO_2 dispersion for a CO_2 leakage rate = 77 t/year, for varying wind conditions. Release pipe height is here assumed to be 2 m.

As can be observed in Figure 19, only under conditions with little wind and only over a limited distance (<10 m) will the CO_2 concentration levels be within a range that noticeably impacts human health. Considering dispersion and CO_2 concentration levels, for a leak to be dangerous to human health (exposure level > 5%), at say 50 m downwind distance, the leakage rate would have to exceed 5000 t/year. This leakage rate was not achieved in any of the scenarios modelled for Getica and LBr-1 in the previous chapter.

The scope of a consequence assessment could also be expanded to include similar considerations for e.g. methane, which could also pose a risk to human health and may also be present if leakage were to occur along a well that has penetrated an oil or gas field.

5.7.2 Consequences – operations

Consequences for operations can be considered in monetary terms. Wellbore leakage could prove costly due to the potentially complicated operations required to reinstate and verify wellbore integrity, such as re-abandonment of a wellbore or performing squeeze cementing. Table 7 shows some cost estimates for various re-abandonment operations, based on IEAGHG (2008). These values have been adjusted for inflation to 2018 costs.

Table 7 Cost estimates for various activities relating to mitigation and remediation of leakage from wells, based on IEAGHG (2008) and adjusted for inflation.

Main objective	Specific objective	Activities	2018 Cost	Cost unit
Location of leakage source	Locate leaky abandoned well	Survey/interpretation	117	k$/survey
	Locate leaky injection well	Diagnostic logs/management charge	352	k$/well
	Cause and source of geological leakage	3D seismic survey/processing/inter-pretation	117	k$/sqm
		Drill new horizontal well	4,700	k$/well
Well plugging	Reinforce wellbore seal	Abandonment/ Re-abandonment	12 - 41	k$/ 1000 m TVD
Well remediation	Repair well	Simple repair	35 - 60	k$/well
		More involved remediation	117	k$/well
	Construct new well	Drill new injection well	1,300	k$/ 1000 m TVD

5.7.3 Consequences – environment

Consequences with respect to the environment should consider the diversity of the receptors (animals, flora, fauna, vegetation, soil, groundwater) in the area of interest. Threshold limits similar to those for humans can be established for some species and estimates similar to those in Chapter 5.7.1 can be produced. Animals and vegetation have about the same and double the thresholds as humans, respectively. The location of abandoned wells within the area of interest is also relevant as to the level of risk it poses, and to which receptors. Environmental consequences should also consider factors such as

areas of special importance, special protection areas, biosphere reserves, ecological corridors and migration corridors for animals.

The concern for contamination of groundwater due to lack of CO_2 storage reservoir integrity could lead to leakage into shallow aquifers through lack of physical trapping and lateral gas leakage into shallow aquifers. Stratigraphic studies should be performed to show how impermeable geologic layers are distributed, and whether CO_2 can be trapped by the external low permeability/impermeable environment of the wells. Due to movement of water and dispersion, CO_2 migration can create a slow-moving plume within the aquifer. Measurements of pH, conductivity and groundwater level from local hydrogeological well(s) should be periodically performed to confirm the lack of leakage into potable water sources.

6 Cement and cement chemistry

Cements are used to keep steel well casings in place and prevent flow of liquid/gas around the annulus during drilling and the production life of the well. Cement is also employed to seal off the reservoir after the production life of a well. This is termed plugging and abandonment of wells. For reservoirs used in CO_2 storage, it is of interest to investigate the suitability of cement to maintain its integrity decades after the injection of CO_2 has ended.

Portland cement is the most popular cement used in the oil and gas industry. Ordinary Portland cement (OPC) is manufactured by heating limestone ($CaCO_3$) with some clays and quartz bearing minerals at 1400^{o}C. The resulting mixtures are ground together with small quantities of gypsum ($CaSO_4 \cdot 2H_2O$) to give a fine Portland cement powder which consists of

1. Tricalcium silicate $(CaO)_3 \cdot SiO_2$ also noted as C_3S
2. Dicalcium silicate $(CaO)_2 \cdot SiO_2$ also noted as C_2S
3. Tricalcium aluminate $(CaO)_3 \cdot Al_2O_3$ also noted as C_3A
4. Tetracalcium aluminoferrite $(CaO)_4 \cdot Al_2O_3 \cdot Fe2O_3$ also noted as C_4AF
5. Gypsum $CaSO_4 \cdot 2H_2O$ which is added to regulate the setting time of the cement

The cement is classified according to the different proportions of these constituents and the size of the powder grains. More detail about cement classification is given in Appendix 1. The cement powder is mixed with water at a given water to cement (w/c) ratio. The reaction with water leads to an exothermic hydration reaction process. The hydration process leads to the formation of the phases shown in Table 8. A brief summary of the hydration process can be found in Zhang and Bachu (2011), and a more detailed review in Lea (1998). The time taken for the hydration process to transition the mixture from slurry to an elastic solid is termed the setting time and this factor is governed mainly by the quantity of C_3A and C_3S in the cement. The C_2S in the cement is responsible for the length of time it takes for the cement to harden and the final strength of the cement. Note that when the cement slurry is set and hardens, the cement slurry often shrinks. This leaves some pores in the cement and may leave some space in the annulus. Additives (pozzolans) are often added to the OPC cement to mitigate this and improve other properties of the cement. This will, depending on the additives used, alter the ratio of the phases given in Table 8.

Table 8 Cement Phases in hydrated Ordinary Portland Cement. Adapted from Carey (2013).

Phase	Formula	Volume (%)	Notes
Calcium-silicate-Hydrate (C-S-H)	$(CaO)_r \cdot SiO_2 \cdot mH_2O$	48%	Ideal $r = 1.7$
Portlandite (CH)	$Ca(OH)_2$	19%	Most reactive to CO_2
Monosulfate (AFm)	$(CaO)_3 \cdot Al_2O_3 \cdot CaSO_4 \cdot 12H_2O$	18%	-
Trisulfate (AFt)	$(CaO)_3 \cdot Al_2O_3 \cdot 3(CaSO_4 \cdot 12H_2O)$	9%	-

Note that the liquid inside cement pores could also be an issue for CO_2 storage sites, since the cement pore water affects the reactivity of cement. During the hydration process, it is common practice to add more water to the cement. This is called curing. In laboratory experiments (Appelo 2017, Rochelle et al. 2014) the cements cores are usually cured by inserting them in high pH solutions. In that way, one is certain of the composition of the cement pore water. More detail on cement water composition used in experiments by the British Geological Survey is given in Appendix 1 (Rochelle et al. 2014). However, there are techniques for squeezing out the pore fluid left in ‘dry’ hydrated cements (Lea, 1998). Analysis of the

pore fluid shows that the composition is often alkaline NaOH and KOH and affected in principle by the period and type of storage, types of additives, water-cement ratio, and sample preparation procedure (Lea 1998). Carbonation has been reported to reduce the concentration of Na and K in hydrated cements.

Calcium-silicate-hydrates (C-S-Hs) and portlandite are the main phases in the hydrated cement. The C-S-H phases are often described as 'gels', and usually comprise nano-sized needles that fill the water space. Spaces not filled by the gels are called capillary pores and spaces in the gel itself are called gel spaces. CH phases essentially form the grains of the cement, as CH precipitates in the form of relatively large crystals, with a width of several micrometers (Lea 1998). Monosulfate (AFm) and trisulfate (Aft) phases are present in amounts that depend on the amount of C_3A and C_4AF initially present in the cement (see Table 2) and the degree of hydration.

6.1 State of CO_2

The reactivity of CO_2 with cement or rock will depend on, amongst other factors, the state of CO_2. In laboratory experiments or at certain reservoir conditions, CO_2 can exist in the following states:

- Gaseous state, which could be wet or dry.
- As liquid CO_2
- As a highly dense fluid
- As CO_2 dissolved in brine also known as carbonated water. This is the most reactive form of CO_2.

Most research into the carbonation in cement/concrete has been performed with gaseous CO_2.
Figure 20 shows the phase diagram for pure CO_2 at different pressures and temperatures. CO_2 storage sites are usually selected such that the temperature and pressure result in storage of CO_2 in its highly dense phase for maximum efficiency.

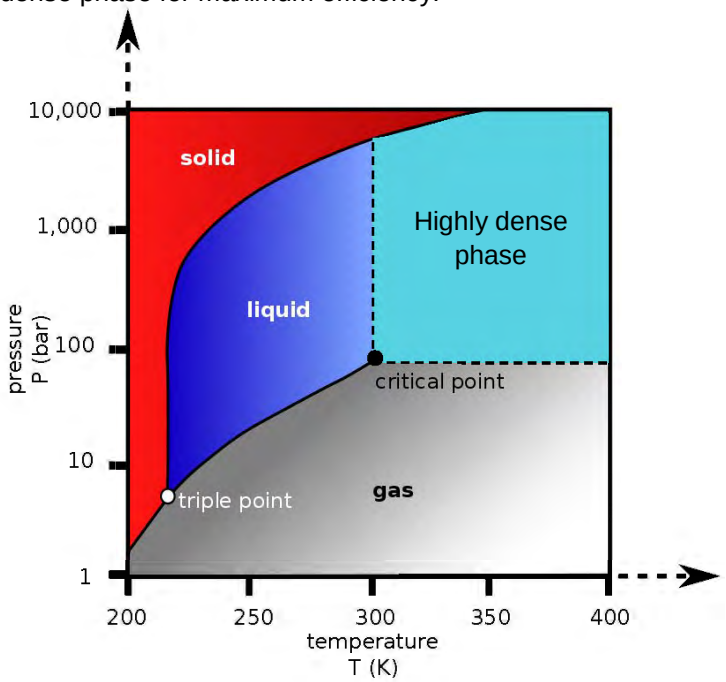

Figure 20: Phase diagram of CO_2 (Finney and Jacobs 2010).

6.2 CO_2 and carbonic acid

In the following section, the descriptions and notations described in Appelo and Postma (1999) are followed.

The solubility of CO_2 in brine is quite high relative to solubility of other gasses. CO_2 dissolves in water as shown in Eqn.[2]] forming $CO2_{(aq)}$. The $CO_{2(aq)}$ then reacts with water to form carbonic acid as shown in Eqn.[3]]

$$CO_{2(g)} \leftrightarrows CO_{2(aq)} \quad [2]$$

$$CO_{2(aq)} + H_2O \leftrightarrows H_2CO_3 \quad [3]$$

The total dissolved CO_2 at this point (which is $CO_{2(aq)}$ + H_2CO_3) is by convention denoted as H_2CO_3*. Depending on the pH of the solution, the carbonic acid can release one proton as in Eqn. [4]] to form a bicarbonate ion. At even highervalues of pH, the stable form of dissolved CO_2 is its carbonate ion as in Eqn. [5]].

$$H_2CO_3^* \leftrightarrows H^+ + HCO_3^- \quad [4]$$

$$HCO_3^- \leftrightarrows H^+ + CO_3^{2-} \quad [5]$$

$$H_2O \leftrightarrows H^+ + OH^- \quad [6]$$

The above equations, together with the dissociation of water (Eqn. [6]]), determine the distribution of forms that CO_2 will take when in contact with water.

6.3 Mineral solubility

The main phases/minerals of cements are listed in Table 8 as portlandite, C-S-H, Aft, and AFm. Other phases/minerals can exist in smaller proportions e.g. kaotite ($(CaO)_3 \cdot Al_2O_3 \cdot 6H_2O$), its ferric form ($(CaO)_3 \cdot Fe_2O_3 \cdot 6H_2O$) and in the case of incomplete hydration, some of the original cement powder components (see Table 10). The relative amount of the mineral phases may differ significantly depending on cement type, hydration process, etc. The solubility of these minerals is important as a change in the mineral composition would lead to a change in porosity, permeability and strength of the cement.

The main change with relevance to CO_2 is the portlandite phase which can be dissolved and transformed to calcite (or its other polymorphs). The decalcification of C-S-H (see equation [11]]) is also an important reaction where the Ca in C-S-H phases is consumed and may be transformed into calcite.

The components of dissolved cement phases may precipitate out as other phases that have larger molar volumes than the parent phases. If this occurs, the cement porosity and permeability will reduce. This situation is termed self-healing. A good example of this is the transformation of portlandite to calcite. On

the other hand, if there is low precipitation and the molar volumes of the precipitates are less than the original cement phases, porosity and permeability would increase. In the worst-case scenario, fractures or flow paths might be opened. Such a scenario is termed fracture opening.

6.3.1 Calcite

Calcite can undergo a dissolution/precipitation reaction as given in Eqn. [7]]. The direction of the reaction is dependent on the concentration of $Ca^{2+}$and $O_3{}^{2-}$ in solution. The concentration of these ions in solution is, in this study, determined by the amount of cement that has been dissolved or is in solution and the amount of $CO_2(g)$ that has been converted into $O_3{}^{2-}$.

$$CaCO_3 \leftrightarrows Ca^{2+} + CO_3{}^{2-} \quad [7]$$

Calcite is the main precipitation product that can be formed in cement when it is exposed to CO_2. Combining Eqns. [2]], [3]], [4]], [5]] and [7]] allows arrival at Eqn. [8]] which illustrates the dynamics of the calcite solubility processes at play. We can see that for cement healing/calcite precipitation to take place the reaction in Eqn. [8]] must move to the left, with calcite dropping out of solution to form a solid. This is favoured when there is a higher concentration of $Ca^{2+}$and $O_3{}^{2-}$ compared to the dissolved CO_2 concentration.

$$CO_2(g) + H_2O + CaCO_3 \leftrightarrows Ca^{2+} + O_3{}^{-} \quad [8]$$

The reaction can also go the right, causing calcite to dissolve. This is the case at high CO_2 concentrations.

Simulation and experimental studies have encountered zones of calcite precipitation distal (deeper into the cement) from the CO_2 source and zones of calcite dissolution close to the CO_2 source (Walsh et al. 2014, Iyer et al. 2017) as a result of reactions with minerals and pore waters within the reservoir. In practice, calcite will be precipitated in the cement at the interphase between the cement, pristine pore water, and carbonated water where CO_2 concentrations are low and precipitated calcite will be re-dissolved when the main CO_2 front arrives (Huerta et al. 2016).

6.3.2 Portlandite

Portlandite is one of the main phases of cements that is responsible for the larger grains around which the silicate gels are located. However, portlandite can be attacked in acidic environments in accordance with the reaction in Eqn. [9].

$$Ca(OH)_2 + 2H^+ \leftrightarrows Ca^{2+} + 2H_2O \quad [9]$$

In the context of cement carbonation, the reaction of Portlandite with CO_2 can be written as a combination of Eqns. [2]], [3]], [8]] and [9]] to give Eqn. [10]]. This equation describes the so-called self-healing of cement i.e. the dissolution of portlandite and subsequent precipitation of calcite. This reaction is expected to decrease the porosity of the cement, as calcite has a higher molar volume than portlandite. The decrease in porosity would likely lead to decrease in permeability of the cement. Note that very often, in simple mechanistic simulations of the carbonation reaction, it is the total hydrated CaO that is modelled as the 'portlandite' phase (Rezagholilou, Papadakis, and Nikraz 2017, Hyvert et al. 2010)

$$Ca(OH)_2 + CO_{2(g)} \leftrightarrows CaCO_3 + H_2O \quad [10]$$

6.3.3 C-S-H

The C-S-H phases as noted earlier very often have varying Ca to Si ratios, *r*, with the mean value for *r* of 1.7 and varying levels of hydration, *m*. The reaction with CO_2 can be written as in Eqn. [11]] (Carey 2013) where *y* is the degree of the carbonation, with *y* = *r* for complete carbonation. The reaction of the C-S-H for complete dissolution is given in Eqn. [12]]

$$(CaO)_r \cdot SiO_2 \cdot mH_2O + yCO_{2(g)} \leftrightarrows (CaO)_{r-y} \cdot SiO_2 \cdot (m-y)H_2O + yCaCO_3 + y\,H_2O \quad [11]$$

$$(CaO)_r \cdot SiO_2 \cdot mH_2O + 2r\,H^+ \leftrightarrows r\,Ca^{2+} + SiO_2 + (r+m)\,H_2O \quad [12]$$

6.3.4 Monosulfate (AFm)

AFm is one of the main phases of cements. This could be either Calcium-Aluminate-Sulphate-Hydrate $(CaO)_3 \cdot Al_2O_3 \cdot CaSO_4 \cdot 12H_2O$ or ,Calcium-ferrous-Sulphate-Hydrate $(CaO)_3 \cdot Fe_2O_3 \cdot CaSO_4 \cdot 12H_2O$, or some combination of the two. It can dissociate according to Eqn. [13] potentially leading to precipitation of gypsum, alumina, calcite, or Friedel's salt.

$$(CaO)_3 \cdot Al_2O_3 \cdot CaSO_4 \cdot 12H_2O + 4\,H^+ \leftrightarrows 4\,Ca^{2+} + 2Al(OH)_4^- + SO_4^{2-} + 10\,H_2O \quad [13]$$

6.3.5 Trisulfate (AFt)

AFt is another of the main phases in hydrated cement. It occurs as either Calcium-Aluminate-Trisulphate-Hydrate $(CaO)_3 \cdot Al_2O_3 \cdot 3CaSO_4 \cdot 32H_2O$ or, Calcium-ferrous-Trisulphate-Hydrate $(CaO)_3 \cdot Fe_2O_3 \cdot 3CaSO_4 \cdot 32H_2O$, or some combination of the two. The Aluminate form of the mineral is also called Ettringite and its dissolution can be given as in Eqn. [14] and can result in precipitation of gypsum, calcite, aluminate, or Friedel's salt depending on the availability of other ions.

$$(CaO)_3 \cdot Al_2O_3 \cdot 3CaSO_4 \cdot 32H_2O + 4\,H^+ \leftrightarrows 6\,Ca^{2+} + 2Al(OH)_4^- + 3\,SO_4^{2-} + 30\,H_2O \quad (14)$$

6.3.6 Friedel's salt

Friedel's salt ($Ca_4Al_2Cl_2O_6 \cdot 10H_2O$) is formed mainly as a secondary phase due to the interaction of primary phases (AFt and AFm) and brines rich in calcium and chloride at high pH (Koukouzas et al. 2017). It is highly soluble and may dissolve again after the pH of the brine has been lowered by CO_2 dissolution. Its dissolution reaction can be given as in Eqn. [15].

$$Ca_4Al_2Cl_2O_6 \cdot 10H_2O + 4\,H^+ \leftrightarrows 4\,Ca^{2+} + 2Al(OH)_4^- + 2\,Cl^- + 8\,H_2O \quad [15]$$

6.3.7 Kaotite

Kaotite ($(CaO)_3 \cdot Al_2O_3 \cdot 6H_2O$) is a mineral phase produced via the hydration of Tricalcium aluminate ($(CaO)_3 \cdot Al_2O_3$).

6.3.8 Amorphous phases

These are formed from the precipitation of the dissolution products from the reactions detailed above, and they include amorphous forms of silica (SiO_2), silicates ($Ca_xNa_{1-2x}Al_ySi_{6-y}O_{12}\cdot 6H_2O$), alumina ($Al(OH)_3$), ferric hydroxide ($Fe(OH)_3$), and iron sulphide (FeS).

Other phases can also be precipitated based on the local conditions. Such phases include brucite ($Mg(OH)_2$) and pyrite (Fe_2S).

6.4 Reaction rates

The reactions rates for the minerals listed above are dependent on pH, amongst other factors. For simulation purposes, care should be taken to implement reaction constants that are representative of a high pH (initial condition of cement) and low pH (conditions after cement is in contact with CO_2) environments as appropriate. Databases (Marty et al. 2015, Palandri and Kharaka 2004) with reaction rates at a wide range of pH values can provide the relevant data.

7 Reactivity of Cement with CO_2

A number of studies (experimental and simulation) have been carried out to investigate the reactivity of CO_2 with cements giving a broad literature database from which to start assessing the reactivity of CO_2 with wellbore cement. The two most important factors affecting the reactivity of CO_2 are the phase of the CO_2 (this would affect the dissolution of CO_2 in the cement pore water) and the transport mechanism of the CO_2 through the cement or rock surface.

7.1 Dry CO_2

If a dry gas is injected into a porous media that is saturated with brine, the gas would displace the brine until a certain critical saturation is reached such that it cannot physically displace any more brine. In addition to the physical displacement, a mass transfer of water from the brine to the gas phase would occur. This has the effect of increasing the wetness (relative humidity) of the gas and increasing the salinity of the brine.

The increasing salinity of the brine may lead to salt precipitation and to subsequent decrease in permeability and/or porosity of the porous media. Such a scenario is called precipitation due to salt dry-out. It is typical in reservoir engineering laboratory experiments of two-phase flow to use a gas phase that is 100% humid to avoid such precipitation in experiments. This is also the case far from the injector where the CO_2 has been saturated with water.

CO_2 induced salt dry-outs have been studied for reservoir rocks. But there are few studies considering dry CO_2 injection in cements with regards to CO_2 storage. Researchers from BGS (Purser et al. 2013) carried out experiments where they injected 100% humidified CO_2 into permeable cement cores initially filled with alkaline water ($Ca(OH)_2$). They reported the development of three zones in the core: a fully carbonated zone where precipitation of $CaCO_3$ and silica had taken place, a reaction front with reduced permeability, and a third zone that was largely unaffected. The depth of the reaction front in their experiment was approximately 3 cm into the cement core following injection of gaseous CO_2 at a rate of 2.125 mL/hr for about 10 days. The permeability of the cement was reduced by half of its original value after CO_2 injection. It will later be seen that the injection speed and volume are important in the reactivity of CO_2 with cement.

Others (Garrabrants and Kosson 2003, Galan et al. 2011), have investigated the effect of CO_2 relative humidity in the carbonation of cement. The authors reported that at very low humidities gaseous CO_2 can increase the dry-out of the water in the cement and reduce the dissolution of the cement because of the increased concentration of the salts in the brine. At very high relative humilities, the diffusion of CO_2 gas is limited, and condensation of water increases. This will lower the carbonation rate (Thiery et al. 2007). However, experimental evidence suggests that the carbonation of cement is fastest at a relative humidity of 50 - 70% (Ashraf 2016). In principle, if the pores of cements are completely filled with brine, the CO_2 can only permeate the cement through diffusion, provided that the entry capillary pressure is not exceeded. This will slow down the carbonation reaction. If on the other hand the pores are completely free of water, then the carbonation reaction will not proceed at all. In practice, the cement pores are only partly filled with brine. The carbonation reaction in cement pores is thus limited by the transport of CO_2 into pores. This transport/diffusion of CO_2 is affected by a huge number of variables e.g. pressure of CO_2, temperature, relative humidity of the CO_2, the water/cement ratio in the cement, the extent of carbonation, amount and types of cement phases, and the porosity/fracturing of the cement. In elaborate mechanistic simulations of cement carbonation with gaseous CO_2 (Saetta, Scotta, and Vitaliani 1998, Thiery et al. 2007), it is often assumed that the once the CO_2 has invaded the pores, then carbonation has occurred. Thus, the depth of carbonation is usually assumed to be the depth at which CO_2 invaded the cement. The depth of carbonation is often scaled with the square-root of time.

7.2 High density CO_2 and liquid CO_2

The reaction mechanisms for high density and liquid CO_2 are similar to the reactions of gaseous CO_2, with the exception that the rate of percolation of the CO_2 through the cement and the amount of CO_2 that is able to dissolve in the cement water are different. This is as a result of the higher pressures and temperatures required to form high density or liquid CO_2 phases. The reactivity of pure, dry, CO_2 is very low (see the following section for more details).

7.3 Carbonated water

CO_2 has relatively high solubility in water and, as discussed earlier, forms carbonic acid when in solution in water. In scenarios where the cement is fully saturated with water, carbonated water has a faster reaction with cement than pure CO_2 (gas, liquid or high density) (Jung and Um 2013). The majority of the experiments performed to examine the integrity of cement in CO_2 storage environments have been performed with carbonated water.

The superior reactivity of carbonated water compared to pure CO_2 phases is due to the ease with which dissolved CO_2 can diffuse from carbonated water through cement pore water compared with diffusion/entry of the pure CO_2 phase into cement.

Figure 21 shows an experiment (Kutchko et al. 2008) where the top half of a cement plug was exposed to supercritical CO_2 and the other half was submerged in brine in equilibrium with the highly dense phase CO_2. It is clear that the carbonation was much faster with the carbonated brine. The same increased carbonation by carbonated formation water was also observed in experiments by Jung and Um (2013) using class A cements.

7.4 Transport of CO_2

The rate of the main carbonation reactions are relatively fast i.e. they are faster than the rate at which reactants or products can be transported from the surface through diffusion (Kutchko et al. 2008) . This means that the carbonation rate is transport controlled, and the mechanism of CO_2 transport is be crucial to the carbonation process. The carbonation reaction considered here is the dissolution of CO_2 in cement pore water, the production of CO_3^{2-}, and subsequent precipitation of calcite.

The result of these reactions makes the rate of cement carbonation essentially a transport problem. In the reaction of carbonated water with intact cement, the early time regime is a Fickian diffusion regime and the depth of carbonation is proportional to the square-root of time. At later times, the diffusion coefficient through the carbonated cement becomes slower and slower. This results in a drop of in the rate of carbonation. In such a scenario, the carbonation depth of penetration often takes the form as shown in Figure 22, which shows rapid carbonation at a constant rate at the initial stage but a diminishing carbonation rate at later times. It should be noted that the rate of carbonation measured in experiments is very dependent on cement type, water-cement ratio and curing procedures such that the rates measured can be quite different (by a factor of 2–3) when similar experiments, but using different cement and cement preparation procedures (Jung and Um 2013, Barlet-Gouedard et al. 2006) are performed.

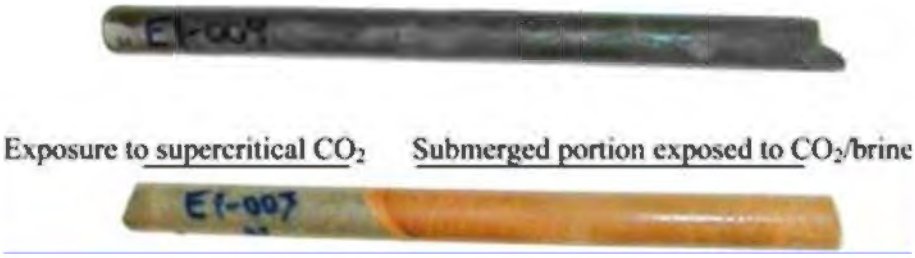

Figure 21 Picture of unreacted cement (Top) and same cement sample exposed to high density CO_2 and Carbonated CO_2. Experiments and Picture by Kutchko et al. (2008).

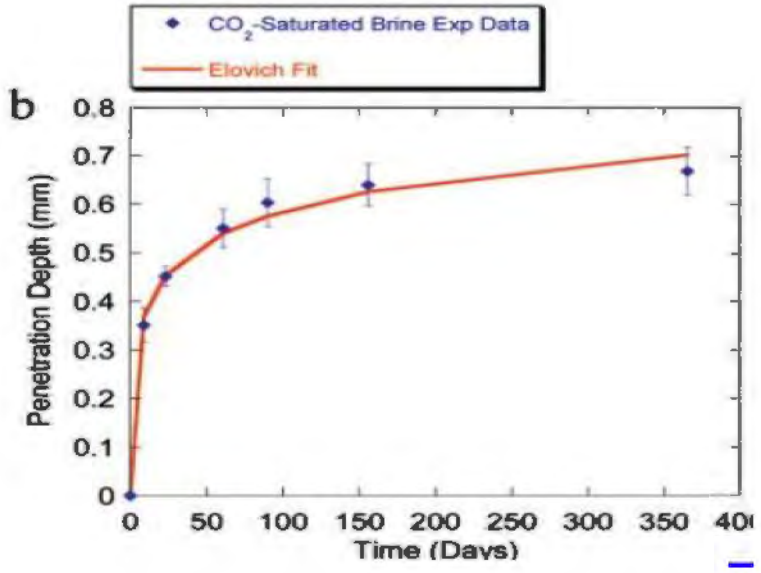

Figure 22: Carbonation depth of Class G cement with carbonated water at 50°C and 30.3 MPa in a batch-type/static experiment. Experimental data from Scanning Electron Microscope examination after the experiment (Kutchko et al. 2008).

The effect of the boundary conditions on the transport of CO_2, and hence the carbonation rate, is very important. The following scenarios could occur in terms of CO_2-cement interaction:

7.4.1 Static

A static no viscous flow situation at the cement-CO_2 boundary. This is the most likely scenario in the field-case when the cement is intact at the time of contact with CO_2. Carbonation can only take place through diffusion and will eventually cease, since the diffusive rate is much slower than the rate of precipitation of calcite. Experiments such as that shown in Figure 22 are designed to capture the carbonation rate in this scenario.

7.4.2 Constant pressure difference driven flow

A constant pressure difference driven flow situation could occur at the cement boundary. The flow could be parallel to the cement surface (such as if it occurs through fractures in the cement) or perpendicular into the surface of a permeable cement (e.g. scenario 8 in Figure 3).

7.4.3 Constant flow rate

A constant flow rate could occur at the cement-rock boundary. As for the static case, this scenario is also studied in laboratory experiments, which can be used to study the rate of carbonation. The main difference between this scenario and that of pressure difference driven flow, is that the constant pressure difference

situation is often followed by an increase or decrease in flow rate due to alteration of the cement properties. This change in flow rate leads to more/less mineral reactions which in turn accelerate the changes in flow rates (i.e. there is a feedback loop). This results in a more significant effect of CO_2 on the cement under constant pressure driven flow compared with constant rate flow. This should be noted when interpreting results from constant rate fractured cement experiments in particular, as field case CO_2 leakage scenarios are expected to be a result of constant pressure differences in fractures.

8 Fractured Cement

Fractures can form in cement and could create pathways for CO_2 leakage. The fractures described in this section include regular fractures in the cement itself, and flow paths or spacing in the annulus between the steel casing and cement or between the cement and rock formation (see Figure 3).

If CO_2 flows through a fracture, it will react with the cement surface along its path. The reaction will dissolve some components of the cement phase and precipitate out some denser, less porous and permeable phases. If the CO_2 is transported quickly enough through the fractures, such that there is limited time for precipitation reactions to take place, then a scenario could occur where more CO_2 is dissolved than precipitated. In such a scenario, the fracture size would be increased because the dissolution reaction would dominate, and, as a result, flow would increase further. If on the other hand, the transport of CO_2 is slow, such that there is time for precipitation reactions to take place, the formation of denser, less porous and permeable minerals would reduce the fracture size and could, eventually, seal the fracture altogether.

Based on the two flow scenarios mentioned above, there would be two main regimes of CO_2 flow in fractured cement; a fracture opening regime and a self-healing regime. The regime that is active would be effectively decided by a critical flow rate above which there is fracture opening and below which there is fracture self-healing. This critical flow rate can be scaled by fracture pore volume injected per unit time (inverse of residence time) and a fracture surface to pore volume ratio (or fracture aperture size). Such scaling was observed in simulations of carbonated water through fracture paths by Brunet et al. (2016), whose work is presented in Figure 23 as shown in Carroll et al. (2016). They concluded that the critical rate in fracture pore volume per minute, $\mathrm{I_c}$, above which there is fracture opening can be given by Eqn. [16], where b is the initial fracture aperture size given in micrometres. Hence, fractures with smaller apertures and longer lengths are more likely to be self-sealing at lower flow rates.

$$\mathrm{I_c} = \frac{1}{(9.8x10^{-4}b^2 + 0.254\,b)} \qquad [16]$$

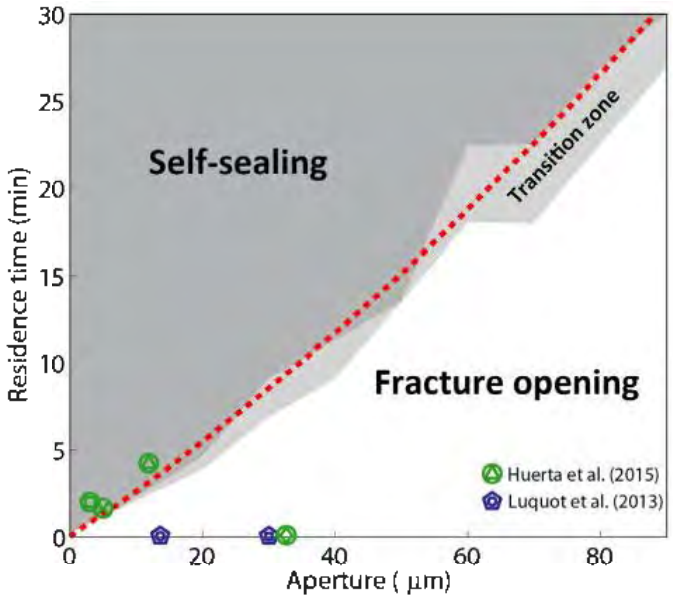

Figure 23 Regimes of self-healing and fracture opening in CO_2 fractured cement simulations (Carroll et al. 2016). Symbols are from actual fractured cement experiments.

9 Review of simulations of Carbonation

Different forms of simulation of CO_2 leakage pathways around the wellbores can be found in the literature, as summarised in this section. The following presents a brief overview of the types of simulations and scenarios that have previously been studied.

9.1 Intact Cement at abandoned wellbores: Carbonated water

In this scenario, it can be assumed that the CO_2 that is in contact with the wellbore is carbonated formation water. Gherardi, Audigane, and Gaucher (2012) studied the escape of CO_2 via carbonated water in a cement-caprock-carbonate interface using the coupled fluid flow-chemistry simulator TOUGHREACT. The only mass transfer mechanism of the CO_2 in the model was through diffusion through the cement and the caprock. The authors also considered chemical reactions of the CO_2 as it diffuses through the caprock and cement. In their model, the diffusivity was considered temperature and porosity dependent. In addition, the porosity was dependent on the changes in the mineral phases, due to chemical reactions with carbonated water. The reservoir considered in this paper was a carbonate reservoir (mainly calcite, which is in itself reactive with carbonated water). The authors concluded that there was short term porosity decrease for the first 10 years as a result of complete transformation of portlandite to calcite. After the portlandite had been consumed, they simulated an increase in porosity (though not up to the original cement porosity) from the re-dissolution of other secondary precipitated phases.

The most serious effect on the cement appears to be the effect of the caprock formation water on the cement-caprock interface. The cap-rock formation water could have some dissolved CO_2 from exposure to the surface (at earlier geological times) or through communication with gas in place. The acidity of the caprock formation resulted in dissolution of the cement over the 1000 years simulation period but the caprock formation water led to precipitation of minor amounts of calcite along the contact boundary, hence an overall porosity loss along the cement-caprock interface, as shown in Figure 25 .

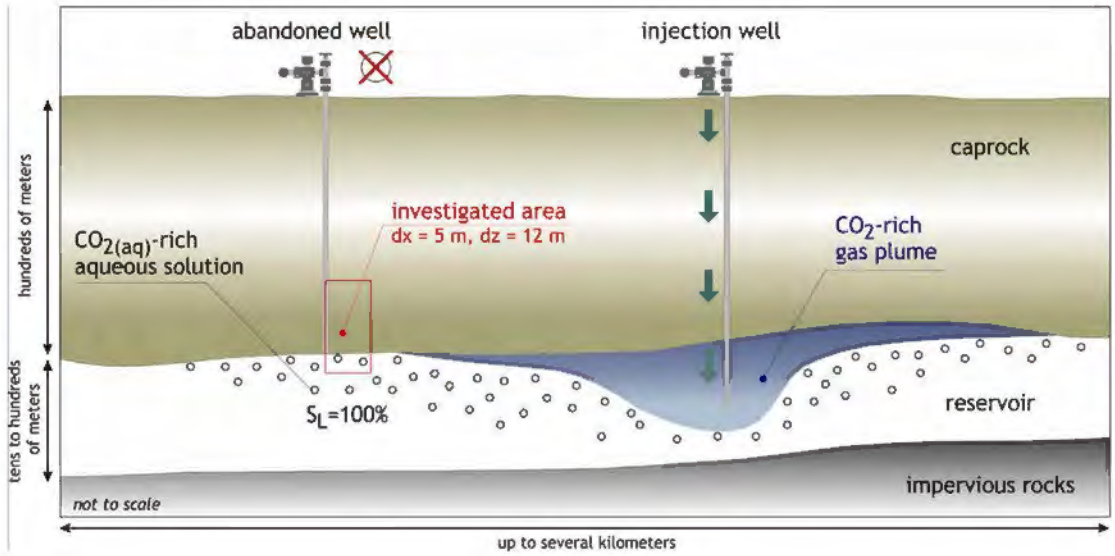

Figure 24 Conceptual model of carbonated water meeting an abandoned wellbore (Gherardi, Audigane, and Gaucher 2012)

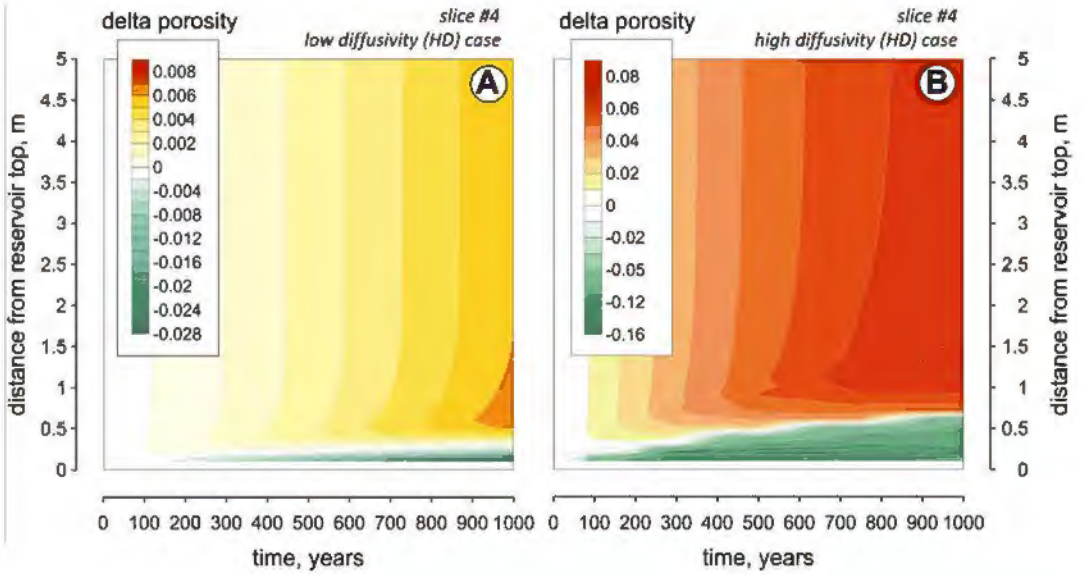

Figure 25: Simulated (Gherardi, Audigane, and Gaucher 2012) porosity evolution at the cement-caprock interface at specified distances from reservoir top. Scenario A: low diffusivity assumed and Scenario B: High diffusivity assumed. Porosity decrease from CO_2 carbonated water influx into the cement. Porosity increase from caprock-formation water influx into the cement.

Other studies (Koukouzas et al. 2017) have investigated the reactive transport of carbonated water in hydrated cement, largely at the mm scale. These 1D simulations usually consider the diffusion of carbonated water into the cements and subsequent reaction with the cement. These simulations often report the development of reaction zones; an outer zone with complete dissolution of portlandite and C-S-H phases, an intermediate zone of predominantly calcite precipitation, and an inner zone of largely unaltered cement.

9.2 Intact Cement at wellbores: gas/high density CO_2

This scenario is similar to that shown in Figure 24, but with the free phase CO_2 front, rather than dissolved CO_2 front, meeting the abandoned well. A similar situation could also occur at the injection well. As stated earlier, the cement can be assumed to be 100% saturated with cement pore water. This will enable the CO_2 to attack the cement only through diffusion (which will result in a similar scenario to that described in Section 10.1) and through the physical displacement of water. The physical displacement by CO_2 of water from the cement requires that the pressure in the CO_2 exceeds the entry capillary pressure in the cement.

Carey and Lichtner (2011) studied the imbibition of high density CO_2 into cements due to a difference in capillary pressure between the cement and reservoir rocks or shale caprock. They concluded, from their numerical study, that the high density CO_2 will not flow through intact cement, and that the dominant leakage pathways are gaps along the interface between the cement and cap-rock/casing.

9.3 Fractured cement at wellbore

Flow through fractures/micro-annuli, or other flow-paths along the wellbore, constitute the most likely pathways for CO_2 leakage. Other studies have investigated the flow of CO_2 in *the form of carbonated water* through such pathways (Huerta et al. 2014). It is concluded that the transformation of cement phases to other precipitated phases may in fact reduce the porosity and permeability of the pathways depending on the residence time of the carbonated water in the fracture.

An identified gap in the currently available literature is, therefore, a study of the reactivity of cement phases when in contact with high density or gaseous CO_2 in the fractures.

10 Simulation of cement/CO_2/brine interaction during CO_2 leakage through wellbore interface path-ways

The aim here is to use a simulation tool (CMG-GEM) to investigate the flow of high density CO_2 through pathways around the cement. The focus here is on the micro-annulus spacing between the cement and the reservoir/cap-rock. It is of interest to study the self-healing of cement under conditions closely related to the LBr-1 injections. It is again stressed that the aim here is to demonstrate the use of simulator tools to model the self-healing of cement by CO_2, rather than to model a specific case, since the parameters are expected to vary for each well.

10.1 The base-case model

In order to simplify LBr-1 injection scenario, it was necessary to create an idealized cartesian 2-D model to represent a vertical cross-section of the cement-rock interface (Figure 26). The rock section is further divided into four layers (a top, water-filled, aquifer, a low permeability aquifer, a main reservoir section with mainly high density CO_2 and residual water saturation, and an underlying aquifer filled with water). The model uses volume modifiers to simulate the condition of constant pressure difference between the top aquifer and the main reservoir. The volume modifier for the top aquifer is placed on the right-most cell of the top aquifer and that of the main reservoir is placed on the top-rightmost cell of the main reservoir section.

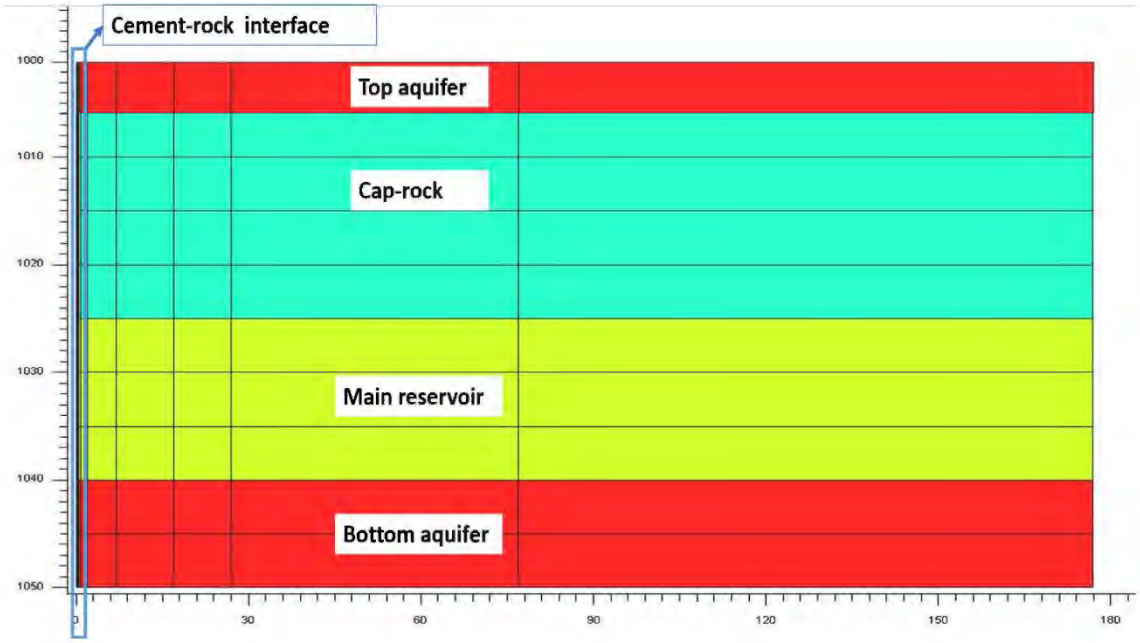

Figure 26: Cross section of the geo-model showing the cement-rock interface, top aquifer (5m thick), cap-rock (20m thick), main reservoir section (15 m thick) and bottom aquifer (10 m thick). Volume multipliers are used in the right end of the top aquifer and main reservoir to simulate constant differential pressure conditions between the top aquifer and main reservoir.

10.2 Fracture in cement-rock interface

The cement interface is modelled as shown in Figure 27. The fracture cells are modelled as a high permeability linear feature, with a mix of fracture permeability and cement matrix permeability. The fracture

permeability is modelled as a permeable rectangular tube with aperture size, b and width, w. In the base-case simulation, the fracture permeability is estimated to be $2x10^5$ milliDarcy based on a fracture aperture of 50 µm and the fracture width of 0.7 m, which is approximately equal to the circumference of a 9.625 inch casing. The cement matrix in the fracture cell is modelled to be 95 mm. The implication of this is that the CO_2 in the fracture has a reaction depth of 95 mm into the cement matrix.

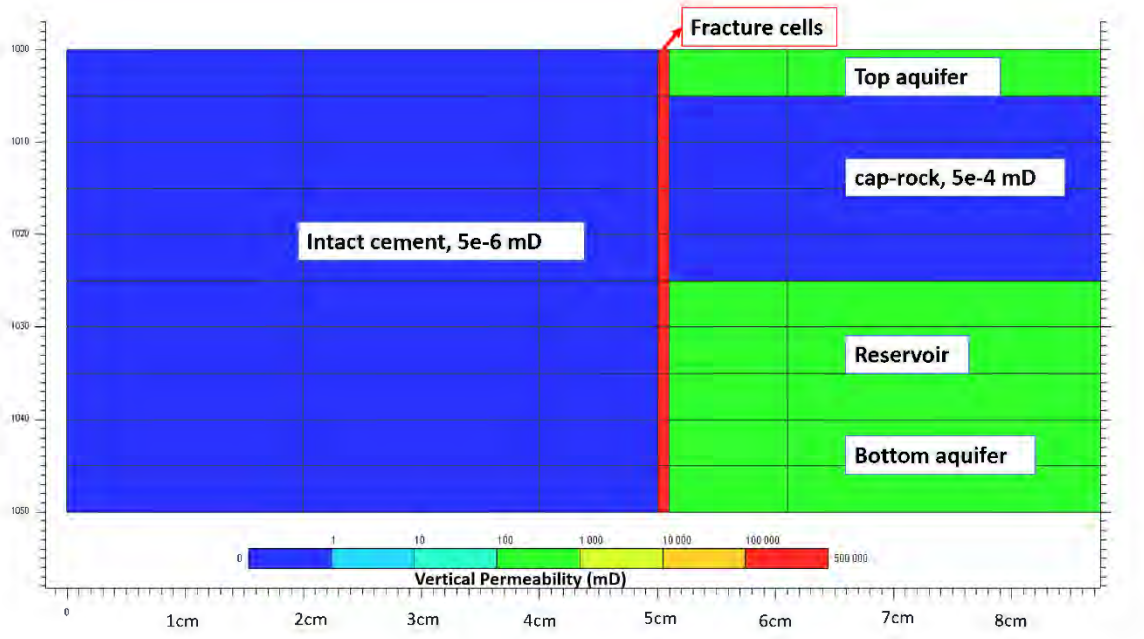

Figure 27: Cement-rock interface. The figure has strong horizontal exaggeration so that the x-axis is in cm and the z-axis is in meters.

10.2.1.1 Geochemistry

Implementation of the geochemistry was performed in the CMG-GEM simulator with the Geochem V2 option. The cement phase is represented by portlandite ($Ca(OH)_2$) since it is the most reactive phase. The conversion of portlandite to calcite (see equation [10]) was implemented as the reaction responsible for CO_2 cement healing. In addition, the formation of the aqueous CO_2 chemistry was also implemented with equilibrium constants for equations [2]-[6]. The reaction rate constants for portlandite and calcite dissolution and precipitation were sourced from literature (Palandri and Kharaka 2004). The initial portlandite concentration of the cement was assumed to be 40% of the cement volume.

Other properties of CO_2 and/or water, such as the solubility of CO_2 in water with varying pressure, viscosity of CO_2, density of CO_2, etc., were modelled with CMG's WINPROP.

10.2.1.2 Porosity-permeability correlation

As stated earlier, the molar volume of calcite is greater than the molar volume of portlandite. A conversion of portlandite to calcite will therefore reduce the porosity of the cement phase. This porosity reduction should lead to a reduction of the permeability of the cement/fracture. The relationship between the porosity and permeability is modelled in CMG-GEM by a Kozeny-Carman type formula (eqn. [17]).

$$\frac{K_2}{K_1} = \left(\frac{\phi_1}{\phi_2}\right)^n \left(\frac{1-\phi_2}{1-\phi_1}\right)^2 \qquad [17]$$

Where K_1, ϕ_1 and K_2, $\phi_2$are permeability and porosity at the previous and current time-steps, respectively. The n-exponent is a design criterion in the model which was designed to give intact cement permeability when the porosity of the intact cement is reached at the fracture cells. Other important model properties are given in Table 9.

Table 9: Important properties of the base-case model.

Properties	Values	Comments
Dimension (nx, ny, nz)	15, 1, 10	
Dx _cement (cm)	2, 2, 1	
Dx_ fracture cells (mm)	1	5% of cell consist of open fracture
Dx_rocks (m)	0.01, 0.05, 0.1, 0.1, 0.5, 1, 5, 10, 10, 50, 100	
Dy (m)	0.768	Circumference of 9.625 inch casing
Dz (m)	5	Constant Dz, top depth at 1000m
Cement porosity	0.18	
Fracture cell porosity	0.22	
Rock porosity	0.18	
Cement permeability (mD)	5E-6	
Fracture cells perm. (mD)	2E5	Vertical permeability
Aquifer & reservoir perm. (mD)	500	
Cap-rock perm(mD)	5E-4	
Volume modifiers	1E4	
Main reservoir saturations	Sw = Swr =0.2; Sg = 0.8	Everywhere else has Sw= 1
Main reservoir Pressure	20 bar overpressures	Everywhere else has hydrostatic pressures
Cement composition	40% portlandite	Trace composition of calcite in other sections
Distance between top aquifer and main reservoir (m)	20	This is the fracture length

10.3 Results of base-case model

The model was first used to explore the leakage rate into the top aquifer, ignoring healing of the cement due to contact with CO_2. It is observed that the leakage rate is highly dependent on the horizontal permeability of the fracture. The horizontal permeability of the fracture limits the flow rate, such that the lower the horizontal permeability, the lower the flow rate. The leakage rate for the base-case model (with high horizontal permeability) in the fracture is given in Figure 28. The figure shows the migration of CO_2 through the fractured cells from the main reservoir to the top aquifer. The leakage rate is approximately 270 Kg of CO_2 per day. It is stressed that the estimate is based on a worst-case scenario combining an over-pressure of 20 bar, a high fracture aperture of 50 µm and a very short fracture length/cement section of 20 m.

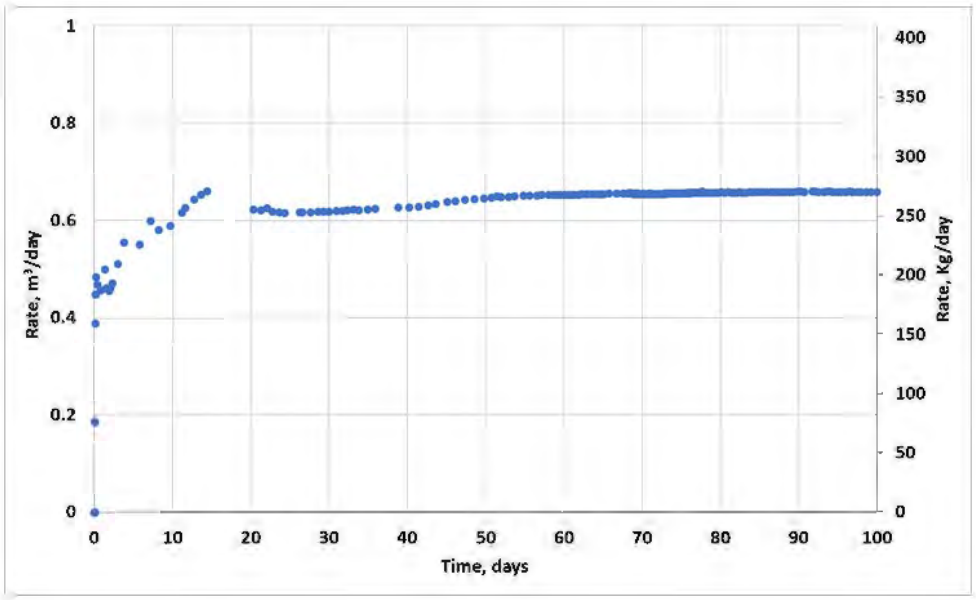

Figure 28: CO_2 Leakage rate into the top aquifer for the base-case model

10.4 Results of simulations including self-healing of cement

In this scenario, low horizontal permeability in the fracture is considered, i.e. there is limited communication between the fracture and the reservoirs. This situation is easier for the model to simulate and is more numerically stable. The leakage rates of CO_2 into the main aquifer when the chemical reactions are set to zero and when chemical reactions are simulated are both shown in Figure 29. It is observed that the chemical reactions reduces the leakage rate as a result of the closing/healing of the fractures.

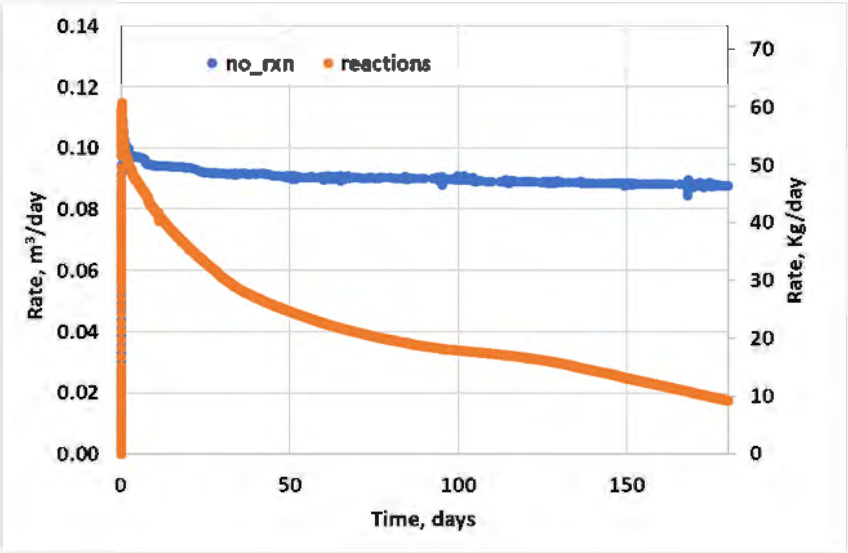

Figure 29: CO_2 Leakage rate into the top aquifer for a no chemical reaction scenario (blue dots) versus a chemical reaction scenario (orange dots) for the model with low horizontal fracture permeability. The inclusion of chemical reactions reduces the rate of the CO_2 leakage as the chemical reactions seal the fracture.

11 Risk evaluation

Risk evaluation involves comparing estimated levels of risk with the risk criteria defined when the context for the study was established, in order to determine the significance of the level and type of risk (ISO/IEC 31010:2009).

The challenge of this phase is often the determination of what is acceptable, and how this can be accomplished, especially considering what, if any, leakage rates are acceptable. To begin with, as the source of the leakage stems from abandoned wellbores, ensuring compliance with existing requirements for P&A is a necessity. Mapping of all abandoned wells and performing a review of the data on these wells versus the requirements is a good first step (typically, requirements concerning length and testing of cement plugs and cement annulus, cement height above perforations, etc. are considered.). However, even if all abandoned wells comply with existing regulations, the risk analysis will provide simulations of potential scenarios where the leakage rate is > 0, and the question then becomes how high can the potential leakage rate be before it is considered unacceptable?

11.1.1 Risk acceptance criteria

There are different approaches to establishing risk acceptance criteria for plugged and abandoned wells. Three such approaches are briefly mentioned here. These are:

1. Well consistency criterion
2. Environmental criterion
3. As Low As Reasonably Practicable (ALARP)

The well consistency criterion consists of three main steps:

1. Select a reference level, e.g. NORSOK D-010, or the prevailing standard relevant to the field in question
2. Choose a barrier system as prescribed in the standard and establish a “worst case” scenario
3. For any well that is subject to the same reference level as chosen in step 1., calculate the leakage probability and leakage rate and compare with the reference level.

A conceptual plot for such a comparison is shown in Figure 30.

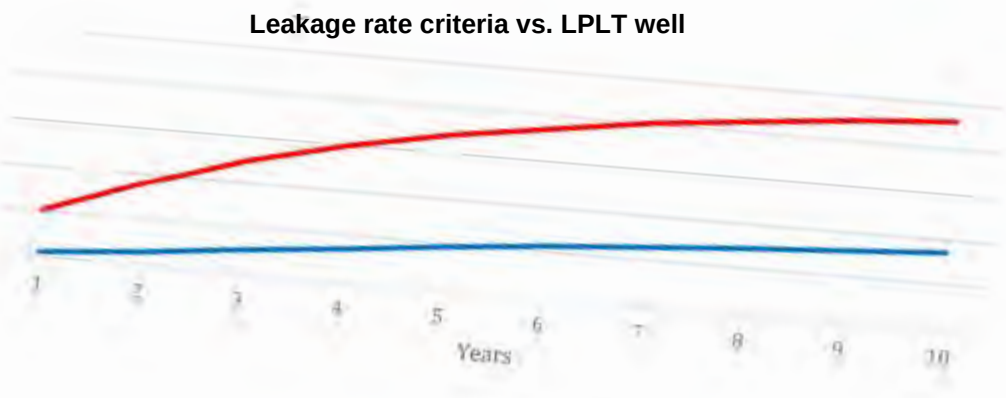

Figure 30: Probability weighted leakage rate comparison for the well consistency criterion (Arild, 2018). Red = Weighted leakage rate reference well; Blue = Weighted leakage rate

The duration for comparison should be aligned with criteria specifying the lifetime of the wells or field. In some cases, requirements for use of the site from an “eternal” perspective could translate into very long durations for practical purposes.

The environmental criterion presumes that the point of reference is natural seepages of gas. Instead of using a constructed reference case, the simulated leakage rates could be compared to flux rates for the area of interest. Alternatively, comparisons could be made with other natural geological CO_2 seepage sites worldwide. According to the DOE (2007), CO_2 leakage rates for sedimentary basins varies between 1.44e-4 to 169 µmol/m^2-s, which also concludes that most such sites have leakage rates below the average soil respiration rate.

Finally, the ALARP approach consists of three main steps:

1. Choose the limit for the “red” region. This could, for example, be the environmental (health) criterion.
2. Choose the limit for the “green” region. This could, for example, be the consistency criterion.
3. If the (probability weighted) leakage rate is in the ALARP region, re-evaluate the P&A design.

The approach is illustrated in Figure 31, using a synthetic case as an example.

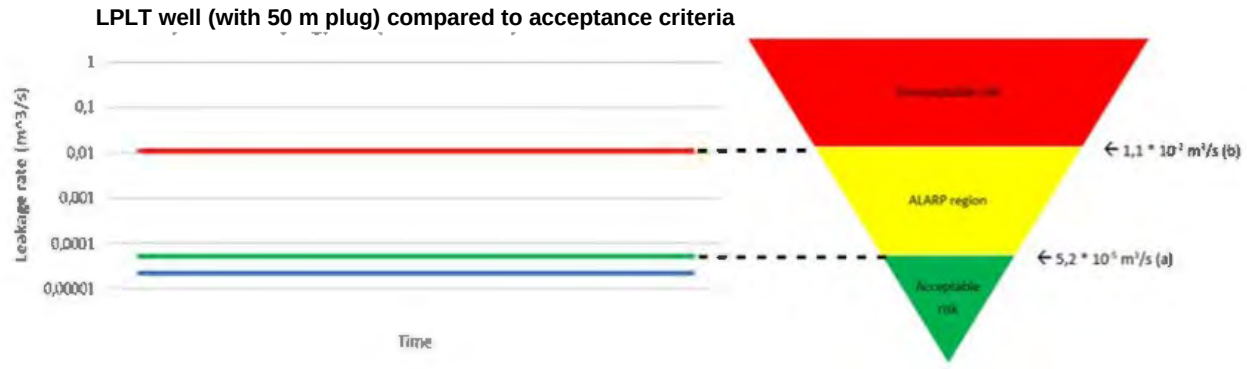

Figure 31 Synthetic example well illustrating the ALARP principle (Arild, 2018).
Red = Environmental risk acceptance (natural seepage)
Green = Consistency between wells (NORSOK req.)
Blue = Average leakage rate

11.1.2 Monitoring measures

The risk evaluation should also outline recommendations on measures that either reduce the probability of a risk occurring or reduce its consequences. Some examples of recommendations for confirming the site is conforming are provided below (Ford et. al., 2016):

- Use of sonic logging tools to monitor possible degradation of cement sheath and tubing due to exposure to CO_2. This is primarily for use in the monitoring wells but could also be done for wells that are going to be re-abandoned.
- Wireline logging of injection and monitoring wells.
- Sensors for continuous measurement of wellhead and downhole pressures and temperatures.
- Use of gas analysis at the compressor and at the injection facility, to avoid injection of contaminated CO_2 (e.g. containing H_2S or other harmful agents).

- Use of atmospheric gas measurements to detect changes in surface concentrations of CO_2 and CH_4, resulting from e.g. leakage along abandoned wellbores or through the caprock. This can be achieved through closed- or open-chamber soil CO_2 flux monitoring, one-way vent-based CO_2 flux detection, or eddy covariance-based CO_2 flux monitoring.
- Use of microseismic monitoring should be considered, such as accelerometer, hydrophone, or geophone arrays, in monitoring wells, to ensure that injection pressure stays below the levels that induce seismicity, to control caprock seal integrity and fault behaviour.
- Use of soil gas surveys to obtain gas measurements at fixed locations around injection wells, as indicator/warning for elevated levels of CO_2 and CH_4.
- Annual ground water sampling and chemical analyses to reveal any potential contamination.
- Prioritized locations for permanent soil gas flux and atmospheric measurements, which should be selected based on the main findings from the risk assessment

11.1.3 Overall evaluation

Once the identified and analysed risks have been reviewed in light of the chosen decision criteria, taking into consideration the available preventive and mitigative measures, an overall summary should be prepared. This could typically be carried out using e.g. a risk matrix, as shown in Figure 32. Not only should proper documentation of the risk assessment process be provided to decision makers, but the document should also state risks that require further treatment, prioritized task lists for treatment, and plans for follow-up. The main recommendations of the assessment should be clearly stated, including which assumptions have been made, the limitations of the review and the uncertainties influencing the recommendations. Based on the EU Storage Directive (and supporting guidance documents), all CO_2 storage sites will have a monitoring plan including liability, obligations, and corrective measures, that must be actioned if there are any indications that the storage site is not responding as anticipated to the injected CO_2, as well as a plan for mitigation and remediation.

Consequence / Probability		1 - Insignificant	2 – Minor	3 - Moderate	4 - Major	5 - Catastrophic
	Safety	Medical treatment, minor health effects, first aid case, or less	Medical treatment with restricted duty or medium health effects	One or more lost time workday cases or significant medical treatment	Permanent disability, multiple hospitalizations, or major health effects	Fatality, Public hospitalization, or severe health effects
	Operational	0-10M USD	10-100M USD	100M-1MM USD	1-10MM USD	> 10MM USD
	Environmental	Small scale and short recovery time	Large scale and short recovery time	Short scale and long recovery time	Large scale and long recovery time	Large scale and long-lasting effect or permanent damage
1	Improbable	< 10^{-6}	Leakage through faults, fractures Leakage into aquifer			
2	Remote	10^{-6} – 10^{-4}	Leakage from an active well to atmosphere		Blowout from an active well	
3	Rare	10^{-4} – 10^{-3}	Leakage from an abandoned well to atmosphere			
4	Probable	10^{-3} – 10^{-2}				
5	Frequent	> 10^{-2}				
	Acceptable area, low level monitoring, unless the risk level changes					
	Acceptable area if the benefits are significant, monitor and be prepared for further measures					
	Acceptable if risk reduction is impracticable or costs is relatively large compared to the risk reduction achieved by the measure					
	Unacceptable area, need injection stop, corrective measures					

Figure 32 Example of a risk matrix summarizing main risks and their probability and consequence classification (Ford et. al., 2016).

12 Conclusions

This report has provided examples of important elements of a risk assessment framework based on ENOS project work and experience from previous work on the REPP-CO_2 project (Ford et. al., 2016), drawing general lessons learned that should prove useful for similar projects.

Examples are provided for all three main steps of a general risk assessment framework; risk identification, risk analysis, and risk evaluation.

The risk identification process highlights both methods that be applied to screen the most important risks.

The risk analysis part provides examples of classification schemes for probabilities and consequences and provides a specific example from the Czech LBr-1 site for assessment of well abandonment status to identify wells that require further examination. The risk analysis also covers a framework that can be applied to estimate CO_2 leakage rates probabilistically, using well Br-62 and a generic well from the Getica field as case examples. The cases investigate micro-annuli between the casing cement and formation wall and examine the impact of varying degrees of knowledge concerning well barrier integrity on the prediction of leakage rates. It is clear from the example model outcomes shown that a combination of a large, vertically continuous micro-annuli gap and a driving pressure are required to reach high levels (~100 t/year) of CO_2 leakage. The size of such gaps is related to the effective wellbore permeability, which in turn relates to the bond between borehole completion materials e.g. casing cement and rock formation. As such, the quality of the cement barrier is crucial, and the information that exists determining its state and quality directly impacts the level of confidence in the leakage rate analysis.

The risk evaluation chapter discusses primarily the aspect of acceptable risk in general, and how such levels can be established and used in conjunction with the results from the risk analysis. Some examples are also provided concerning the potential impact which various leakage rates may have on human health.

The overall contribution of the risk assessment is a general framework where certain aspects are detailed, providing the means to identify, quantify and evaluate the risks related to abandoned wells. The framework does not provide *all* of the answers and should rather be viewed as a collection of tools and techniques that together provide *one* set of answers, and a starting point for risk analysis in similar projects.

A simplified model of the LBr-1 injection well was used to study the reactivity of the CO_2 in a micro annulus gap between the cement and the reservoir rock under a worst-case scenario (20 bar over-pressure in the reservoir, 20m cement depth and 50 µm annulus gap, with a circumference of 0.7 m). The simulation results show that the leakage rate was reduced by 80% over a 180 day period due to the self-healing action of CO_2 on cement.

The feasibility study has also confirmed that modern pressure gauges installed in the wells can help in detecting the occurrence of very low levels of wellbore leakage. Taking LBr-1 wellbore and reservoir parameters as reference, we can conclude that PDGs are capable of measuring pressure deviations due to leakage with rates starting from 0.1 cubic meters per day, therefore enhancing the list of currently available field monitoring technics and making the storage safer by providing early warning system.

References

Abdel-Rahman, A.A. (2008): *On The Atmospheric Dispersion and Gaussian Plume Model*, 2nd International Conference on WASTE MANAGEMENT, WATER POLLUTION, AIR POLLUTION, INDOOR CLIMATE (WWAI'08) Corfu, Greece, October 26-28, 2008. ISBN:

978-960-474-017-8.

Anderson, J. (editor) (1989): *The Joint SKI/SKB Scenario Development Project*. SKB Report TR 89-35 and SKI Report No. TR 89:14, Stockholm, Sweden.

Appelo, C. A. J. 2017. "Solute transport solved with the Nernst-Planck equation for concrete pores with 'free' water and a double layer." *Cement and Concrete Research* 101. doi: https://doi.org/10.1016/j.cemconres.2017.08.030.

Appelo, C. A. J., and Dieke Postma. 1999. *Geochemistry, groundwater and pollution*. 4th corrected print. ed. Rotterdam ; Brookfield, VT: Balkema.

Ashraf, Warda. 2016. "Carbonation of cement-based materials: Challenges and opportunities." *Construction and Building Materials* 120 (C):558-570. doi: https://doi.org/10.1016/j.conbuildmat.2016.05.080.

Arild, Ø, Ford, E.P., Lohne, H.P., Majoumerd, M.M., Havlova, V. (2017): *A Comparison of FEP-analysis and Barrier Analysis for CO_2 Leakage Risk Assessment on an Abandoned Czech Oilfield*, Energy Procedia, Vol. 114, July 2017, pp. 4237 – 4255.

Arild, Ø. (2018): *Discussion of acceptance criteria for risk-based P&A design*, Presentation given at P&A seminar October 18th, 2018, Sola, Norway.

Barlet-Gouedard, Veronique, Gaetan Rimmele, Bruno Goffe, and Olivier Porcherie. 2006. "Mitigation strategies for the risk of CO_2 migration through wellbores." IADC/SPE Drilling Conference, Miami, Florida, USA, 2006/1/1/.

Bourdet, D. (2002). Well Test Analysis: The Use of Advanced Interpretation Models. Elsevier.

Brunet, Jean-Patrick Leopold, Li Li, Zuleima T. Karpyn, and Nicolas J. Huerta. 2016. "Fracture opening or self-sealing: Critical residence time as a unifying parameter for cement–CO_2–brine interactions." *International Journal of Greenhouse Gas Control* 47:25-37. doi: https://doi.org/10.1016/j.ijggc.2016.01.024.

Carey, Bill, and Peter C. Lichtner. 2011. "Computational Studies of Two-Phase Cement/CO_2/Brine Interaction in Wellbore Environments." *SPE Journal*. doi: 10.2118/126666-PA.

Carey, J. William. 2013. "Geochemistry of wellbore integrity in CO_2 sequestration: Portland cement-steel-brine-CO_2 interactions." *Reviews in Mineralogy and Geochemistry* 77 (1):505-539. doi: https://doi.org/10.2138/rmg.2013.77.15.

Carroll, Susan, J. William Carey, David Dzombak, Nicolas J. Huerta, Li Li, Tom Richard, Wooyong Um, Stuart D. C. Walsh, and Liwei Zhang. 2016. "Review: Role of chemistry, mechanics, and transport on well integrity in CO_2 storage environments." *International Journal of Greenhouse Gas Control* 49:149-160. doi: https://doi.org/10.1016/j.ijggc.2016.01.010.

Celia, M.A., Bachu, S., Nordbotten, J.M., Gasda, S., Dahle, H.K. (2005): Quantitative estimation of CO_2 leakage from geological storage: Analytical models, numerical models, and data needs. Paper ID #228 for GHGT-7.

Downhole Pressure Gauges, Schlumberger

https://www.slb.com/services/characterization/testing/drillstem/downhole_test_tools.aspx

Fabbri, A., Jacquemet, N., Seyedi, D.M. (2011): A chemo-poromechanical model of oilwell cement carbonation under CO_2 geological storage conditions. CCR (42), p. 8-19.

Finney, B. and M. Jacobs. 2010. Carbon dioxide pressure-temperature phase diagram. Wikimedia.

Ford, E., Lohne, H.P., Arild, Ø., Havlová, V., Štván, F., Klempa, M., Bujok, P., Hladik, V. (2016): *REPP-CO_2 Deliverable V4.3 – Final risk assessment report*, 30-11-2016.

Ford, E.P., Moeinikia, F., Lohne, H.P., Arild, Ø., Majoumerd, M.M., Fjelde, K.K. (2017): *Leakage Calculator for Plugged and Abandoned Wells*, SPE-185890-MS.

Galan, I., C. Andrade, M. Castellote, N. Rebolledo, J. Sanchez, L. Toro, I. Puente, J. Campo, and O. Fabelo. 2011. "Neutron diffraction for studying the influence of the relative humidity on the carbonation process of cement pastes." *Journal of Physics: Conference Series* 325 (1):012015. doi: https://doi.org/10.1088/1742-6596/325/1/012015.

Garrabrants, Andrew C., and David S. Kosson. 2003. "Modeling Moisture Transport from a Portland Cement-Based Material During Storage in Reactive and Inert Atmospheres." *Drying Technology* 21 (5):775-805. doi: https://doi.org/10.1081/DRT-120021686.

Gherardi, Fabrizio, Pascal Audigane, and Eric C. Gaucher. 2012. "Predicting long-term geochemical alteration of wellbore cement in a generic geological CO_2 confinement site: Tackling a difficult reactive transport modeling challenge." *Journal of Hydrology* 420-421:340-359. doi: https://doi.org/10.1016/j.jhydrol.2011.12.026.

Global CCS Institute (2018): http://hub.globalccsinstitute.com/publications/getica-ccs-demo-project-feasibility-study-overview-report/executive-summary

Global CCS Institute, 2018. The Global Status of CCS: 2018. Australia.

Hladik, V., Berenblyum, R. Pereszlenyi, M., Krejci, O., Francu, J., Riis, F., Ford, E., Kollbotn, L., Khrulenko, A. 2017. " LBr-1 – Research CO2 Storage Pilot in the Czech Republic." *Energy Procedia,* Vol. 114, July 2017, pp. 5742-5747.

Hollnagel, E. (1999): *Accidents and barriers*, pp. 175-180 in Proceedings CSAPC'99, In Hoc JM, Millot P, Hollnagel E, Cacciabue PC (Eds.). Villeneuve d'Asq. France: Presses Universitaires de Valenciennes.

Huerta, Nicolas J., Marc A. Hesse, Steven L. Bryant, Brian R. Strazisar, and Christina Lopano. 2016. "Reactive transport of CO_2-saturated water in a cement fracture: Application to wellbore leakage during geologic CO_2 storage." *International Journal of Greenhouse Gas Control* 44:276-289. doi: https://doi.org/10.1016/j.ijggc.2015.02.006.

Huerta, Nicolas J., Brian R. Strazisar, Steven L. Bryant, and Marc A. Hesse. 2014. "Time-dependent Fluid Migration From a Storage Formation via Leaky Wells." *Energy Procedia* 63:5724-5736. doi: https://doi.org/10.1016/j.egypro.2014.11.605.

Hyvert, N., A. Sellier, F. Duprat, P. Rougeau, and P. Francisco. 2010. "Dependency of C-S-H carbonation rate on CO_2 pressure to explain transition from accelerated tests to natural carbonation." *Cem. Concr. Res.* 40 (11):1582-1589. doi: https://doi.org/10.1016/j.cemconres.2010.06.010.

IEA Greenhouse Gas R&D Programme (IEA GHG) (2008): *Assessment of sub sea ecosystem impacts*. 2008/08, August 2008.

ISO 31000:2018. *Risk Management – Guidelines*.

ISO Guide 73:2009. *Risk management — Vocabulary*.

ISO/IEC 31010:2009: *Risk management – Risk assessment techniques*.

Iyer, Jaisree, Stuart D. C. Walsh, Yue Hao, and Susan A. Carroll. 2017. "Incorporating reaction-rate dependence in reaction-front models of wellbore-cement/carbonated-brine systems." *International Journal of Greenhouse Gas Control* 59 (C):160-171. doi: https://doi.org/10.1016/j.ijggc.2017.01.019.

Jung, Hun Bok, and Wooyong Um. 2013. "Experimental study of potential wellbore cement carbonation by various phases of carbon dioxide during geologic carbon sequestration." *Applied Geochemistry* 35:161-172. doi: https://doi.org/10.1016/j.apgeochem.2013.04.007.

Karlsen, H.C., Ford, E.P. (2014): *BlowFlow – Next Generation Software for Calculating Blowout Rates*, SPE-169226-MS.

Koukouzas, Nikolaos, Zacharenia Kypritidou, Charalampos Vasilatos, Nikolaos Tsoukalas, Christopher A. Rochelle, and Gemma Purser. 2017. "Geochemical modeling of carbonation of hydrated oil well cement exposed to CO_2-saturated brine solution." *Applied Geochemistry* 85:35-48. doi: https://doi.org/10.1016/j.apgeochem.2017.08.002.

Kutchko, Barbara G., Brian R. Strazisar, Gregory V. Lowry, David A. Dzombak, and Niels Thaulow. 2008. "Rate of CO_2 Attack on Hydrated Class H Well Cement under Geologic Sequestration Conditions." *Environmental Science & Technology* 42 (16):6237-6242. doi: http://dx.doi.org/10.1021/es800049r.

Lea, F. M. 1998. "Lea's chemistry of cement and concrete." In, ed P. C. Hewlett: Arnold

Copublished in North, Central, and South America by J. Wiley.

Marty, Nicolas C. M., Francis Claret, Arnault Lassin, Joachim Tremosa, Philippe Blanc, Benoit Madé, Eric Giffaut, Benoit Cochepin, and Christophe Tournassat. 2015. "A database of dissolution and precipitation rates for clay-rocks minerals." *Applied Geochemistry* 55:108-118. doi: https://doi.org/10.1016/j.apgeochem.2014.10.012.

National Risk Assessment Partnership (NRAP) (2017): *Probability Distributions for* Effective Permeability of Potentially Leaking Wells at CO_2 Sequestration Sites, NRAP-TRS-III-021-2017, 21 April 2017.

NORSOK D-010:2013. *Well integrity in drilling and well operations*. Rev. 4, June.

Palandri, James L, and Yousif K Kharaka. 2004. A compilation of rate parameters of water-mineral interaction kinetics for application to geochemical modeling. DTIC Document.

Petroleum Experts (2018): *Prosper – Multiphase Well and Pipeline Nodal Analysis,* http://www.petex.com/products/ipm-suite/prosper/

Purser, G., A. E. Milodowski, J. F. Harrington, C. A. Rochelle, A. Butcher, and D. Wagner. 2013. "Modification to the Flow Properties of Repository Cement as a Result of Carbonation." *Procedia Earth and Planetary Science* 7:701-704. doi: https://doi.org/10.1016/j.proeps.2013.03.102.

Rausand, M. (2013): *Risk Assessment: Theory, Methods, and Applications*. John Wiley & Sons, Jun 12, 2013.

Rezagholilou, Alireza, Vagelis G. Papadakis, and Hamid Nikraz. 2017. "Rate of carbonation in cement modified base course material." *Construction and Building Materials* 150:646-652. doi: https://doi.org/10.1016/j.conbuildmat.2017.05.226.

Rochelle, C., G. Purser, A. Milodowski, and D Wagner. 2014. Results of laboratory carbonation experiments on Nirex Reference Vault Backfill cement. British Geological Survey.

Saetta, Anna, Roberto Scotta, and Renato Vitaliani. 1998. "Mechanical Behavior of Concrete under Physical-Chemical Attacks." *Journal of Engineering Mechanics* 124 (10):1100-1109. doi: https://doi.org/10.1061/(ASCE)0733-9399(1998)124:10(1100).

Savage, D. – Maul, P. R. – Benbow, S. – Walke, R. C. (2004): *A generic FEP database for the assessment of long-term performance and safety of the geologic storage of* CO_2. Quintessa Report QRS-1060A-1; 2004; 73pp (http://www.quintessa-online.com/FED_DB_report.pdf)

Scherer, George W., Michael A. Celia, Jean-Hervé Prévost, Stefan Bachu, Robert Bruant, Andrew Duguid, Richard Fuller, Sarah E. Gasda, Mileva Radonjic, and Wilasa Vichit-Vadakan. 2005. "Chapter 10 - Leakage of CO_2 Through Abandoned Wells: Role of Corrosion of Cement." In *Carbon Dioxide Capture for Storage in Deep Geologic Formations*, edited by David C. Thomas, 827-848. Amsterdam: Elsevier Science.

Schlumberger (2018): *OLGA Dynamic Multiphase Flow Simulator*, https://www.software.slb.com/products/olga

Sintef (2018): *SINTEF Offshore Blowout Database*, https://www.sintef.no/en/projects/sintef-offshore-blowout-database/

Sklet, S. (2005): *Safety Barriers on Oil and Gas Platforms – Means to Prevent Hydrocarbon Releases*. Doctoral thesis for the degree of doktor ingeniør. Trondheim, December 2005. Norwegian University of Science and Technology, Department of Production and Quality Engineering.

Stormont, J.C., Fernandez, S.G., Taha, M.R., Matteo, E.N. (2018): *Gas flow through cement-casing micro-annuli under varying stress conditions*, Geomechanics for Energy and the Environment 13 (2018) 1-13.

CO_2Thiery, M., G. Villain, P. Dangla, and G. Platret. 2007. "Investigation of the carbonation front shape on cementitious materials: Effects of the chemical kinetics." *Cement and Concrete Research* 37 (7):1047-1058. doi: https://doi.org/10.1016/j.cemconres.2007.04.002.

U.S. Department of Energy (DOE) (2007): *Final Risk Assessment Report for the FutureGen Project Environmental Impact Statement*, DE-AT26-06NT42921, Rev. 2 October 2007.

Walsh, Stuart D. C., Harris E. Mason, Wyatt L. Du Frane, and Susan A. Carroll. 2014. "Experimental calibration of a numerical model describing the alteration of cement/caprock interfaces by carbonated brine." *International Journal of Greenhouse Gas Control* 22:176-188. doi: https://doi.org/10.1016/j.ijggc.2014.01.004.

Zhang, Min, and Stefan Bachu. 2011. "Review of integrity of existing wells in relation to CO_2 geological storage: What do we know?" *International Journal of Greenhouse Gas Control* 5 (4):826-840. doi: https://doi.org/10.1016/j.ijggc.2010.11.006.

Appendix 1

Classes of Cements

Cements are classified based on the proportions of the different constituents in them and their particle sizes. Type G and H are the most common cements currently used in the Oil and Gas industry. Type A was most commonly used in the 1980s.

Table 10 Classes of OPC Cement. (Scherer et al. 2005)

API Class	ASTM type	$(CaO)_3 \cdot SiO_2$ (%)	$(CaO)_2 \cdot SiO_2$ (%)	$(CaO)_3 \cdot Al_2O_3$ (%)	$(CaO)_4 \cdot Al_2O_3 \cdot Fe2O_3$ (%)
A	I	53	24	8	8
B	II	47	32	5	12
C	III	58	16	8	8
D		26	54	2	12
E		26	54	2	12
F		-	-	-	-
G		50	30	5	12
H		50	30	5	12

Cement pore water composition

Hydrated cement contains brine that is left behind after hydration. This pore brine is often alkaline, and its composition is often variable depending on the storage time and condition. The pore water is principally composed of K and Na hydroxides. An example of one such pore water composition used in experiments by BGS is given in Table 11. However, the hydrated cements can be exposed to formation water and there would be some leaching of the formation water into the cement so that the final mixture is some combination of the formation water and cement pore water. BGS evaluated the carbonation with three brines: cement pore water, evolved water and an intermediate brine. All brines used were alkaline.

Table 11: Cement pore water composition (Rochelle et al. 2014)

Chemical component	Cement pore water (mg/L)
CaO	168.30
NaOH	2812.45
KOH	5217.20
SiO_2	48.06

Appendix 2

Well profiles with stratigraphy, well logs, lithology and well design

See accompanying pdf

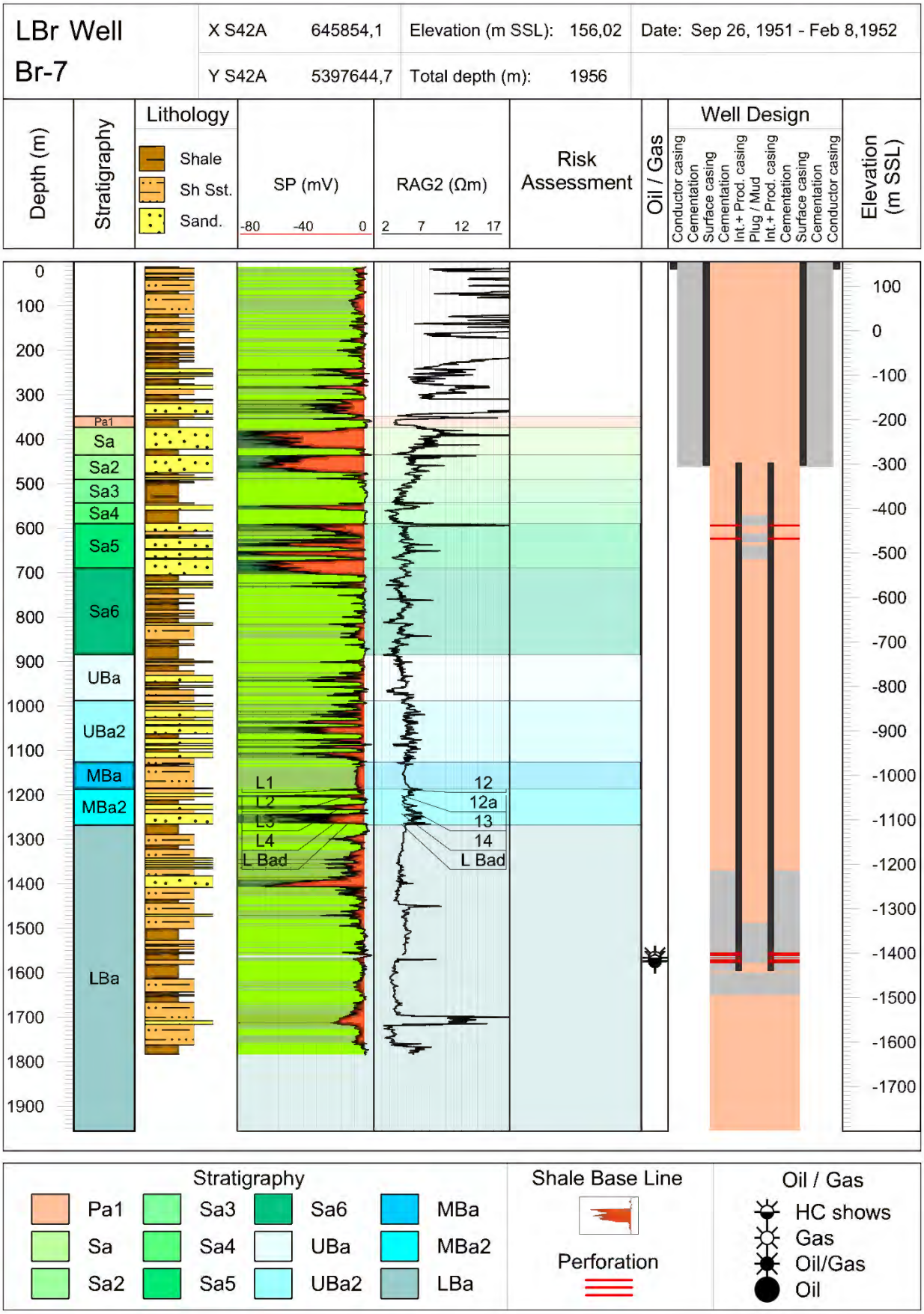
LBr Well
Br-7
X S42A 645854,1
Y S42A 5397644,7
Elevation (m SSL): 156,02
Total depth (m): 1956
Date: Sep 26, 1951 - Feb 8,1952
Depth (m)
Stratigraphy
Lithology
Shale
Sh Sst.
Sand.
SP (mV)
-80 -40 0
RAG2 (Ωm)
2 7 12 17
Risk Assessment
Oil / Gas
Well Design
Conductor casing
Cementation
Surface casing
Cementation
Int.+ Prod. casing
Plug / Mud
Int.+ Prod. casing
Cementation
Surface casing
Cementation
Conductor casing
Elevation (m SSL)
0
100
200
300
400
500
600
700
800
900
1000
1100
1200
1300
1400
1500
1600
1700
1800
1900
Pa1
Sa
Sa2
Sa3
Sa4
Sa5
Sa6
UBa
UBa2
MBa
MBa2
LBa
L1
L2
L3
L4
L Bad
12
12a
13
14
L Bad
100
0
-100
-200
-300
-400
-500
-600
-700
-800
-900
-1000
-1100
-1200
-1300
-1400
-1500
-1600
-1700
Stratigraphy
Pa1
Sa
Sa2
Sa3
Sa4
Sa5
Sa6
UBa
UBa2
MBa
MBa2
LBa
Shale Base Line
Perforation
Oil / Gas
HC shows
Gas
Oil/Gas
Oil

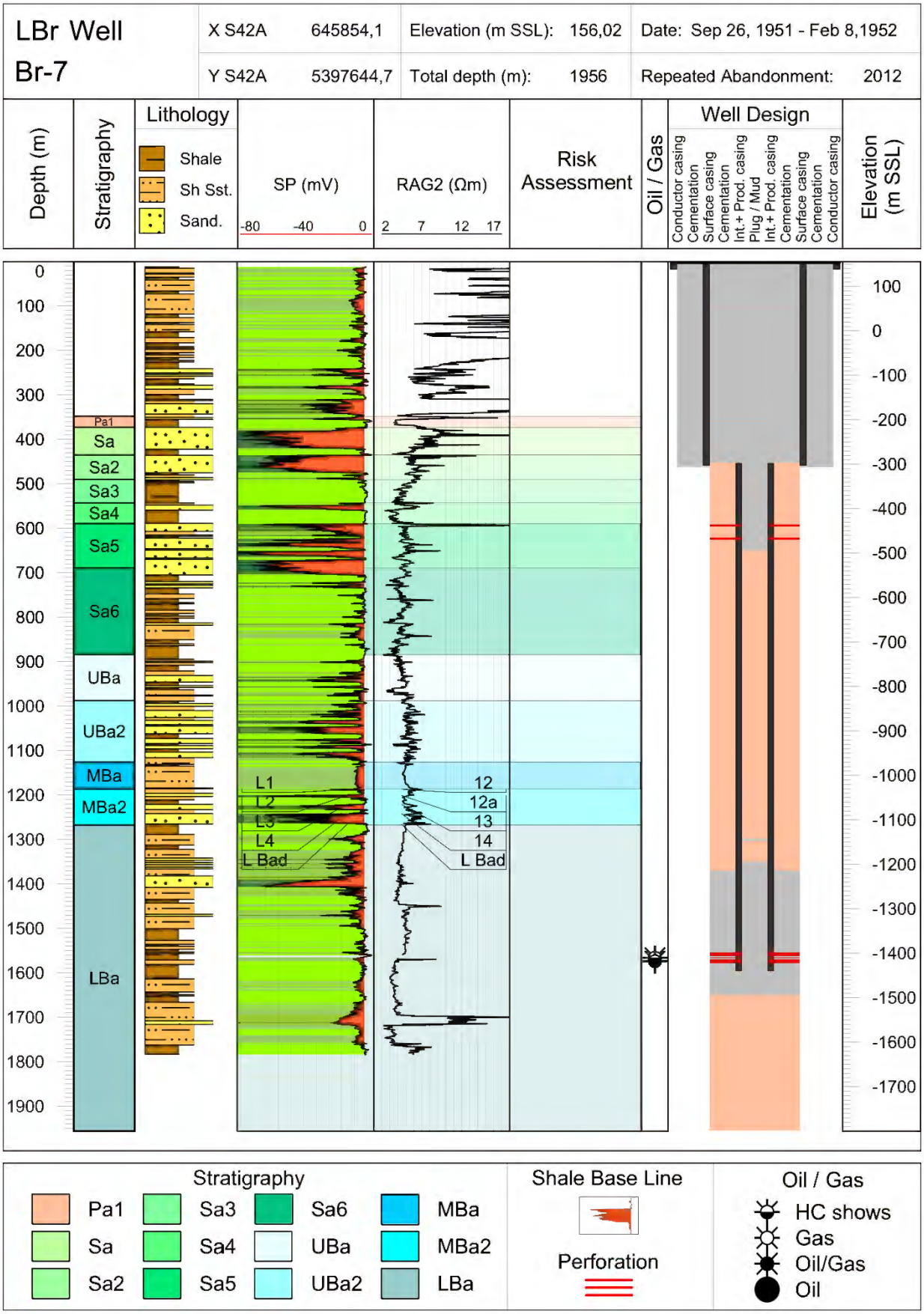
LBr Well
Br-7
X S42A 645854,1
Y S42A 5397644,7
Elevation (m SSL): 156,02
Total depth (m): 1956
Date: Sep 26, 1951 - Feb 8,1952
Repeated Abandonment: 2012
Depth (m)
Stratigraphy
Lithology
Shale
Sh Sst.
Sand.
SP (mV)
-80 -40 0
RAG2 (Ωm)
2 7 12 17
Risk Assessment
Oil / Gas
Well Design
Conductor casing
Cementation
Surface casing
Cementation
Int.+ Prod. casing
Plug / Mud
Int.+ Prod. casing
Cementation
Surface casing
Cementation
Conductor casing
Elevation (m SSL)
0
100
200
300
400
500
600
700
800
900
1000
1100
1200
1300
1400
1500
1600
1700
1800
1900
Pa1
Sa
Sa2
Sa3
Sa4
Sa5
Sa6
UBa
UBa2
MBa
MBa2
LBa
L1
L2
L3
L4
L Bad
12
12a
13
14
L Bad
100
0
-100
-200
-300
-400
-500
-600
-700
-800
-900
-1000
-1100
-1200
-1300
-1400
-1500
-1600
-1700
Stratigraphy
Pa1
Sa
Sa2
Sa3
Sa4
Sa5
Sa6
UBa
UBa2
MBa
MBa2
LBa
Shale Base Line
Perforation
Oil / Gas
HC shows
Gas
Oil/Gas
Oil

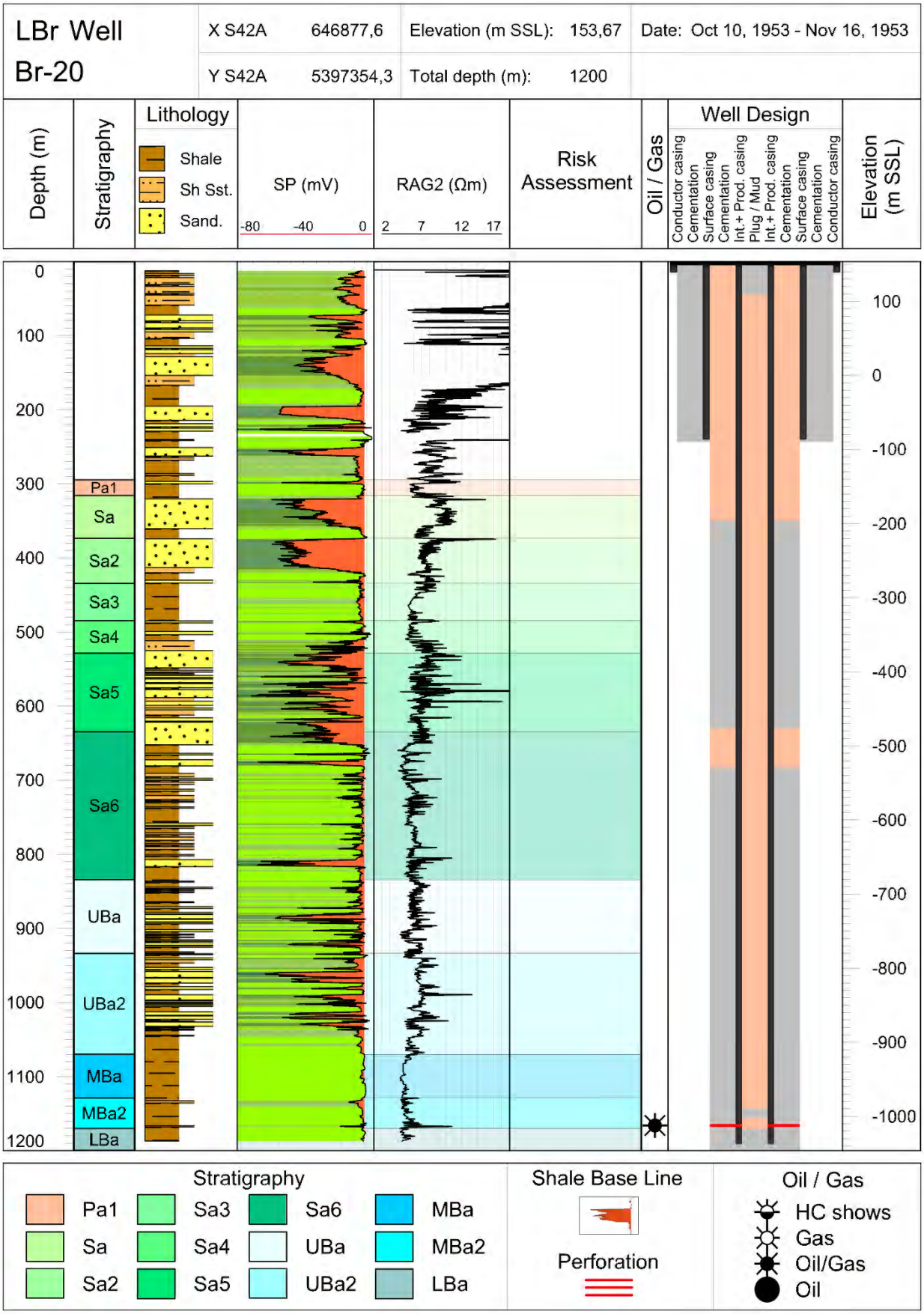
LBr Well
Br-20
X S42A 646877,6
Y S42A 5397354,3
Elevation (m SSL): 153,67
Total depth (m): 1200
Date: Oct 10, 1953 - Nov 16, 1953
Depth (m)
Stratigraphy
Lithology
Shale
Sh Sst.
Sand.
SP (mV)
-80 -40 0
RAG2 (Ωm)
2 7 12 17
Risk Assessment
Oil / Gas
Well Design
Conductor casing
Cementation
Surface casing
Cementation
Int.+ Prod. casing
Plug / Mud
Int.+ Prod. casing
Cementation
Surface casing
Cementation
Conductor casing
Elevation (m SSL)
0
100
200
300
400
500
600
700
800
900
1000
1100
1200
Pa1
Sa
Sa2
Sa3
Sa4
Sa5
Sa6
UBa
UBa2
MBa
MBa2
LBa
100
0
-100
-200
-300
-400
-500
-600
-700
-800
-900
-1000
Stratigraphy
Pa1
Sa
Sa2
Sa3
Sa4
Sa5
Sa6
UBa
UBa2
MBa
MBa2
LBa
Shale Base Line
Perforation
Oil / Gas
HC shows
Gas
Oil/Gas
Oil

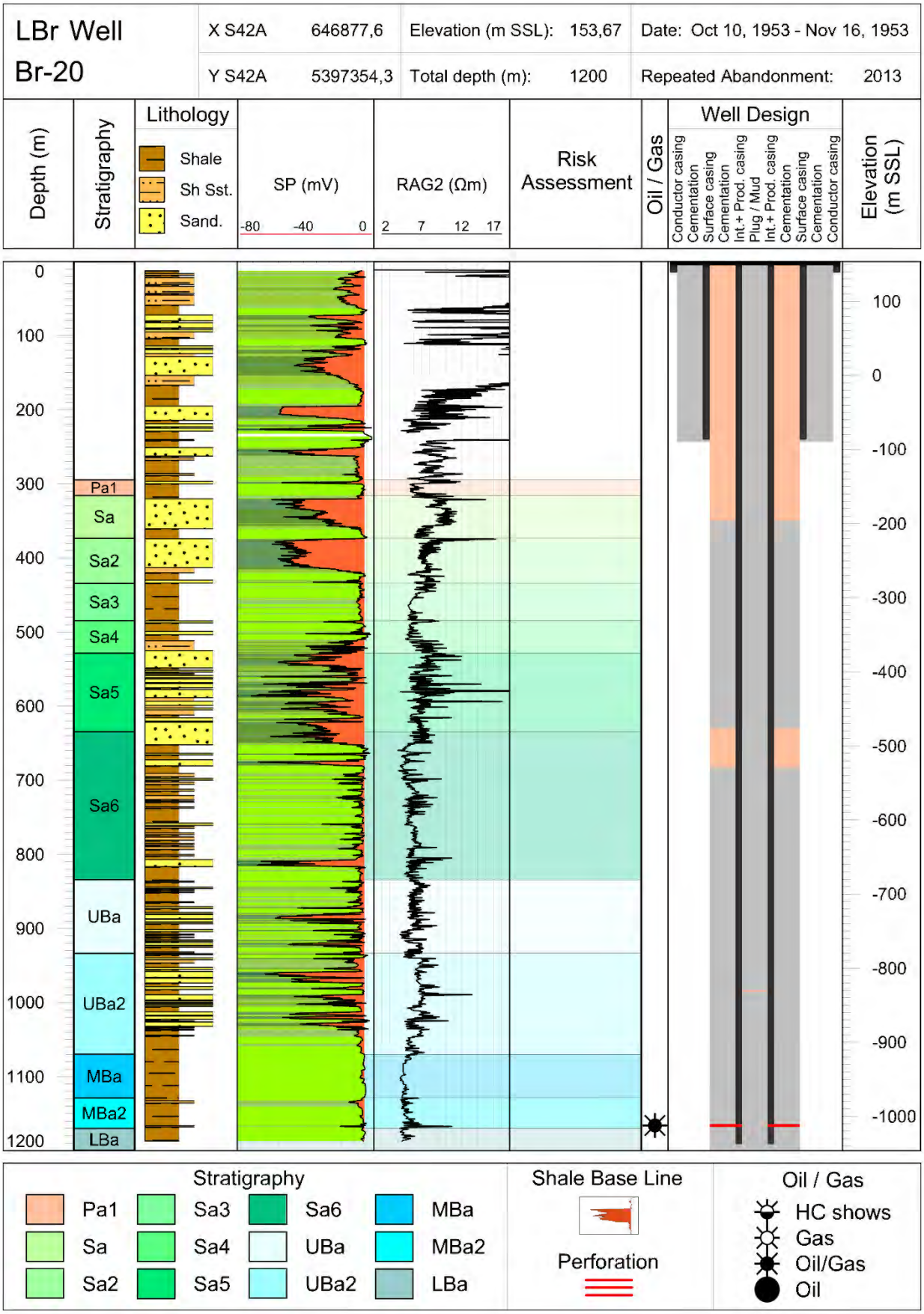
LBr Well
Br-20
X S42A 646877,6
Y S42A 5397354,3
Elevation (m SSL): 153,67
Total depth (m): 1200
Date: Oct 10, 1953 - Nov 16, 1953
Repeated Abandonment: 2013
Depth (m)
Stratigraphy
Lithology
Shale
Sh Sst.
Sand.
SP (mV)
-80 -40 0
RAG2 (Ωm)
2 7 12 17
Risk Assessment
Oil / Gas
Well Design
Conductor casing
Cementation
Surface casing
Cementation
Int.+ Prod. casing
Plug / Mud
Int.+ Prod. casing
Cementation
Surface casing
Cementation
Conductor casing
Elevation (m SSL)
0
100
200
300
400
500
600
700
800
900
1000
1100
1200
Pa1
Sa
Sa2
Sa3
Sa4
Sa5
Sa6
UBa
UBa2
MBa
MBa2
LBa
100
0
-100
-200
-300
-400
-500
-600
-700
-800
-900
-1000
Stratigraphy
Pa1
Sa
Sa2
Sa3
Sa4
Sa5
Sa6
UBa
UBa2
MBa
MBa2
LBa
Shale Base Line
Perforation
Oil / Gas
HC shows
Gas
Oil/Gas
Oil

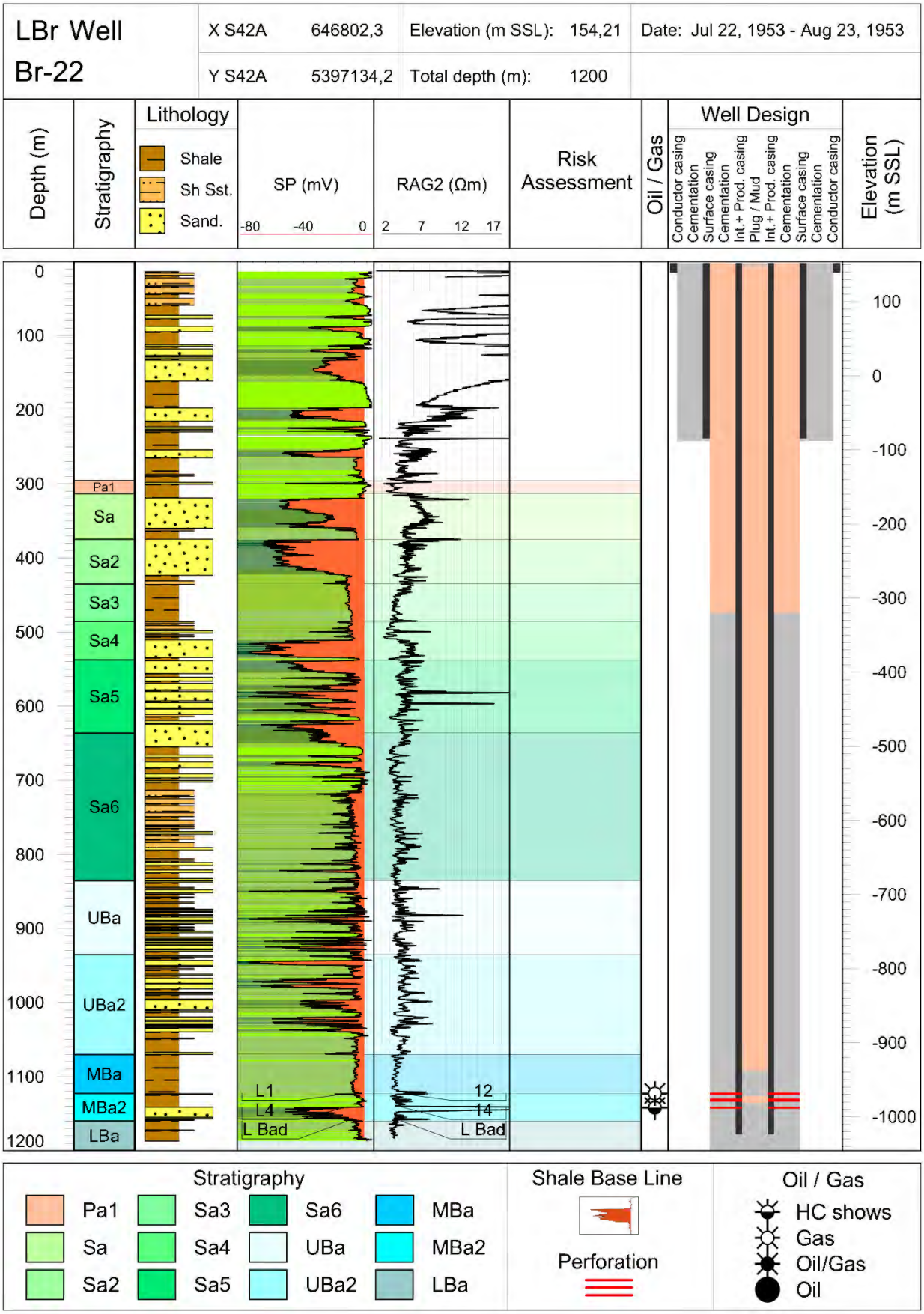
LBr Well
Br-22
X S42A 646802,3
Y S42A 5397134,2
Elevation (m SSL): 154,21
Total depth (m): 1200
Date: Jul 22, 1953 - Aug 23, 1953
Depth (m)
Stratigraphy
Lithology
Shale
Sh Sst.
Sand.
SP (mV)
-80 -40 0
RAG2 (Ωm)
2 7 12 17
Risk Assessment
Oil / Gas
Well Design
Conductor casing
Cementation
Surface casing
Cementation
Int.+ Prod. casing
Plug / Mud
Int.+ Prod. casing
Cementation
Surface casing
Cementation
Conductor casing
Elevation (m SSL)
0
100
200
300
400
500
600
700
800
900
1000
1100
1200
Pa1
Sa
Sa2
Sa3
Sa4
Sa5
Sa6
UBa
UBa2
MBa
MBa2
LBa
L1
L4
L Bad
12
14
L Bad
100
0
-100
-200
-300
-400
-500
-600
-700
-800
-900
-1000
Stratigraphy
Pa1
Sa
Sa2
Sa3
Sa4
Sa5
Sa6
UBa
UBa2
MBa
MBa2
LBa
Shale Base Line
Perforation
Oil / Gas
HC shows
Gas
Oil/Gas
Oil

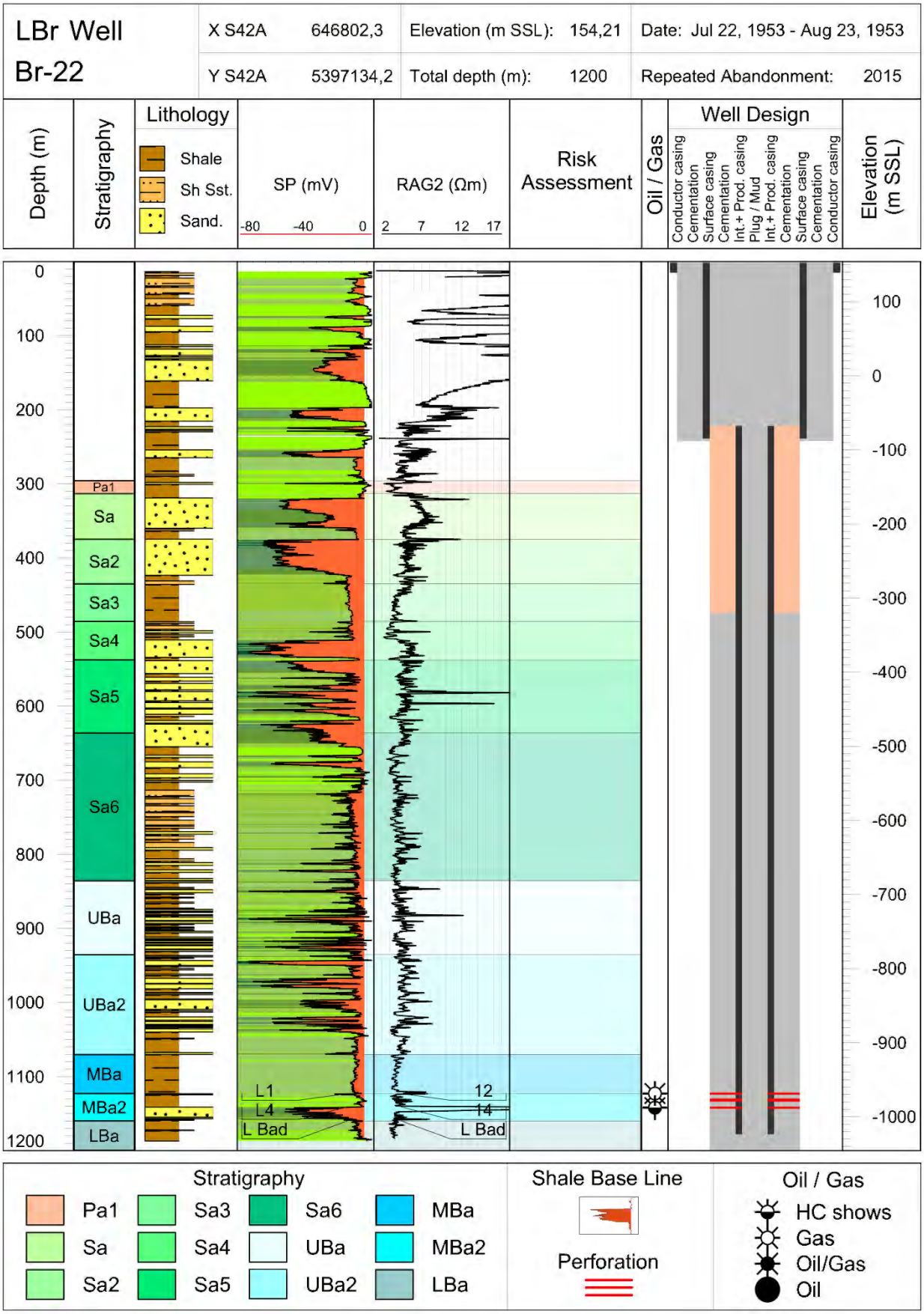
LBr Well
Br-22
X S42A 646802,3
Y S42A 5397134,2
Elevation (m SSL): 154,21
Total depth (m): 1200
Date: Jul 22, 1953 - Aug 23, 1953
Repeated Abandonment: 2015
Depth (m)
Stratigraphy
Lithology
Shale
Sh Sst.
Sand.
SP (mV)
-80 -40 0
RAG2 (Ωm)
2 7 12 17
Risk Assessment
Oil / Gas
Well Design
Conductor casing
Cementation
Surface casing
Cementation
Int.+ Prod. casing
Plug / Mud
Int.+ Prod. casing
Cementation
Surface casing
Cementation
Conductor casing
Elevation (m SSL)
0
100
200
300
400
500
600
700
800
900
1000
1100
1200
Pa1
Sa
Sa2
Sa3
Sa4
Sa5
Sa6
UBa
UBa2
MBa
MBa2
LBa
L1
L4
L Bad
12
14
L Bad
100
0
-100
-200
-300
-400
-500
-600
-700
-800
-900
-1000
Stratigraphy
Pa1
Sa
Sa2
Sa3
Sa4
Sa5
Sa6
UBa
UBa2
MBa
MBa2
LBa
Shale Base Line
Perforation
Oil / Gas
HC shows
Gas
Oil/Gas
Oil

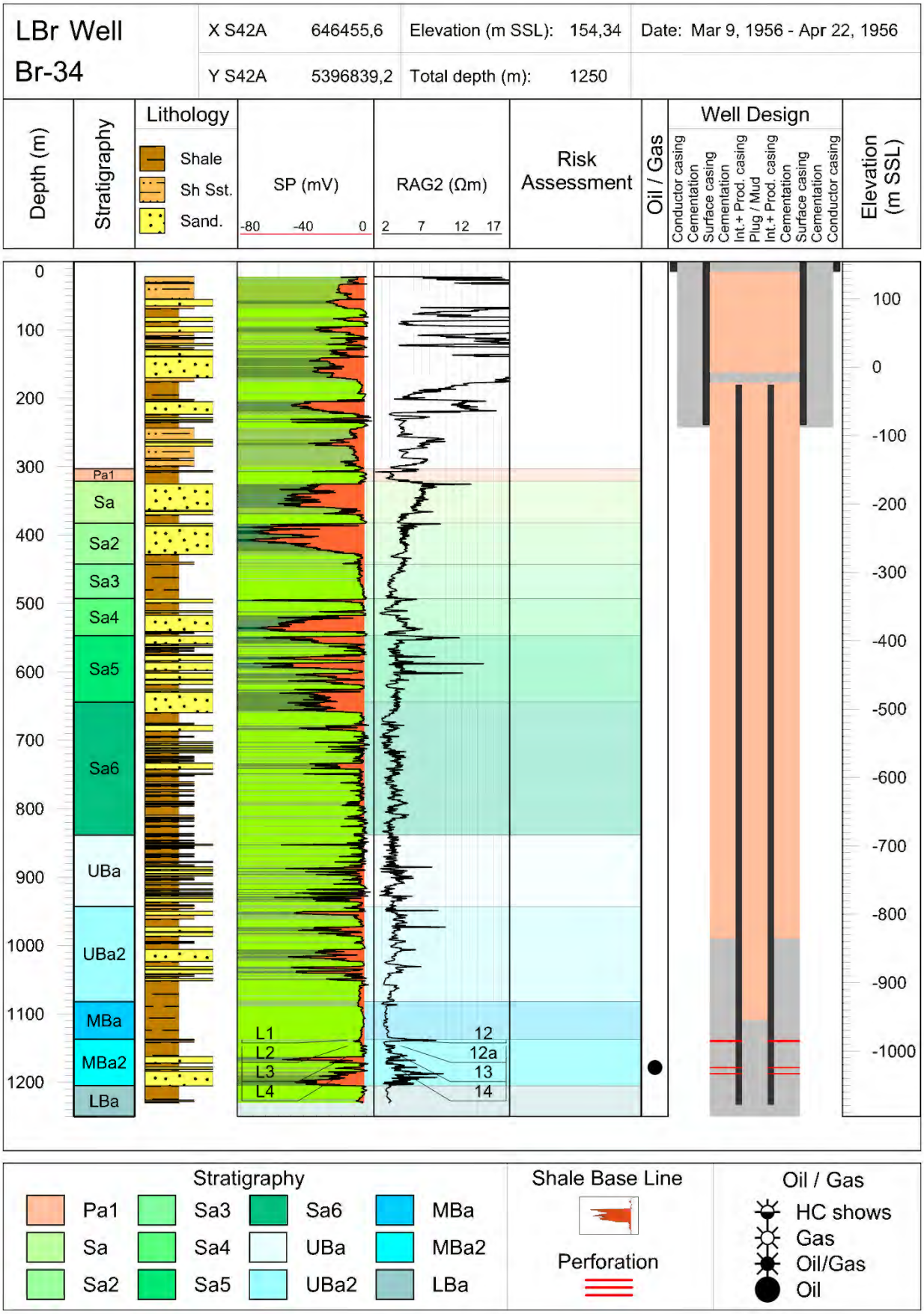
LBr Well
Br-34
X S42A 646455,6
Y S42A 5396839,2
Elevation (m SSL): 154,34
Total depth (m): 1250
Date: Mar 9, 1956 - Apr 22, 1956
Depth (m)
Stratigraphy
Lithology
Shale
Sh Sst.
Sand.
SP (mV)
-80 -40 0
RAG2 (Ωm)
2 7 12 17
Risk Assessment
Oil / Gas
Well Design
Conductor casing
Cementation
Surface casing
Cementation
Int.+ Prod. casing
Plug / Mud
Int.+ Prod. casing
Cementation
Surface casing
Cementation
Conductor casing
Elevation (m SSL)
0
100
200
300
400
500
600
700
800
900
1000
1100
1200
Pa1
Sa
Sa2
Sa3
Sa4
Sa5
Sa6
UBa
UBa2
MBa
MBa2
LBa
L1
L2
L3
L4
12
12a
13
14
100
0
-100
-200
-300
-400
-500
-600
-700
-800
-900
-1000
Stratigraphy
Pa1
Sa
Sa2
Sa3
Sa4
Sa5
Sa6
UBa
UBa2
MBa
MBa2
LBa
Shale Base Line
Perforation
Oil / Gas
HC shows
Gas
Oil/Gas
Oil

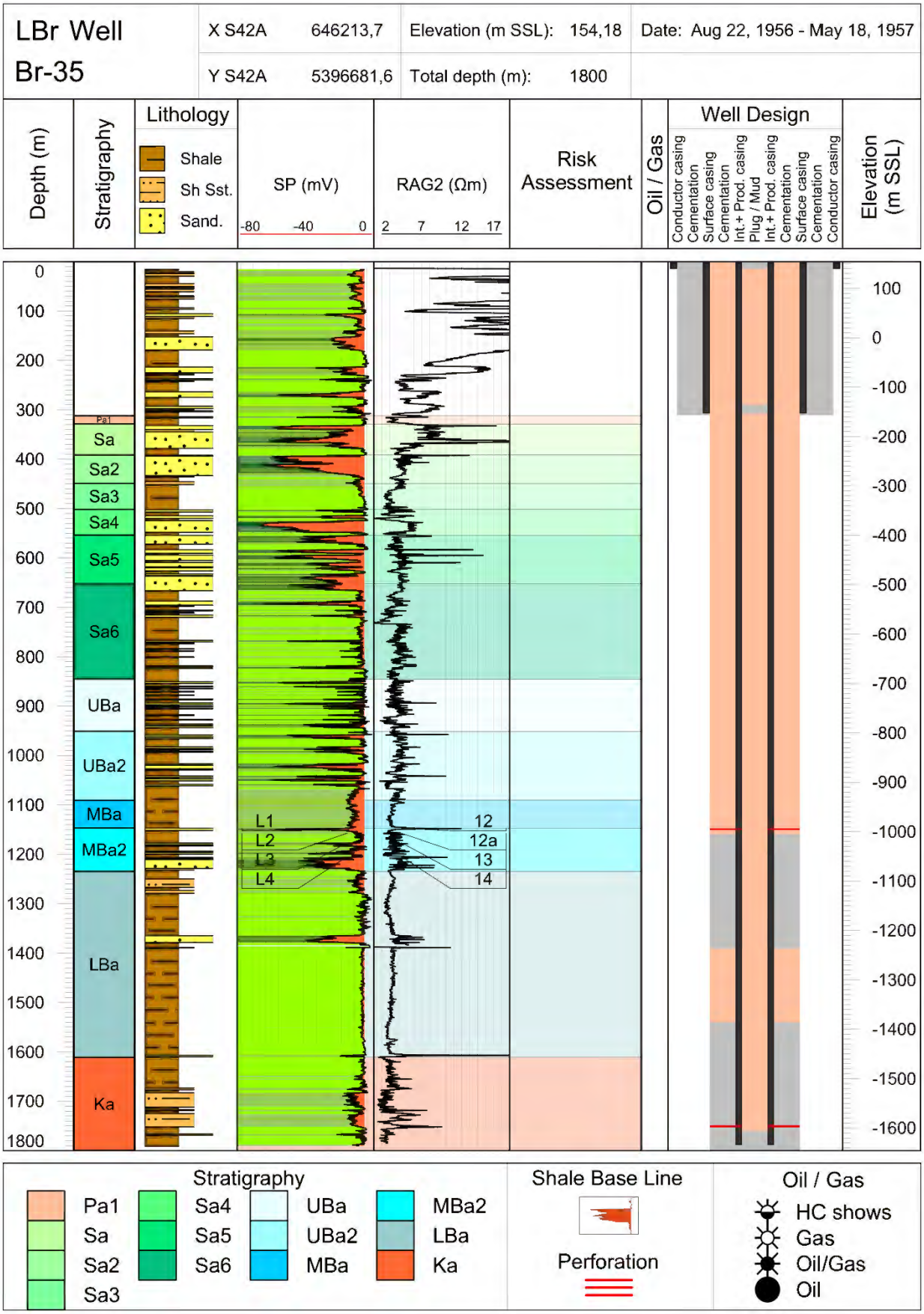
LBr Well
Br-35
X S42A 646213,7
Y S42A 5396681,6
Elevation (m SSL): 154,18
Total depth (m): 1800
Date: Aug 22, 1956 - May 18, 1957
Depth (m)
Stratigraphy
Lithology
Shale
Sh Sst.
Sand.
SP (mV)
-80 -40 0
RAG2 (Ωm)
2 7 12 17
Risk Assessment
Oil / Gas
Well Design
Conductor casing
Cementation
Surface casing
Cementation
Int.+ Prod. casing
Plug / Mud
Int.+ Prod. casing
Cementation
Surface casing
Cementation
Conductor casing
Elevation (m SSL)
0
100
200
300
400
500
600
700
800
900
1000
1100
1200
1300
1400
1500
1600
1700
1800
Pa1
Sa
Sa2
Sa3
Sa4
Sa5
Sa6
UBa
UBa2
MBa
MBa2
LBa
Ka
L1
L2
L3
L4
12
12a
13
14
100
0
-100
-200
-300
-400
-500
-600
-700
-800
-900
-1000
-1100
-1200
-1300
-1400
-1500
-1600
Stratigraphy
Pa1
Sa
Sa2
Sa3
Sa4
Sa5
Sa6
UBa
UBa2
MBa
MBa2
LBa
Ka
Shale Base Line
Perforation
Oil / Gas
HC shows
Gas
Oil/Gas
Oil

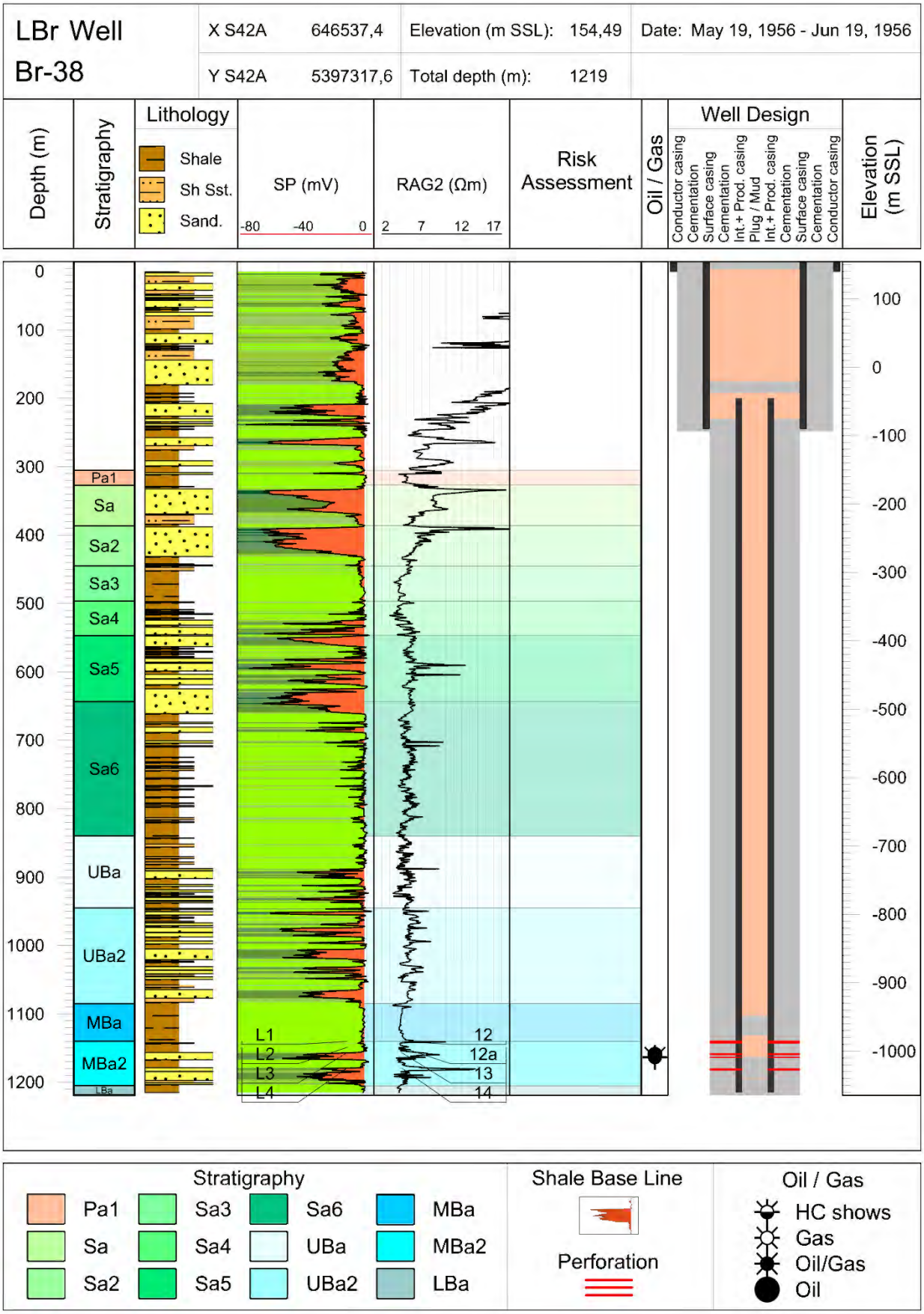
LBr Well
Br-38
X S42A 646537,4
Y S42A 5397317,6
Elevation (m SSL): 154,49
Total depth (m): 1219
Date: May 19, 1956 - Jun 19, 1956
Depth (m)
Stratigraphy
Lithology
Shale
Sh Sst.
Sand.
SP (mV)
-80 -40 0
RAG2 (Ωm)
2 7 12 17
Risk Assessment
Oil / Gas
Well Design
Conductor casing
Cementation
Surface casing
Cementation
Int.+ Prod. casing
Plug / Mud
Int.+ Prod. casing
Cementation
Surface casing
Cementation
Conductor casing
Elevation (m SSL)
0
100
200
300
400
500
600
700
800
900
1000
1100
1200
Pa1
Sa
Sa2
Sa3
Sa4
Sa5
Sa6
UBa
UBa2
MBa
MBa2
LBa
L1
L2
L3
L4
12
12a
13
14
100
0
-100
-200
-300
-400
-500
-600
-700
-800
-900
-1000
Stratigraphy
Pa1
Sa
Sa2
Sa3
Sa4
Sa5
Sa6
UBa
UBa2
MBa
MBa2
LBa
Shale Base Line
Perforation
Oil / Gas
HC shows
Gas
Oil/Gas
Oil

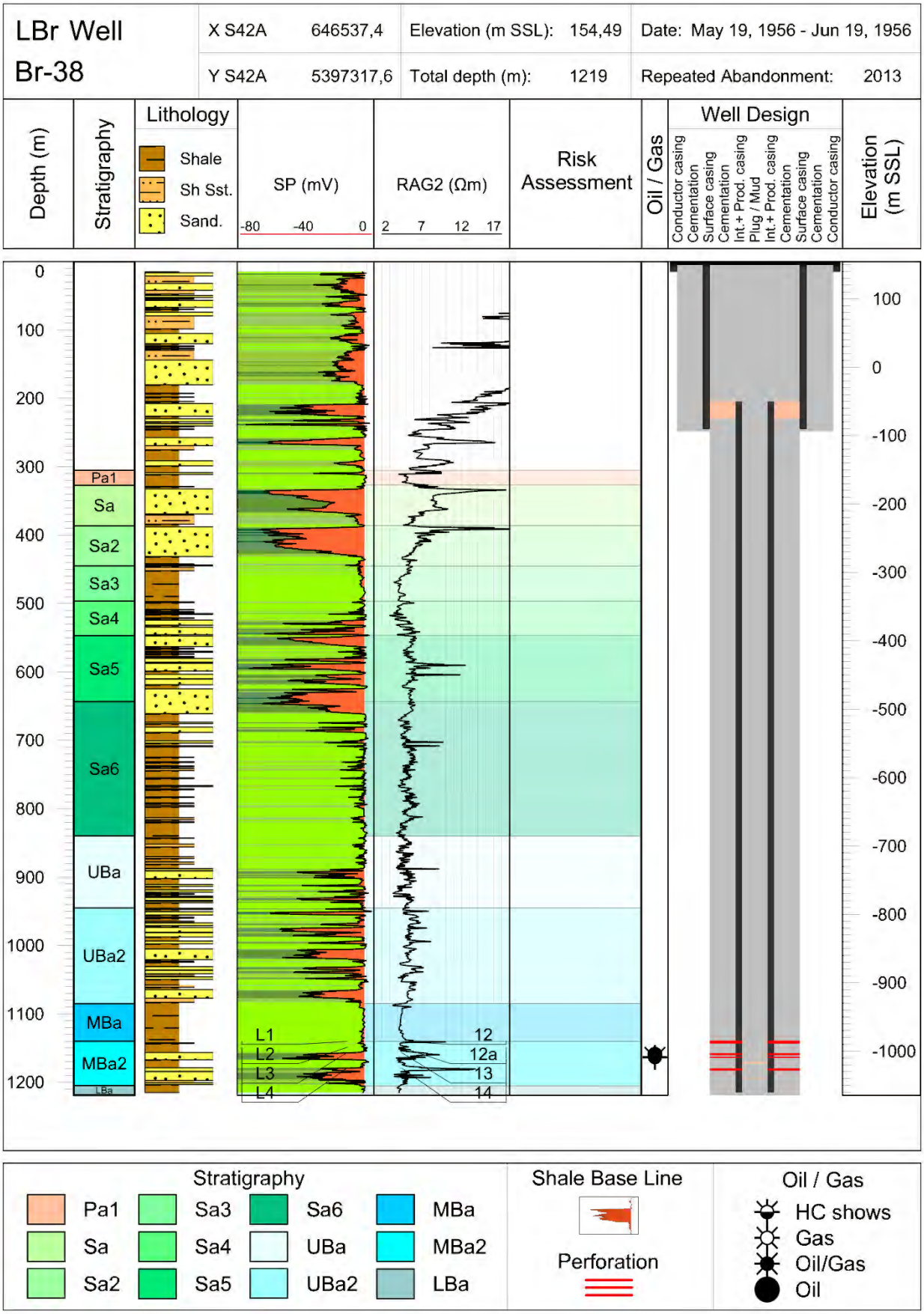
LBr Well
Br-38
X S42A 646537,4
Y S42A 5397317,6
Elevation (m SSL): 154,49
Total depth (m): 1219
Date: May 19, 1956 - Jun 19, 1956
Repeated Abandonment: 2013
Depth (m)
Stratigraphy
Lithology
Shale
Sh Sst.
Sand.
SP (mV)
-80 -40 0
RAG2 (Ωm)
2 7 12 17
Risk Assessment
Oil / Gas
Well Design
Conductor casing
Cementation
Surface casing
Cementation
Int.+ Prod. casing
Plug / Mud
Int.+ Prod. casing
Cementation
Surface casing
Cementation
Conductor casing
Elevation (m SSL)
0
100
200
300
400
500
600
700
800
900
1000
1100
1200
Pa1
Sa
Sa2
Sa3
Sa4
Sa5
Sa6
UBa
UBa2
MBa
MBa2
LBa
L1
L2
L3
L4
12
12a
13
14
100
0
-100
-200
-300
-400
-500
-600
-700
-800
-900
-1000
Stratigraphy
Pa1
Sa
Sa2
Sa3
Sa4
Sa5
Sa6
UBa
UBa2
MBa
MBa2
LBa
Shale Base Line
Perforation
Oil / Gas
HC shows
Gas
Oil/Gas
Oil

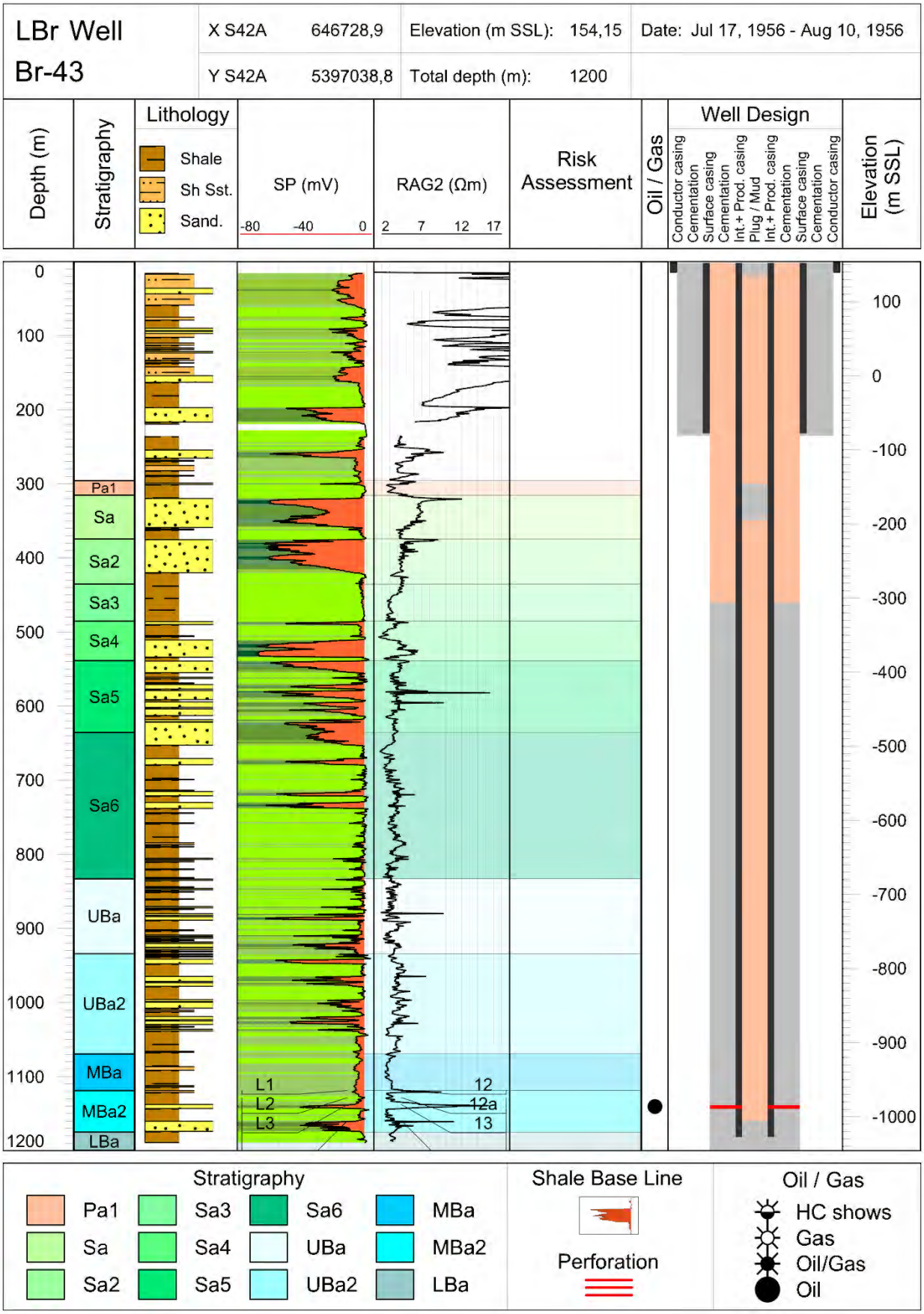
LBr Well
Br-43
X S42A 646728,9
Y S42A 5397038,8
Elevation (m SSL): 154,15
Total depth (m): 1200
Date: Jul 17, 1956 - Aug 10, 1956
Depth (m)
Stratigraphy
Lithology
Shale
Sh Sst.
Sand.
SP (mV)
-80 -40 0
RAG2 (Ωm)
2 7 12 17
Risk Assessment
Oil / Gas
Well Design
Conductor casing
Cementation
Surface casing
Cementation
Int.+ Prod. casing
Plug / Mud
Int.+ Prod. casing
Cementation
Surface casing
Cementation
Conductor casing
Elevation (m SSL)
0
100
200
300
400
500
600
700
800
900
1000
1100
1200
Pa1
Sa
Sa2
Sa3
Sa4
Sa5
Sa6
UBa
UBa2
MBa
MBa2
LBa
L1
L2
L3
12
12a
13
100
0
-100
-200
-300
-400
-500
-600
-700
-800
-900
-1000
Stratigraphy
Pa1
Sa
Sa2
Sa3
Sa4
Sa5
Sa6
UBa
UBa2
MBa
MBa2
LBa
Shale Base Line
Perforation
Oil / Gas
HC shows
Gas
Oil/Gas
Oil

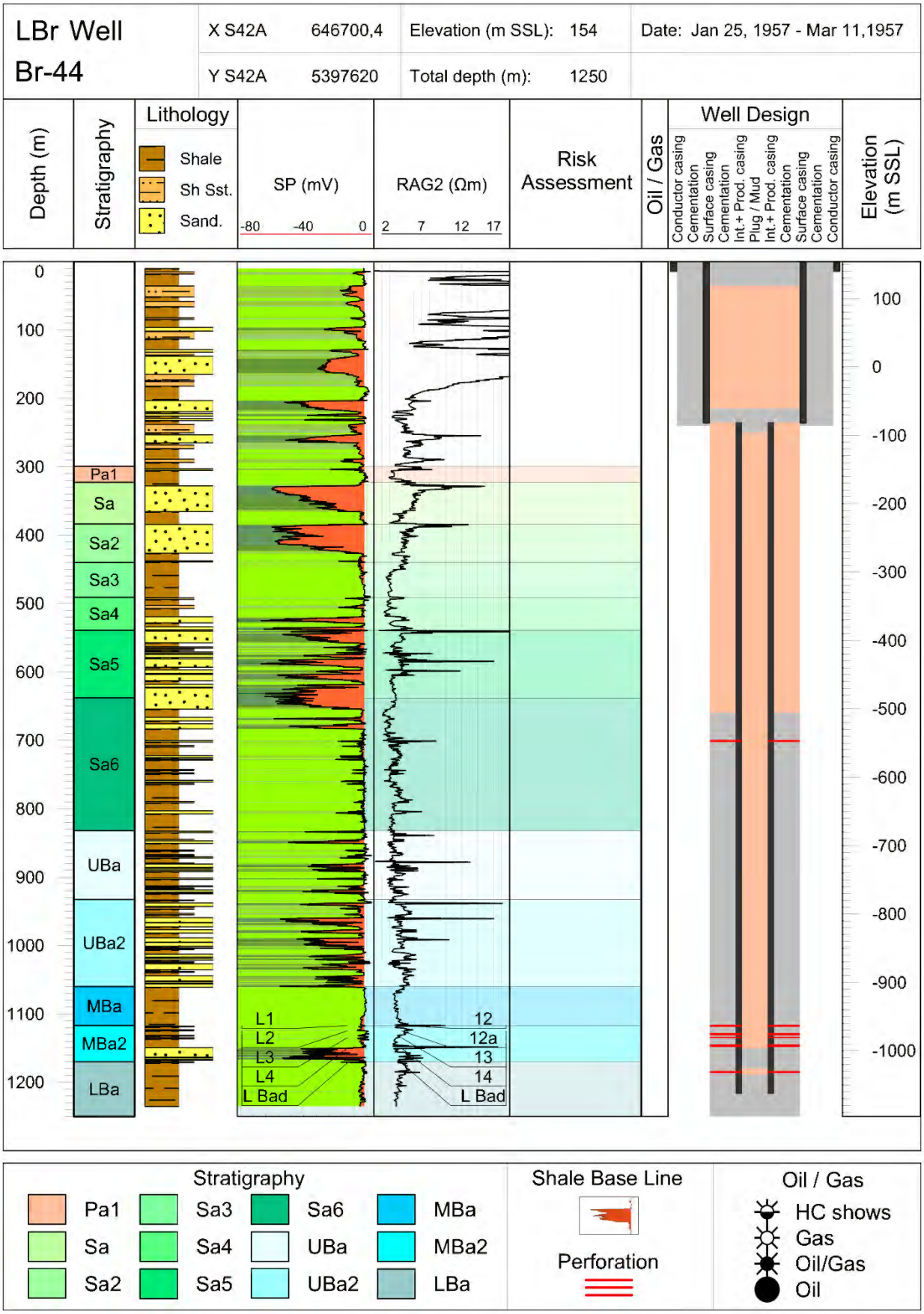
LBr Well
Br-44
X S42A 646700,4
Y S42A 5397620
Elevation (m SSL): 154
Total depth (m): 1250
Date: Jan 25, 1957 - Mar 11,1957
Depth (m)
Stratigraphy
Lithology
Shale
Sh Sst.
Sand.
SP (mV)
-80 -40 0
RAG2 (Ωm)
2 7 12 17
Risk Assessment
Oil / Gas
Well Design
Conductor casing
Cementation
Surface casing
Cementation
Int.+ Prod. casing
Plug / Mud
Int.+ Prod. casing
Cementation
Surface casing
Cementation
Conductor casing
Elevation (m SSL)
0
100
200
300
400
500
600
700
800
900
1000
1100
1200
Pa1
Sa
Sa2
Sa3
Sa4
Sa5
Sa6
UBa
UBa2
MBa
MBa2
LBa
L1
L2
L3
L4
L Bad
12
12a
13
14
L Bad
100
0
-100
-200
-300
-400
-500
-600
-700
-800
-900
-1000
Stratigraphy
Pa1
Sa
Sa2
Sa3
Sa4
Sa5
Sa6
UBa
UBa2
MBa
MBa2
LBa
Shale Base Line
Perforation
Oil / Gas
HC shows
Gas
Oil/Gas
Oil

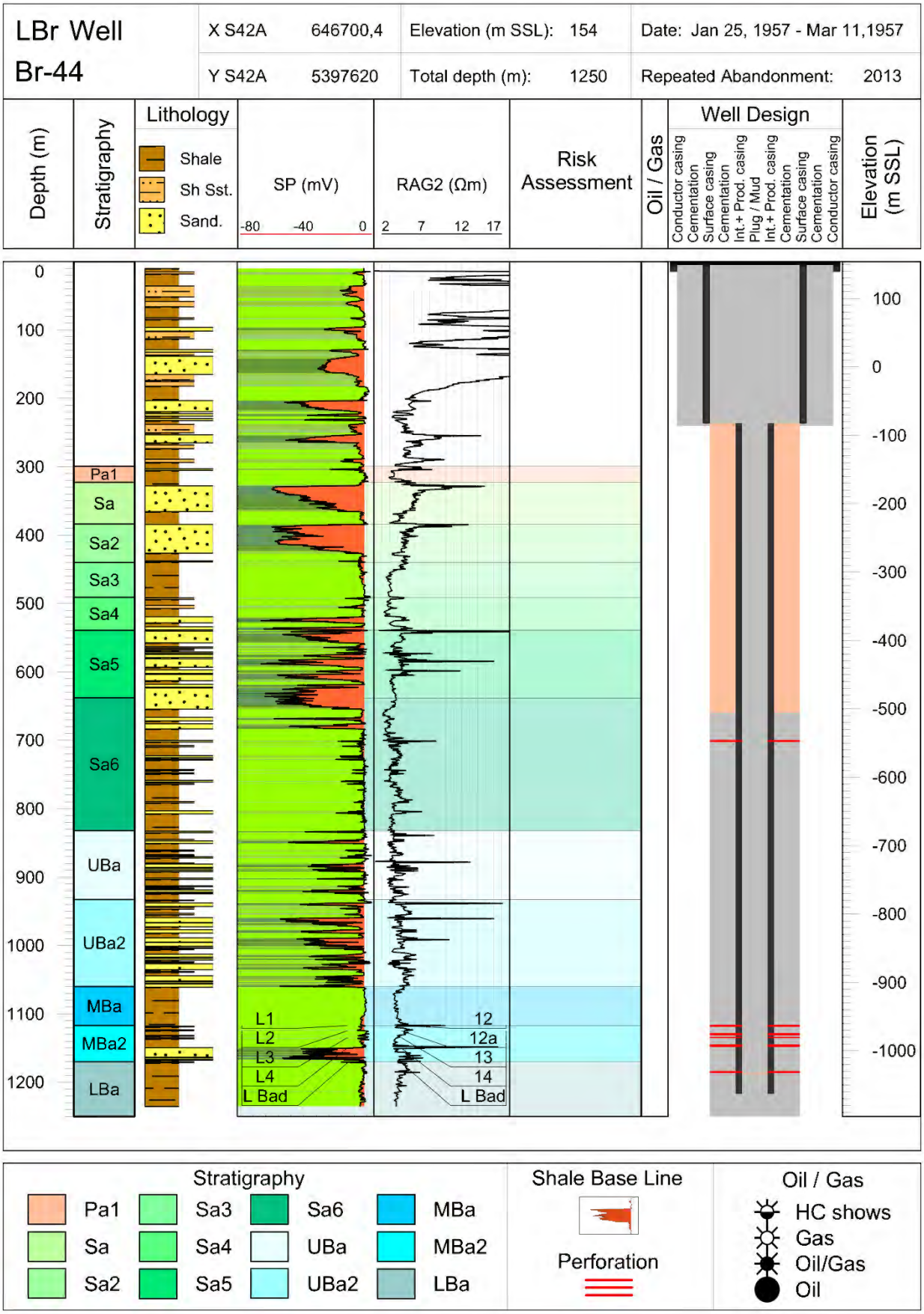
LBr Well
Br-44
X S42A 646700,4
Y S42A 5397620
Elevation (m SSL): 154
Total depth (m): 1250
Date: Jan 25, 1957 - Mar 11,1957
Repeated Abandonment: 2013
Depth (m)
Stratigraphy
Lithology
Shale
Sh Sst.
Sand.
SP (mV)
-80 -40 0
RAG2 (Ωm)
2 7 12 17
Risk Assessment
Oil / Gas
Well Design
Conductor casing
Cementation
Surface casing
Cementation
Int.+ Prod. casing
Plug / Mud
Int.+ Prod. casing
Cementation
Surface casing
Cementation
Conductor casing
Elevation (m SSL)
0
100
200
300
400
500
600
700
800
900
1000
1100
1200
Pa1
Sa
Sa2
Sa3
Sa4
Sa5
Sa6
UBa
UBa2
MBa
MBa2
LBa
L1
L2
L3
L4
L Bad
12
12a
13
14
L Bad
100
0
-100
-200
-300
-400
-500
-600
-700
-800
-900
-1000
Stratigraphy
Pa1
Sa
Sa2
Sa3
Sa4
Sa5
Sa6
UBa
UBa2
MBa
MBa2
LBa
Shale Base Line
Perforation
Oil / Gas
HC shows
Gas
Oil/Gas
Oil

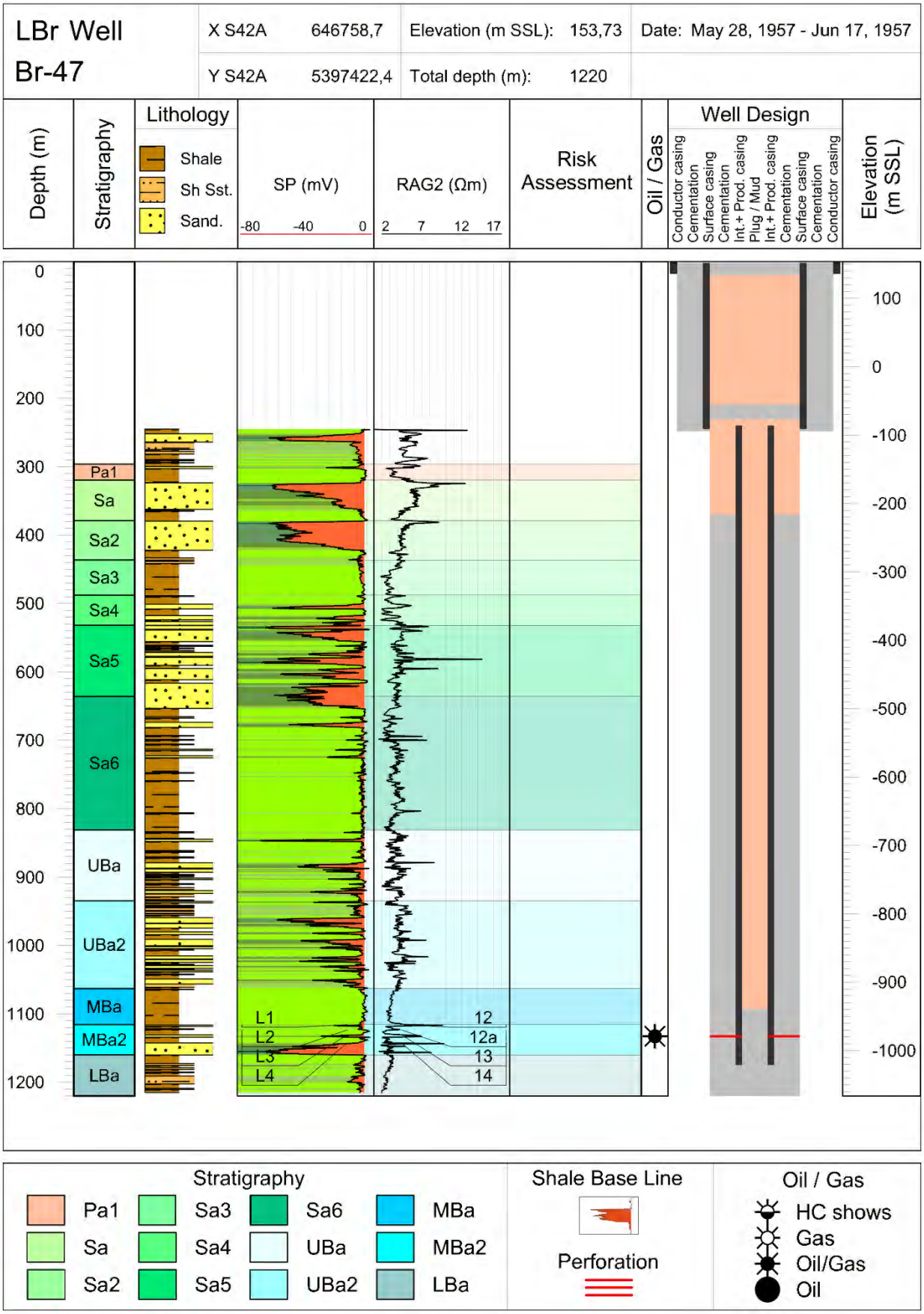
LBr Well
Br-47
X S42A 646758,7
Y S42A 5397422,4
Elevation (m SSL): 153,73
Total depth (m): 1220
Date: May 28, 1957 - Jun 17, 1957
Depth (m)
Stratigraphy
Lithology
Shale
Sh Sst.
Sand.
SP (mV)
-80 -40 0
RAG2 (Ωm)
2 7 12 17
Risk Assessment
Oil / Gas
Well Design
Conductor casing
Cementation
Surface casing
Cementation
Int.+ Prod. casing
Plug / Mud
Int.+ Prod. casing
Cementation
Surface casing
Cementation
Conductor casing
Elevation (m SSL)
0
100
200
300
400
500
600
700
800
900
1000
1100
1200
Pa1
Sa
Sa2
Sa3
Sa4
Sa5
Sa6
UBa
UBa2
MBa
MBa2
LBa
L1
L2
L3
L4
12
12a
13
14
100
0
-100
-200
-300
-400
-500
-600
-700
-800
-900
-1000
Stratigraphy
Pa1
Sa
Sa2
Sa3
Sa4
Sa5
Sa6
UBa
UBa2
MBa
MBa2
LBa
Shale Base Line
Perforation
Oil / Gas
HC shows
Gas
Oil/Gas
Oil

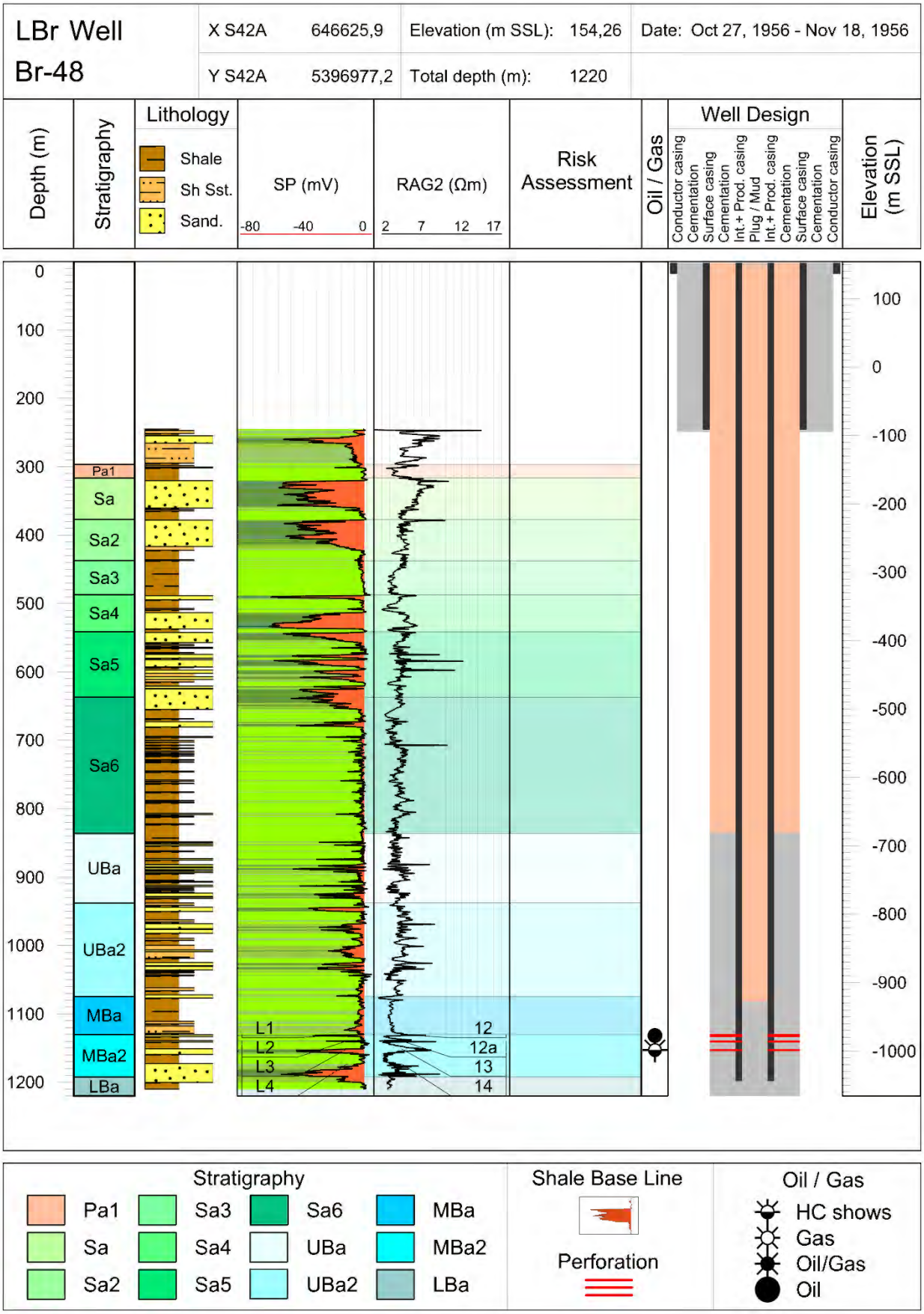
LBr Well
Br-48
X S42A 646625,9
Y S42A 5396977,2
Elevation (m SSL): 154,26
Total depth (m): 1220
Date: Oct 27, 1956 - Nov 18, 1956
Depth (m)
Stratigraphy
Lithology
Shale
Sh Sst.
Sand.
SP (mV)
-80 -40 0
RAG2 (Ωm)
2 7 12 17
Risk Assessment
Oil / Gas
Well Design
Conductor casing
Cementation
Surface casing
Cementation
Int.+ Prod. casing
Plug / Mud
Int.+ Prod. casing
Cementation
Surface casing
Cementation
Conductor casing
Elevation (m SSL)
0
100
200
300
400
500
600
700
800
900
1000
1100
1200
Pa1
Sa
Sa2
Sa3
Sa4
Sa5
Sa6
UBa
UBa2
MBa
MBa2
LBa
L1
L2
L3
L4
12
12a
13
14
100
0
-100
-200
-300
-400
-500
-600
-700
-800
-900
-1000
Stratigraphy
Pa1
Sa
Sa2
Sa3
Sa4
Sa5
Sa6
UBa
UBa2
MBa
MBa2
LBa
Shale Base Line
Perforation
Oil / Gas
HC shows
Gas
Oil/Gas
Oil

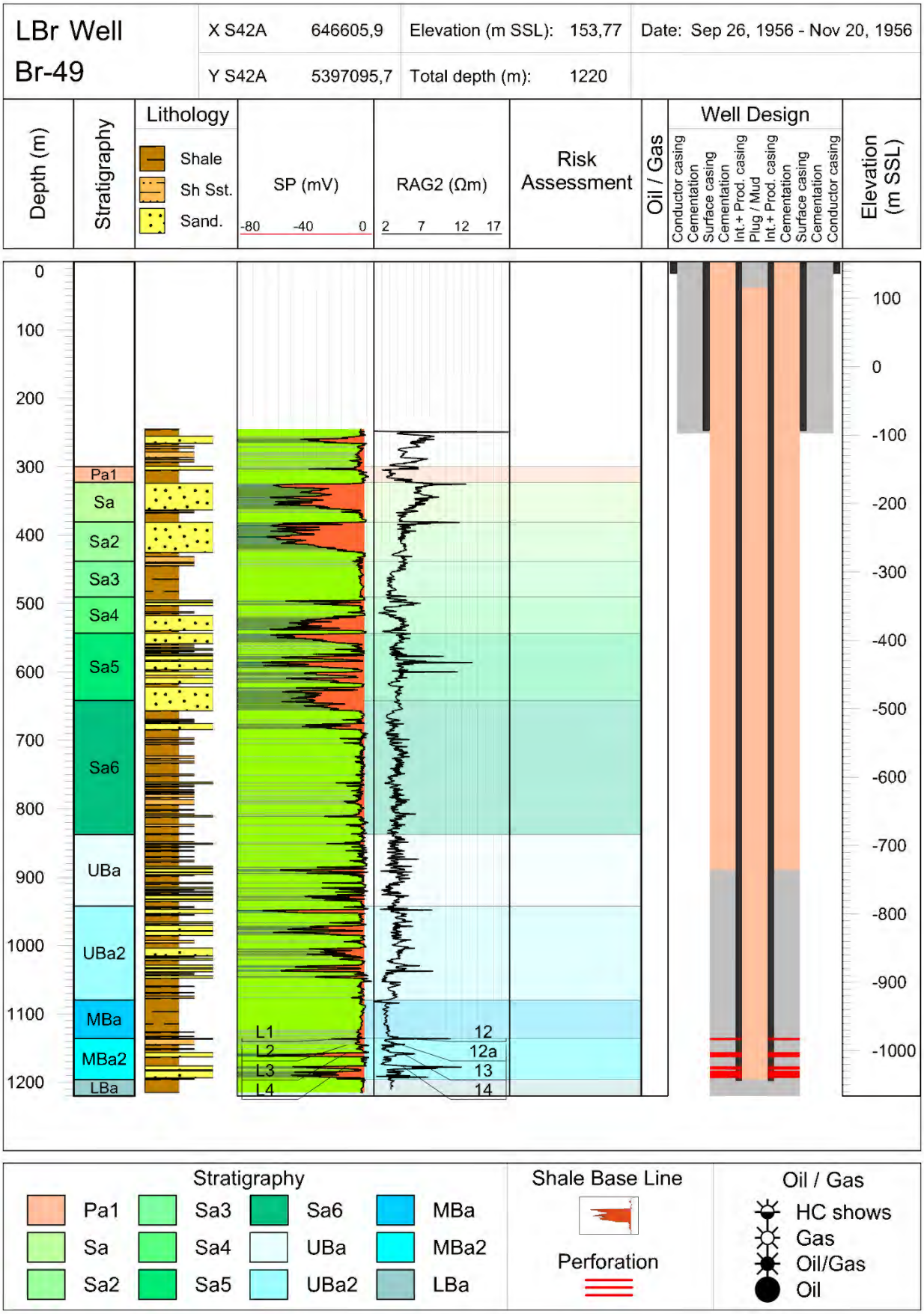
LBr Well
Br-49
X S42A 646605,9
Y S42A 5397095,7
Elevation (m SSL): 153,77
Total depth (m): 1220
Date: Sep 26, 1956 - Nov 20, 1956
Depth (m)
Stratigraphy
Lithology
Shale
Sh Sst.
Sand.
SP (mV)
-80 -40 0
RAG2 (Ωm)
2 7 12 17
Risk Assessment
Oil / Gas
Well Design
Conductor casing
Cementation
Surface casing
Cementation
Int.+ Prod. casing
Plug / Mud
Int.+ Prod. casing
Cementation
Surface casing
Cementation
Conductor casing
Elevation (m SSL)
0
100
200
300
400
500
600
700
800
900
1000
1100
1200
Pa1
Sa
Sa2
Sa3
Sa4
Sa5
Sa6
UBa
UBa2
MBa
MBa2
LBa
L1
L2
L3
L4
12
12a
13
14
100
0
-100
-200
-300
-400
-500
-600
-700
-800
-900
-1000
Stratigraphy
Pa1
Sa
Sa2
Sa3
Sa4
Sa5
Sa6
UBa
UBa2
MBa
MBa2
LBa
Shale Base Line
Perforation
Oil / Gas
HC shows
Gas
Oil/Gas
Oil

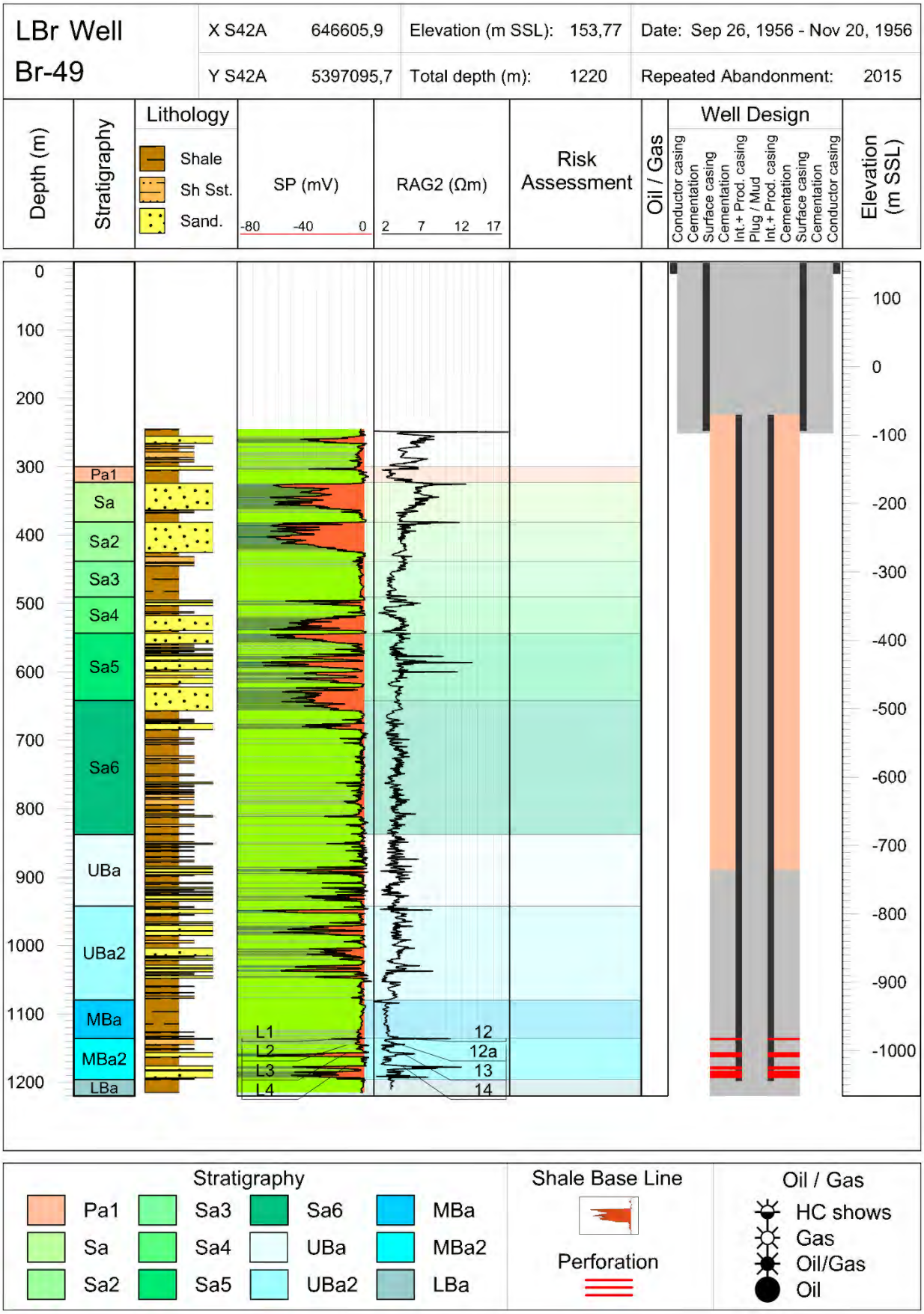
LBr Well
Br-49
X S42A 646605,9
Y S42A 5397095,7
Elevation (m SSL): 153,77
Total depth (m): 1220
Date: Sep 26, 1956 - Nov 20, 1956
Repeated Abandonment: 2015
Depth (m)
Stratigraphy
Lithology
Shale
Sh Sst.
Sand.
SP (mV)
-80 -40 0
RAG2 (Ωm)
2 7 12 17
Risk Assessment
Oil / Gas
Well Design
Conductor casing
Cementation
Surface casing
Cementation
Int.+ Prod. casing
Plug / Mud
Int.+ Prod. casing
Cementation
Surface casing
Cementation
Conductor casing
Elevation (m SSL)
0
100
200
300
400
500
600
700
800
900
1000
1100
1200
Pa1
Sa
Sa2
Sa3
Sa4
Sa5
Sa6
UBa
UBa2
MBa
MBa2
LBa
L1
L2
L3
L4
12
12a
13
14
100
0
-100
-200
-300
-400
-500
-600
-700
-800
-900
-1000
Stratigraphy
Pa1
Sa
Sa2
Sa3
Sa4
Sa5
Sa6
UBa
UBa2
MBa
MBa2
LBa
Shale Base Line
Perforation
Oil / Gas
HC shows
Gas
Oil/Gas
Oil

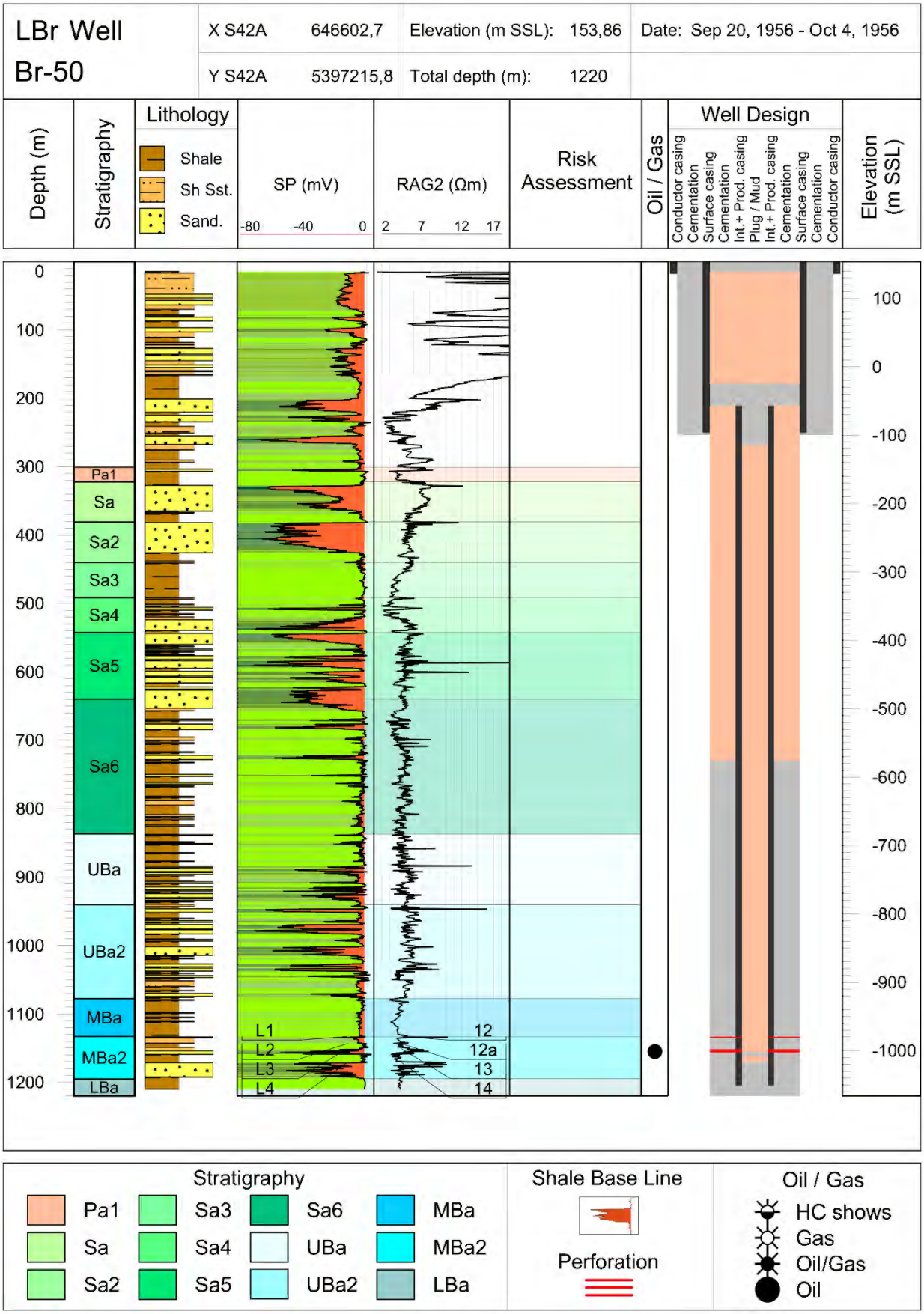
LBr Well
Br-50
X S42A 646602,7
Y S42A 5397215,8
Elevation (m SSL): 153,86
Total depth (m): 1220
Date: Sep 20, 1956 - Oct 4, 1956
Depth (m)
Stratigraphy
Lithology
Shale
Sh Sst.
Sand.
SP (mV)
-80 -40 0
RAG2 (Ωm)
2 7 12 17
Risk Assessment
Oil / Gas
Well Design
Conductor casing
Cementation
Surface casing
Cementation
Int.+ Prod. casing
Plug / Mud
Int.+ Prod. casing
Cementation
Surface casing
Cementation
Conductor casing
Elevation (m SSL)
0
100
200
300
400
500
600
700
800
900
1000
1100
1200
Pa1
Sa
Sa2
Sa3
Sa4
Sa5
Sa6
UBa
UBa2
MBa
MBa2
LBa
L1
L2
L3
L4
12
12a
13
14
100
0
-100
-200
-300
-400
-500
-600
-700
-800
-900
-1000
Stratigraphy
Pa1
Sa
Sa2
Sa3
Sa4
Sa5
Sa6
UBa
UBa2
MBa
MBa2
LBa
Shale Base Line
Perforation
Oil / Gas
HC shows
Gas
Oil/Gas
Oil

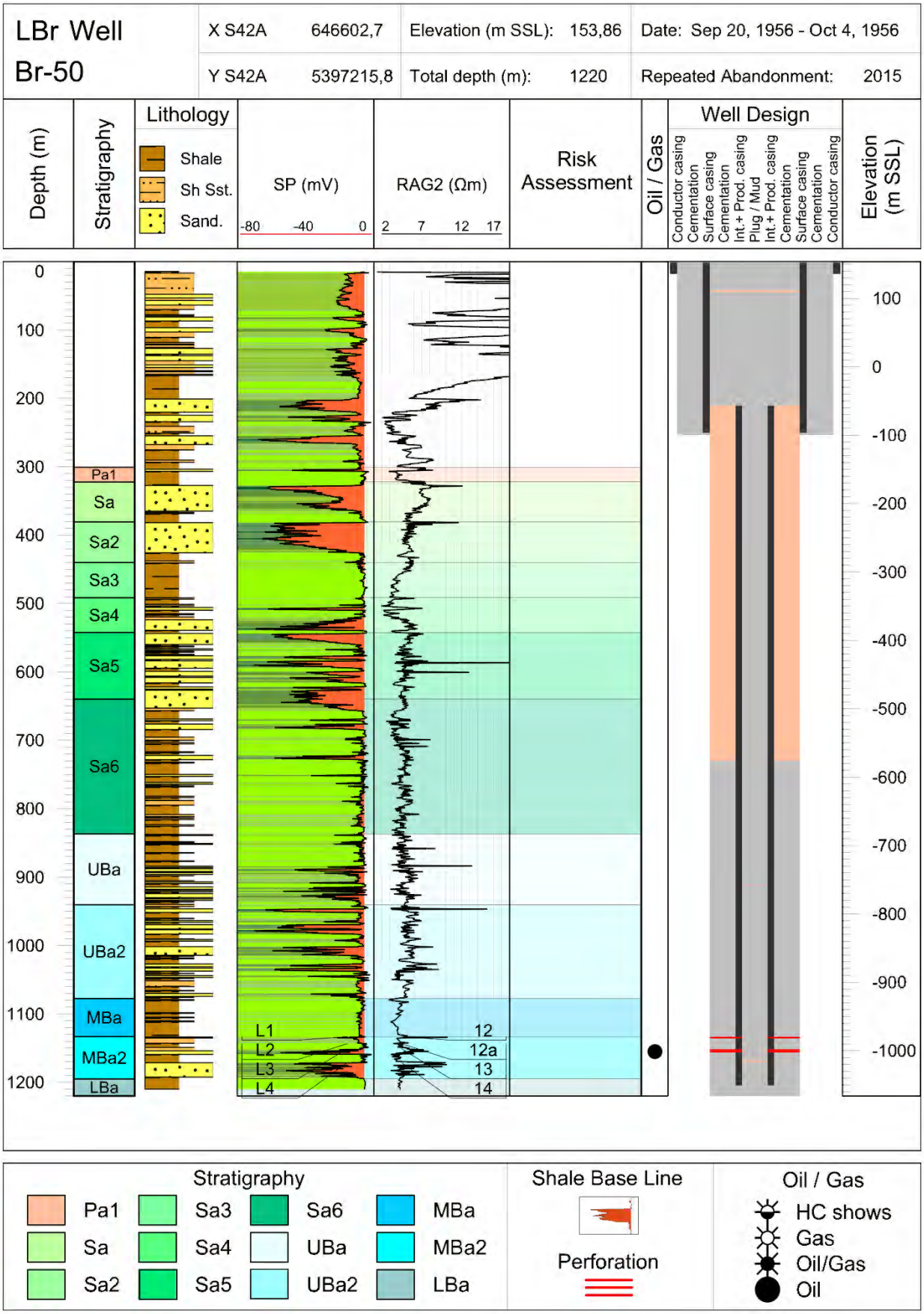
LBr Well
Br-50
X S42A 646602,7
Y S42A 5397215,8
Elevation (m SSL): 153,86
Total depth (m): 1220
Date: Sep 20, 1956 - Oct 4, 1956
Repeated Abandonment: 2015
Depth (m)
Stratigraphy
Lithology
Shale
Sh Sst.
Sand.
SP (mV)
-80 -40 0
RAG2 (Ωm)
2 7 12 17
Risk Assessment
Oil / Gas
Well Design
Conductor casing
Cementation
Surface casing
Cementation
Int.+ Prod. casing
Plug / Mud
Int.+ Prod. casing
Cementation
Surface casing
Cementation
Conductor casing
Elevation (m SSL)
0
100
200
300
400
500
600
700
800
900
1000
1100
1200
Pa1
Sa
Sa2
Sa3
Sa4
Sa5
Sa6
UBa
UBa2
MBa
MBa2
LBa
L1
L2
L3
L4
12
12a
13
14
100
0
-100
-200
-300
-400
-500
-600
-700
-800
-900
-1000
Stratigraphy
Pa1
Sa
Sa2
Sa3
Sa4
Sa5
Sa6
UBa
UBa2
MBa
MBa2
LBa
Shale Base Line
Perforation
Oil / Gas
HC shows
Gas
Oil/Gas
Oil

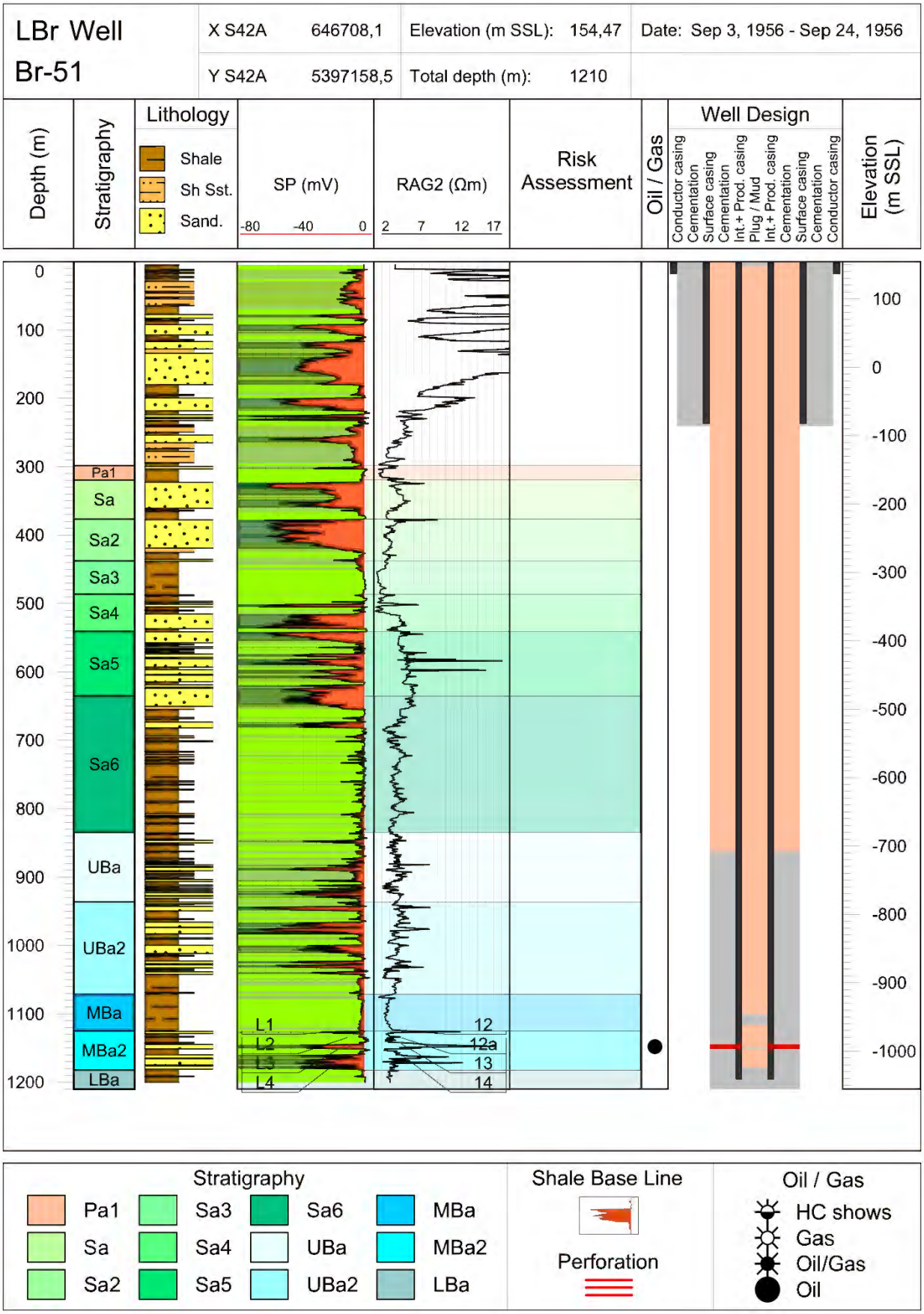
LBr Well
Br-51
X S42A 646708,1
Y S42A 5397158,5
Elevation (m SSL): 154,47
Total depth (m): 1210
Date: Sep 3, 1956 - Sep 24, 1956
Depth (m)
Stratigraphy
Lithology
Shale
Sh Sst.
Sand.
SP (mV)
-80 -40 0
RAG2 (Ωm)
2 7 12 17
Risk Assessment
Oil / Gas
Well Design
Conductor casing
Cementation
Surface casing
Cementation
Int.+ Prod. casing
Plug / Mud
Int.+ Prod. casing
Cementation
Surface casing
Cementation
Conductor casing
Elevation (m SSL)
0
100
200
300
400
500
600
700
800
900
1000
1100
1200
Pa1
Sa
Sa2
Sa3
Sa4
Sa5
Sa6
UBa
UBa2
MBa
MBa2
LBa
L1
L2
L3
L4
12
12a
13
14
100
0
-100
-200
-300
-400
-500
-600
-700
-800
-900
-1000
Stratigraphy
Pa1
Sa
Sa2
Sa3
Sa4
Sa5
Sa6
UBa
UBa2
MBa
MBa2
LBa
Shale Base Line
Perforation
Oil / Gas
HC shows
Gas
Oil/Gas
Oil

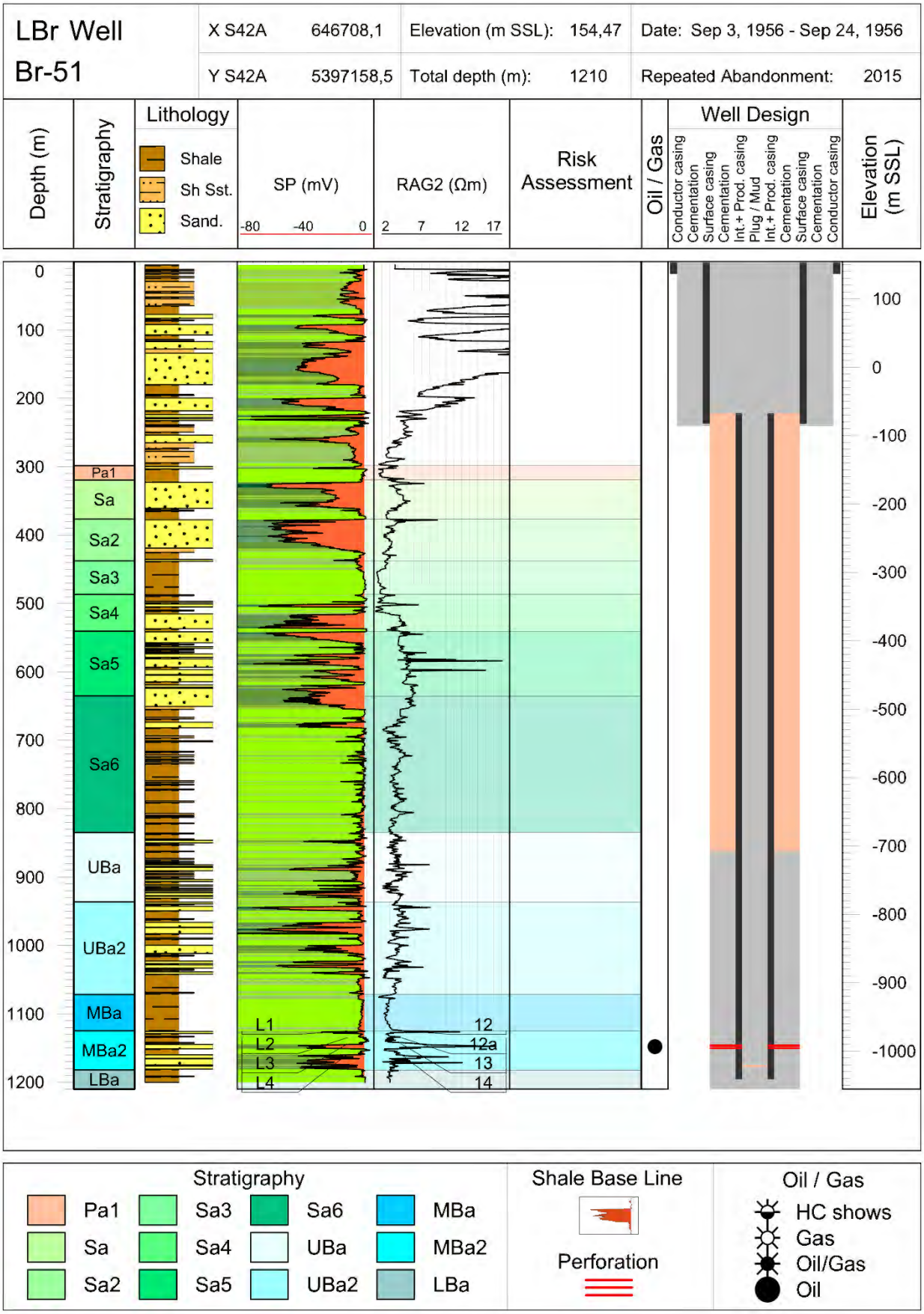
LBr Well
Br-51
X S42A 646708,1
Y S42A 5397158,5
Elevation (m SSL): 154,47
Total depth (m): 1210
Date: Sep 3, 1956 - Sep 24, 1956
Repeated Abandonment: 2015
Depth (m)
Stratigraphy
Lithology
Shale
Sh Sst.
Sand.
SP (mV)
-80 -40 0
RAG2 (Ωm)
2 7 12 17
Risk Assessment
Oil / Gas
Well Design
Conductor casing
Cementation
Surface casing
Cementation
Int.+ Prod. casing
Plug / Mud
Int.+ Prod. casing
Cementation
Surface casing
Cementation
Conductor casing
Elevation (m SSL)
0
100
200
300
400
500
600
700
800
900
1000
1100
1200
Pa1
Sa
Sa2
Sa3
Sa4
Sa5
Sa6
UBa
UBa2
MBa
MBa2
LBa
L1
L2
L3
L4
12
12a
13
14
100
0
-100
-200
-300
-400
-500
-600
-700
-800
-900
-1000
Stratigraphy
Pa1
Sa
Sa2
Sa3
Sa4
Sa5
Sa6
UBa
UBa2
MBa
MBa2
LBa
Shale Base Line
Perforation
Oil / Gas
HC shows
Gas
Oil/Gas
Oil

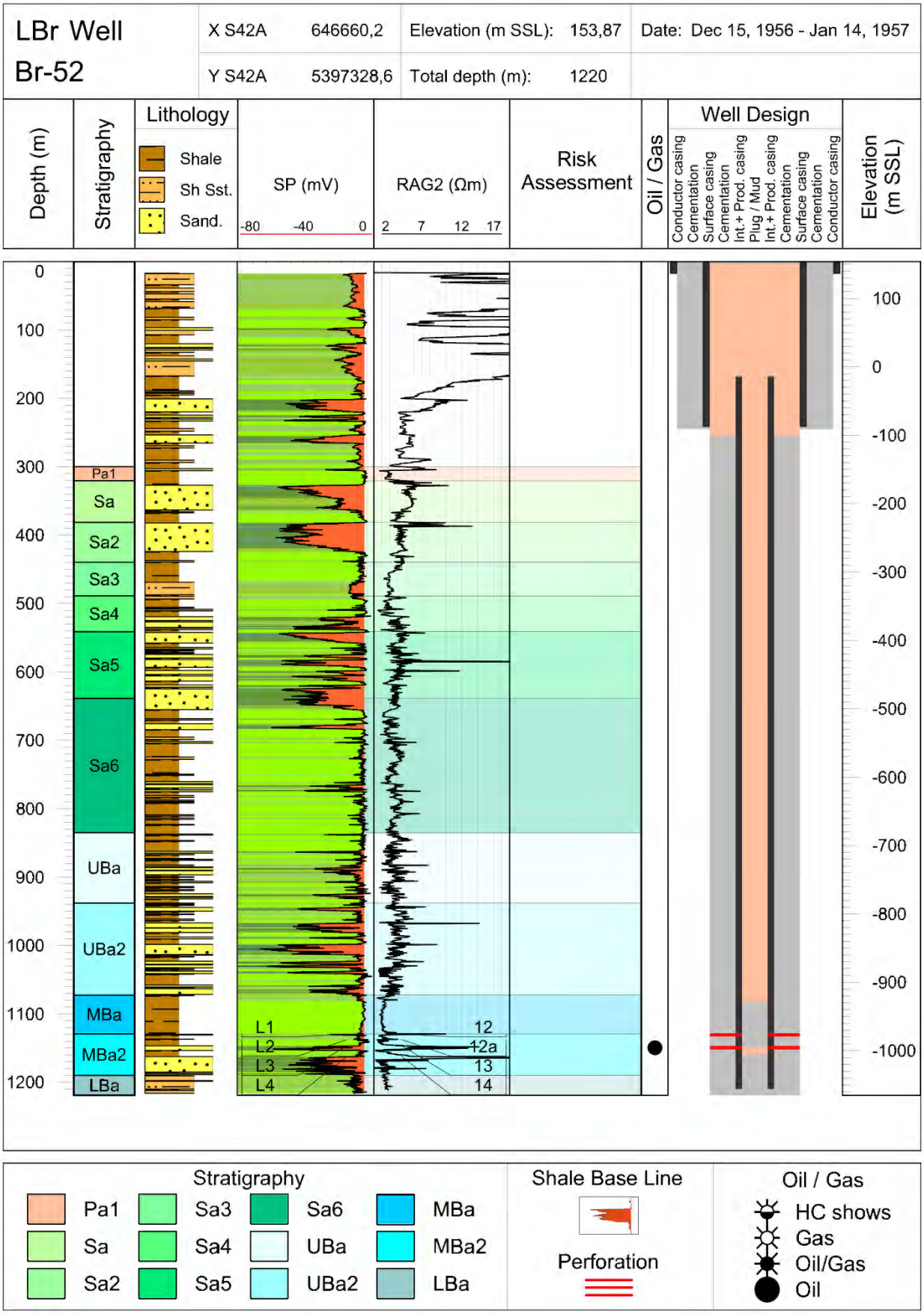
LBr Well
Br-52
X S42A 646660,2
Y S42A 5397328,6
Elevation (m SSL): 153,87
Total depth (m): 1220
Date: Dec 15, 1956 - Jan 14, 1957
Depth (m)
Stratigraphy
Lithology
Shale
Sh Sst.
Sand.
SP (mV)
-80 -40 0
RAG2 (Ωm)
2 7 12 17
Risk Assessment
Oil / Gas
Well Design
Conductor casing
Cementation
Surface casing
Cementation
Int.+ Prod. casing
Plug / Mud
Int.+ Prod. casing
Cementation
Surface casing
Cementation
Conductor casing
Elevation (m SSL)
0
100
200
300
400
500
600
700
800
900
1000
1100
1200
Pa1
Sa
Sa2
Sa3
Sa4
Sa5
Sa6
UBa
UBa2
MBa
MBa2
LBa
L1
L2
L3
L4
12
12a
13
14
100
0
-100
-200
-300
-400
-500
-600
-700
-800
-900
-1000
Stratigraphy
Pa1
Sa
Sa2
Sa3
Sa4
Sa5
Sa6
UBa
UBa2
MBa
MBa2
LBa
Shale Base Line
Perforation
Oil / Gas
HC shows
Gas
Oil/Gas
Oil

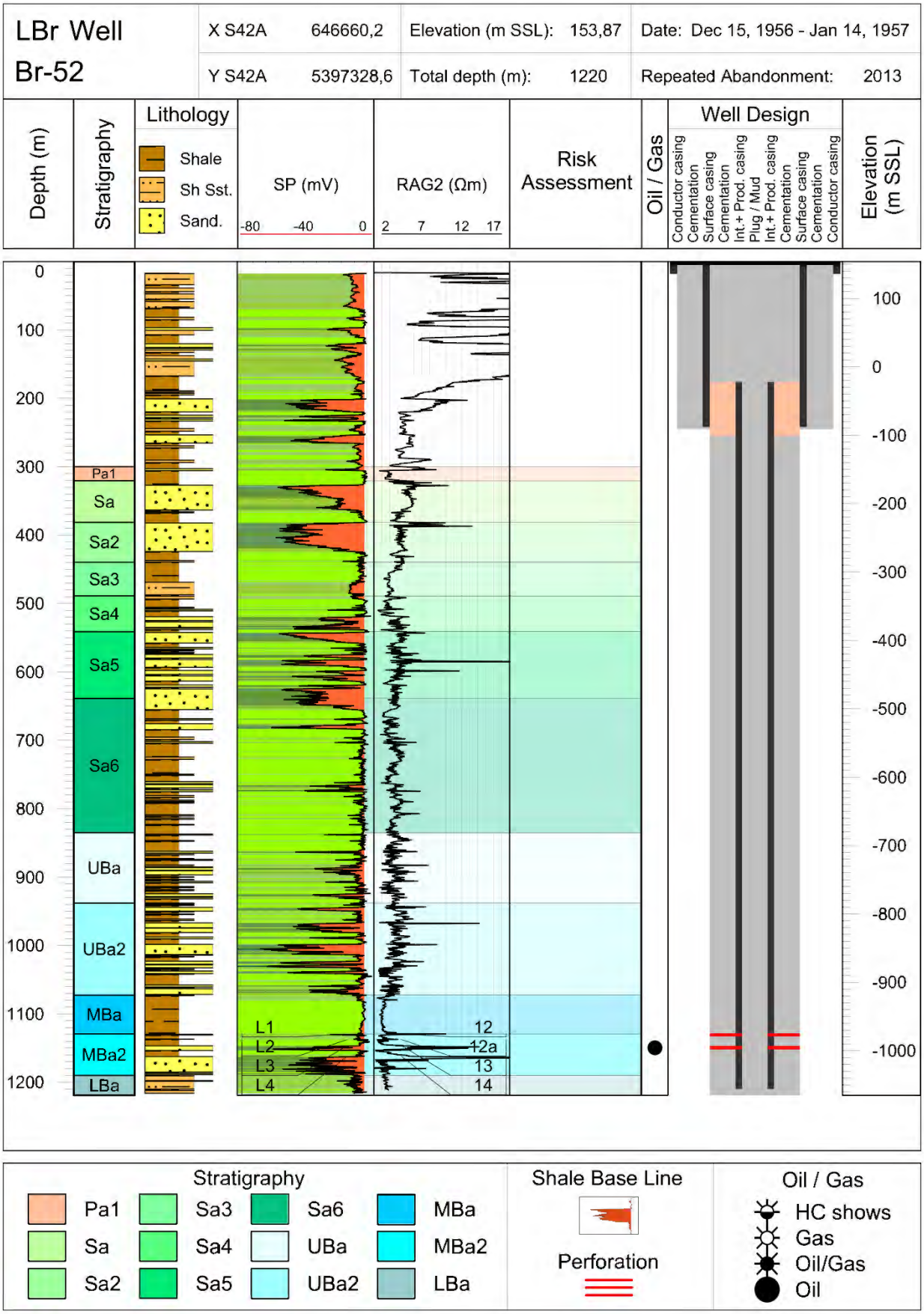
LBr Well
Br-52
X S42A 646660,2
Y S42A 5397328,6
Elevation (m SSL): 153,87
Total depth (m): 1220
Date: Dec 15, 1956 - Jan 14, 1957
Repeated Abandonment: 2013
Depth (m)
Stratigraphy
Lithology
Shale
Sh Sst.
Sand.
SP (mV)
-80 -40 0
RAG2 (Ωm)
2 7 12 17
Risk Assessment
Oil / Gas
Well Design
Conductor casing
Cementation
Surface casing
Cementation
Int.+ Prod. casing
Plug / Mud
Int.+ Prod. casing
Cementation
Surface casing
Cementation
Conductor casing
Elevation (m SSL)
0
100
200
300
400
500
600
700
800
900
1000
1100
1200
Pa1
Sa
Sa2
Sa3
Sa4
Sa5
Sa6
UBa
UBa2
MBa
MBa2
LBa
L1
L2
L3
L4
12
12a
13
14
100
0
-100
-200
-300
-400
-500
-600
-700
-800
-900
-1000
Stratigraphy
Pa1
Sa
Sa2
Sa3
Sa4
Sa5
Sa6
UBa
UBa2
MBa
MBa2
LBa
Shale Base Line
Perforation
Oil / Gas
HC shows
Gas
Oil/Gas
Oil

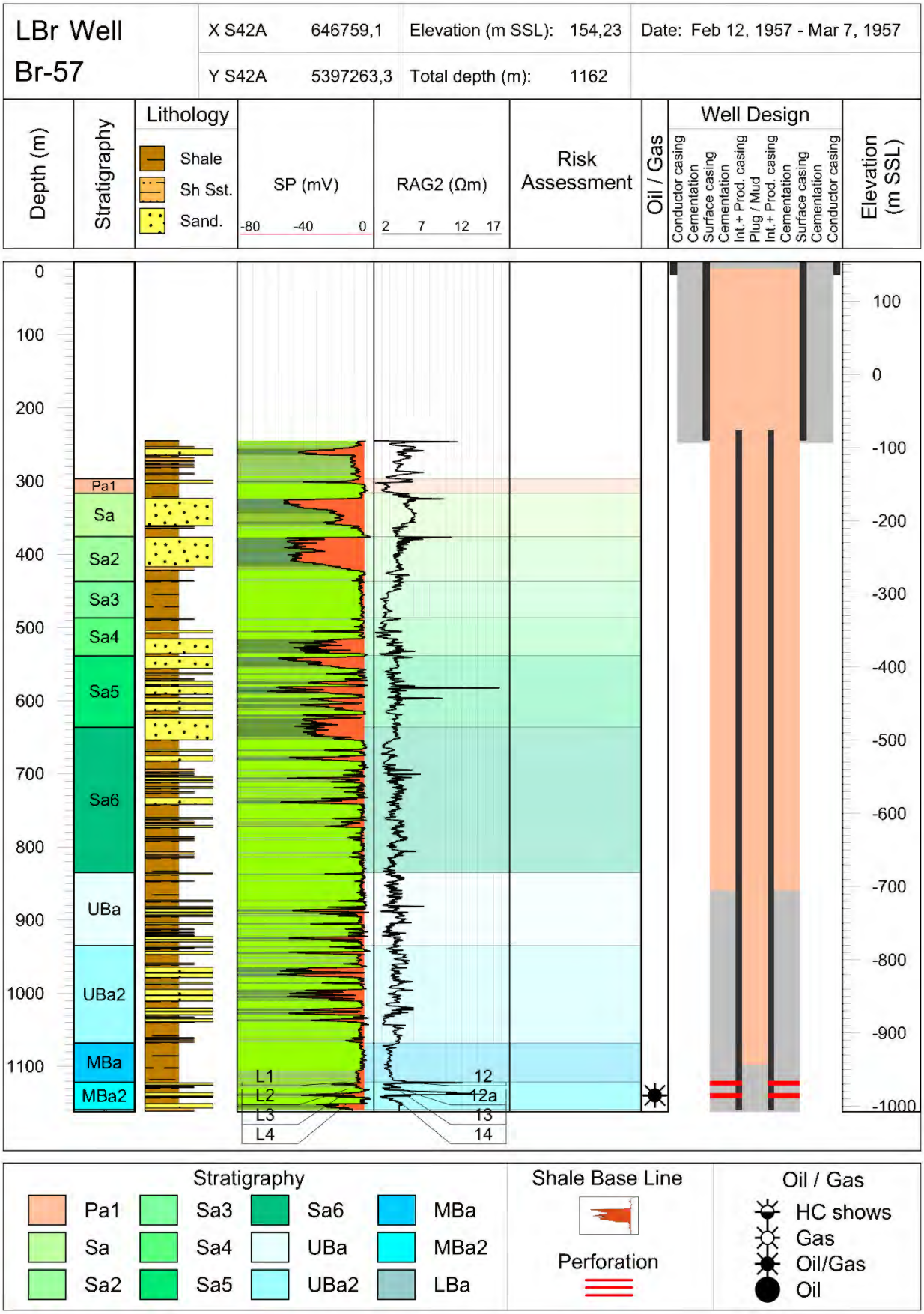
LBr Well
Br-57
X S42A 646759,1
Y S42A 5397263,3
Elevation (m SSL): 154,23
Total depth (m): 1162
Date: Feb 12, 1957 - Mar 7, 1957
Depth (m)
Stratigraphy
Lithology
Shale
Sh Sst.
Sand.
SP (mV)
-80 -40 0
RAG2 (Ωm)
2 7 12 17
Risk Assessment
Oil / Gas
Well Design
Conductor casing
Cementation
Surface casing
Cementation
Int.+ Prod. casing
Plug / Mud
Int.+ Prod. casing
Cementation
Surface casing
Cementation
Conductor casing
Elevation (m SSL)
0
100
200
300
400
500
600
700
800
900
1000
1100
Pa1
Sa
Sa2
Sa3
Sa4
Sa5
Sa6
UBa
UBa2
MBa
MBa2
L1
L2
L3
L4
12
12a
13
14
100
0
-100
-200
-300
-400
-500
-600
-700
-800
-900
-1000
Stratigraphy
Pa1
Sa
Sa2
Sa3
Sa4
Sa5
Sa6
UBa
UBa2
MBa
MBa2
LBa
Shale Base Line
Perforation
Oil / Gas
HC shows
Gas
Oil/Gas
Oil

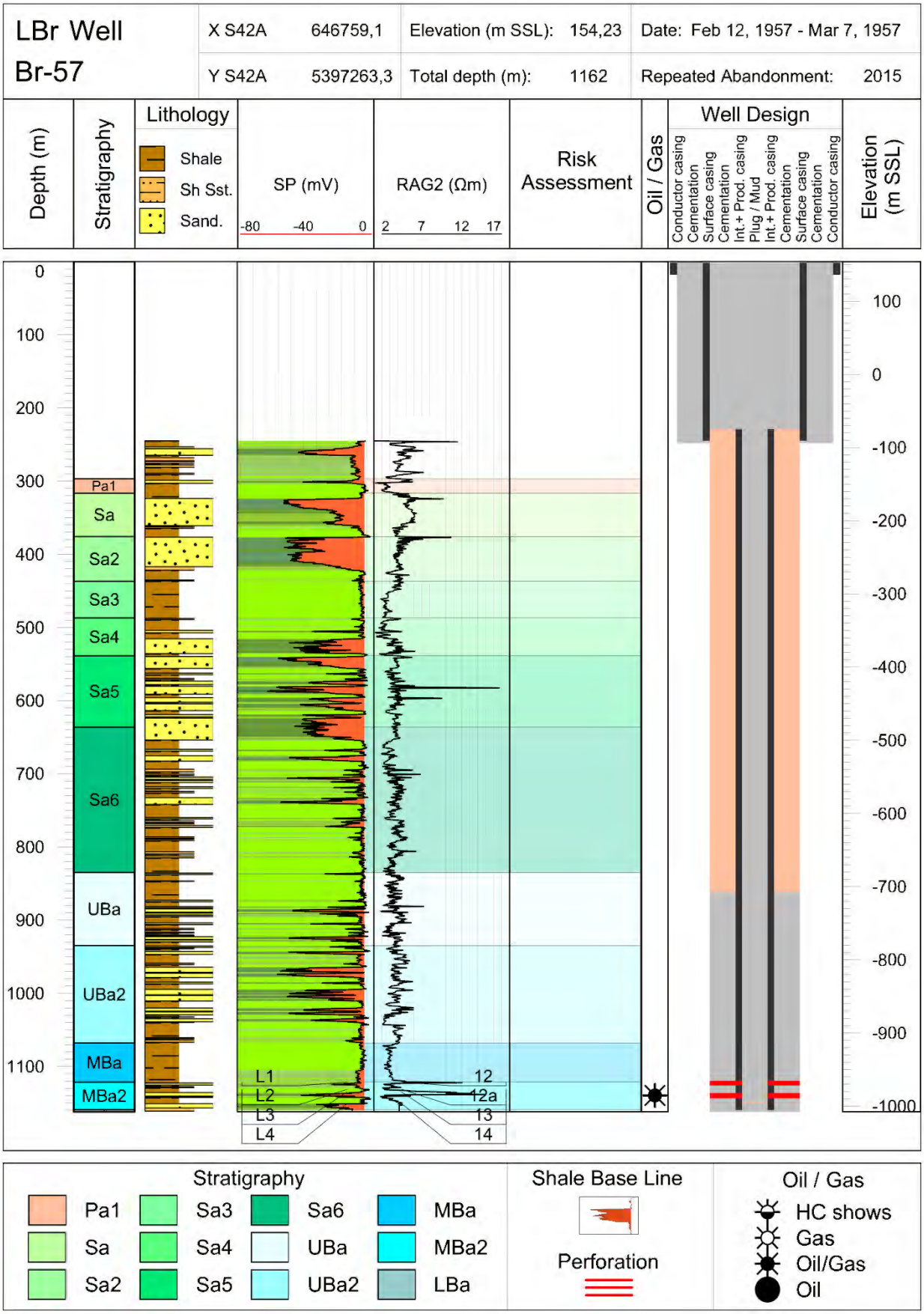
LBr Well
Br-57
X S42A 646759,1
Y S42A 5397263,3
Elevation (m SSL): 154,23
Total depth (m): 1162
Date: Feb 12, 1957 - Mar 7, 1957
Repeated Abandonment: 2015
Depth (m)
Stratigraphy
Lithology
Shale
Sh Sst.
Sand.
SP (mV)
-80 -40 0
RAG2 (Ωm)
2 7 12 17
Risk Assessment
Oil / Gas
Well Design
Conductor casing
Cementation
Surface casing
Cementation
Int.+ Prod. casing
Plug / Mud
Int.+ Prod. casing
Cementation
Surface casing
Cementation
Conductor casing
Elevation (m SSL)
0
100
200
300
400
500
600
700
800
900
1000
1100
Pa1
Sa
Sa2
Sa3
Sa4
Sa5
Sa6
UBa
UBa2
MBa
MBa2
L1
L2
L3
L4
12
12a
13
14
100
0
-100
-200
-300
-400
-500
-600
-700
-800
-900
-1000
Stratigraphy
Pa1
Sa
Sa2
Sa3
Sa4
Sa5
Sa6
UBa
UBa2
MBa
MBa2
LBa
Shale Base Line
Perforation
Oil / Gas
HC shows
Gas
Oil/Gas
Oil

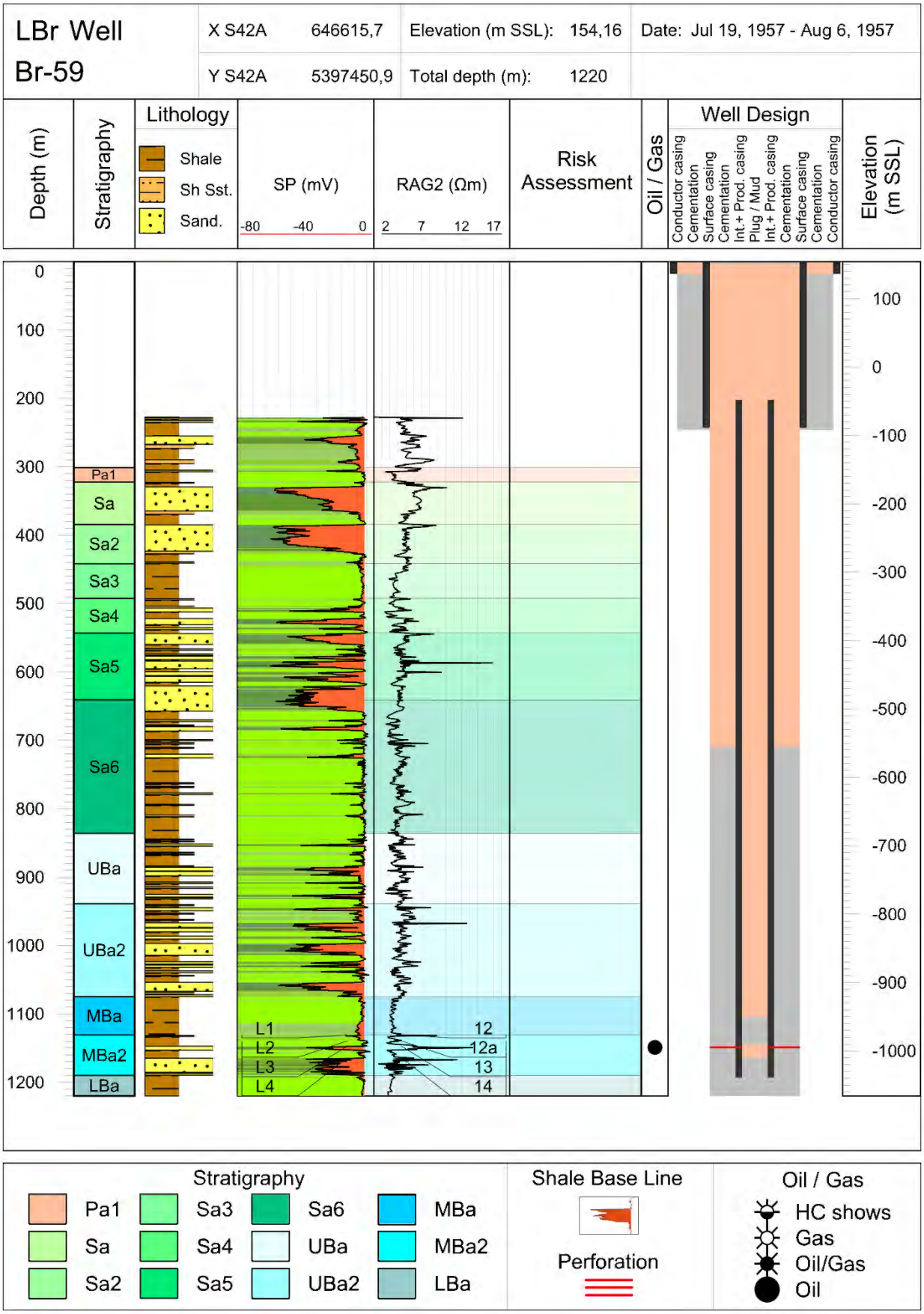
LBr Well
Br-59
X S42A 646615,7
Y S42A 5397450,9
Elevation (m SSL): 154,16
Total depth (m): 1220
Date: Jul 19, 1957 - Aug 6, 1957
Depth (m)
Stratigraphy
Lithology
Shale
Sh Sst.
Sand.
SP (mV)
-80 -40 0
RAG2 (Ωm)
2 7 12 17
Risk Assessment
Oil / Gas
Well Design
Conductor casing
Cementation
Surface casing
Cementation
Int.+ Prod. casing
Plug / Mud
Int.+ Prod. casing
Cementation
Surface casing
Cementation
Conductor casing
Elevation (m SSL)
0
100
200
300
400
500
600
700
800
900
1000
1100
1200
Pa1
Sa
Sa2
Sa3
Sa4
Sa5
Sa6
UBa
UBa2
MBa
MBa2
LBa
L1
L2
L3
L4
12
12a
13
14
100
0
-100
-200
-300
-400
-500
-600
-700
-800
-900
-1000
Stratigraphy
Pa1
Sa
Sa2
Sa3
Sa4
Sa5
Sa6
UBa
UBa2
MBa
MBa2
LBa
Shale Base Line
Perforation
Oil / Gas
HC shows
Gas
Oil/Gas
Oil

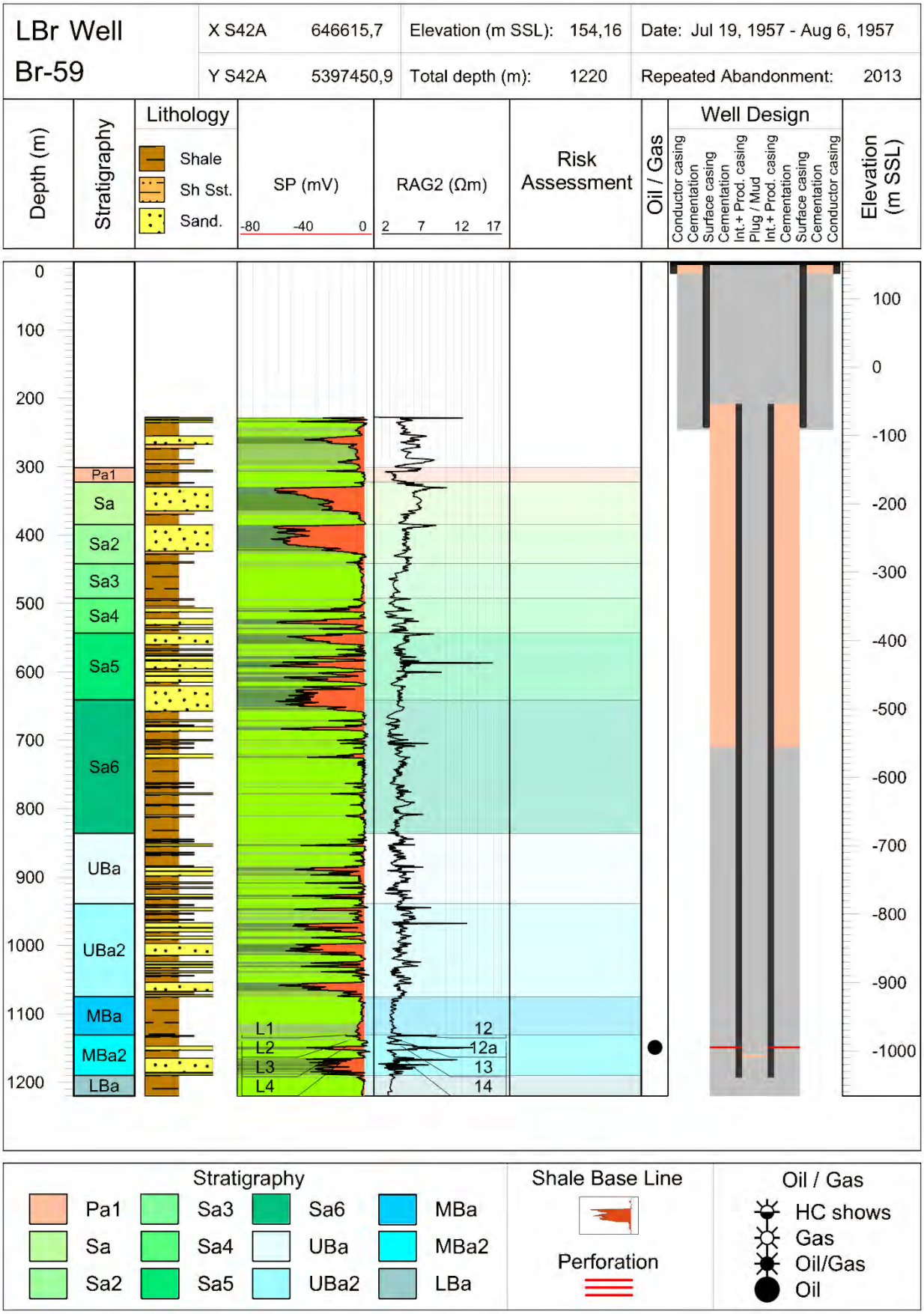
LBr Well
Br-59
X S42A 646615,7
Y S42A 5397450,9
Elevation (m SSL): 154,16
Total depth (m): 1220
Date: Jul 19, 1957 - Aug 6, 1957
Repeated Abandonment: 2013
Depth (m)
Stratigraphy
Lithology
Shale
Sh Sst.
Sand.
SP (mV)
-80 -40 0
RAG2 (Ωm)
2 7 12 17
Risk Assessment
Oil / Gas
Well Design
Conductor casing
Cementation
Surface casing
Cementation
Int.+ Prod. casing
Plug / Mud
Int.+ Prod. casing
Cementation
Surface casing
Cementation
Conductor casing
Elevation (m SSL)
0
100
200
300
400
500
600
700
800
900
1000
1100
1200
Pa1
Sa
Sa2
Sa3
Sa4
Sa5
Sa6
UBa
UBa2
MBa
MBa2
LBa
L1
L2
L3
L4
12
12a
13
14
100
0
-100
-200
-300
-400
-500
-600
-700
-800
-900
-1000
Stratigraphy
Pa1
Sa
Sa2
Sa3
Sa4
Sa5
Sa6
UBa
UBa2
MBa
MBa2
LBa
Shale Base Line
Perforation
Oil / Gas
HC shows
Gas
Oil/Gas
Oil

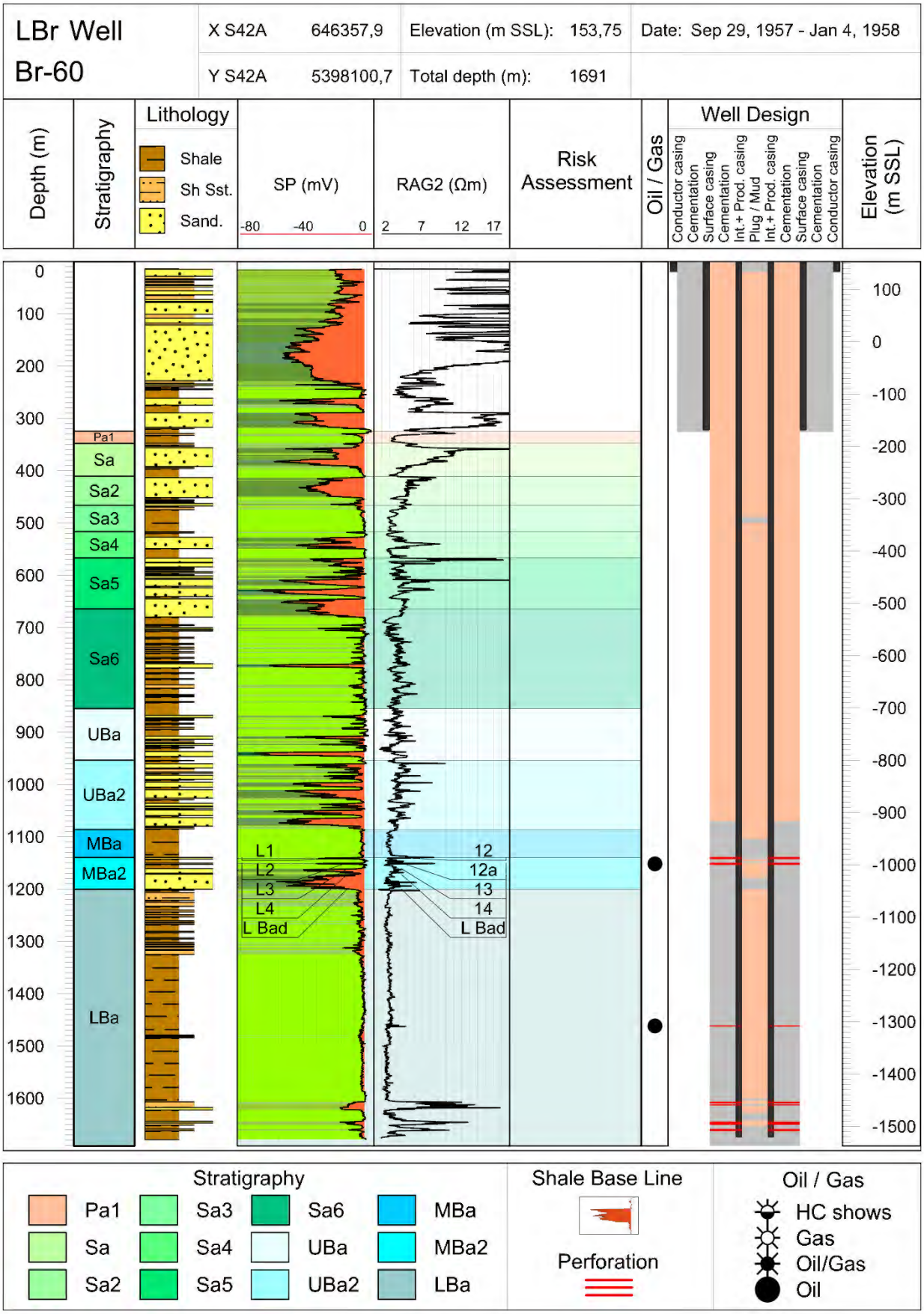
LBr Well
Br-60
X S42A 646357,9
Y S42A 5398100,7
Elevation (m SSL): 153,75
Total depth (m): 1691
Date: Sep 29, 1957 - Jan 4, 1958
Depth (m)
Stratigraphy
Lithology
Shale
Sh Sst.
Sand.
SP (mV)
-80 -40 0
RAG2 (Ωm)
2 7 12 17
Risk Assessment
Oil / Gas
Well Design
Conductor casing
Cementation
Surface casing
Cementation
Int.+ Prod. casing
Plug / Mud
Int.+ Prod. casing
Cementation
Surface casing
Cementation
Conductor casing
Elevation (m SSL)
0
100
200
300
400
500
600
700
800
900
1000
1100
1200
1300
1400
1500
1600
Pa1
Sa
Sa2
Sa3
Sa4
Sa5
Sa6
UBa
UBa2
MBa
MBa2
LBa
L1
L2
L3
L4
L Bad
12
12a
13
14
L Bad
100
0
-100
-200
-300
-400
-500
-600
-700
-800
-900
-1000
-1100
-1200
-1300
-1400
-1500
Stratigraphy
Pa1
Sa
Sa2
Sa3
Sa4
Sa5
Sa6
UBa
UBa2
MBa
MBa2
LBa
Shale Base Line
Perforation
Oil / Gas
HC shows
Gas
Oil/Gas
Oil

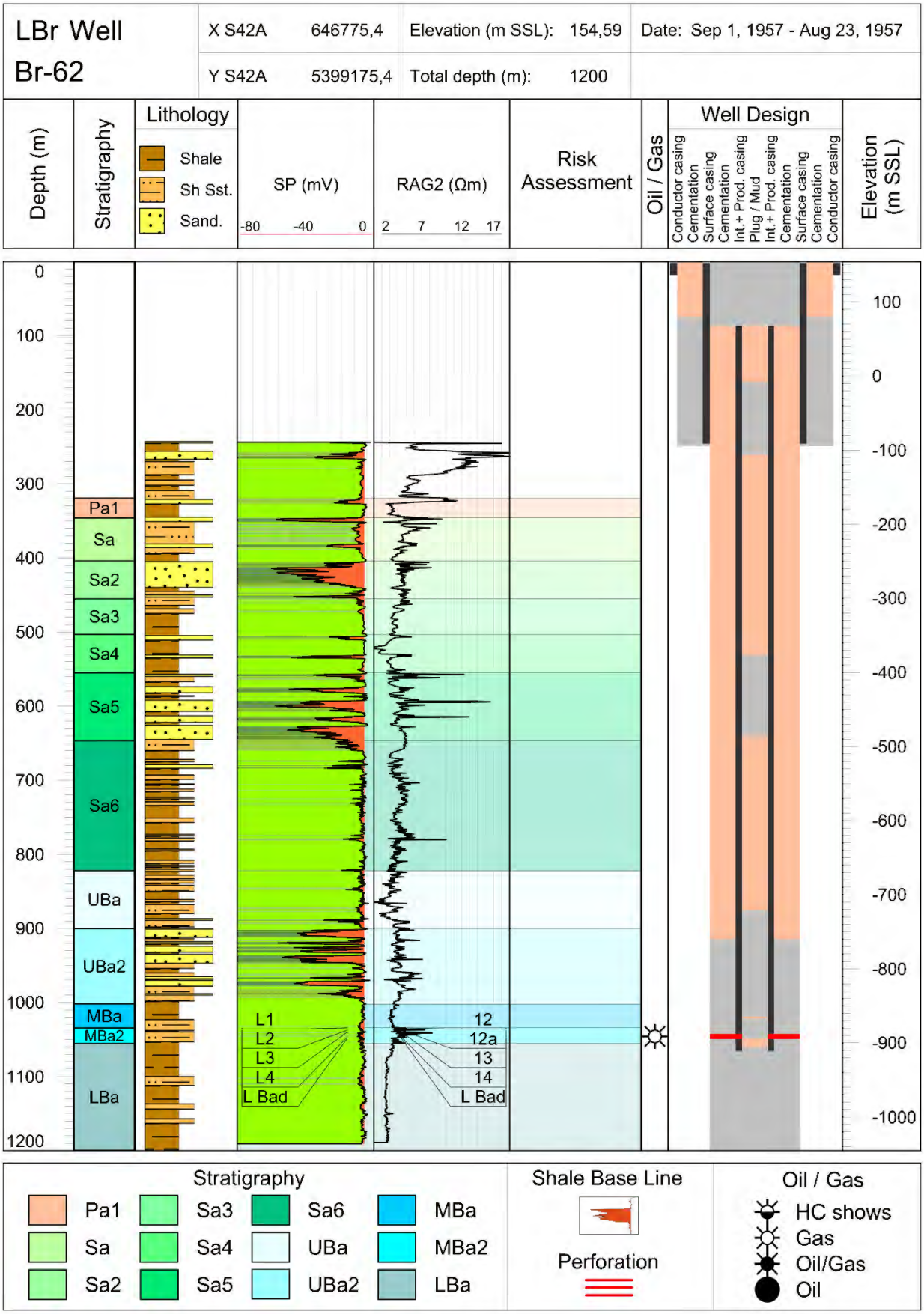
LBr Well
Br-62
X S42A 646775,4
Y S42A 5399175,4
Elevation (m SSL): 154,59
Total depth (m): 1200
Date: Sep 1, 1957 - Aug 23, 1957
Depth (m)
Stratigraphy
Lithology
Shale
Sh Sst.
Sand.
SP (mV)
-80 -40 0
RAG2 (Ωm)
2 7 12 17
Risk Assessment
Oil / Gas
Well Design
Conductor casing
Cementation
Surface casing
Cementation
Int.+ Prod. casing
Plug / Mud
Int.+ Prod. casing
Cementation
Surface casing
Cementation
Conductor casing
Elevation (m SSL)
0
100
200
300
400
500
600
700
800
900
1000
1100
1200
Pa1
Sa
Sa2
Sa3
Sa4
Sa5
Sa6
UBa
UBa2
MBa
MBa2
LBa
L1
L2
L3
L4
L Bad
12
12a
13
14
L Bad
100
0
-100
-200
-300
-400
-500
-600
-700
-800
-900
-1000
Stratigraphy
Pa1
Sa
Sa2
Sa3
Sa4
Sa5
Sa6
UBa
UBa2
MBa
MBa2
LBa
Shale Base Line
Perforation
Oil / Gas
HC shows
Gas
Oil/Gas
Oil

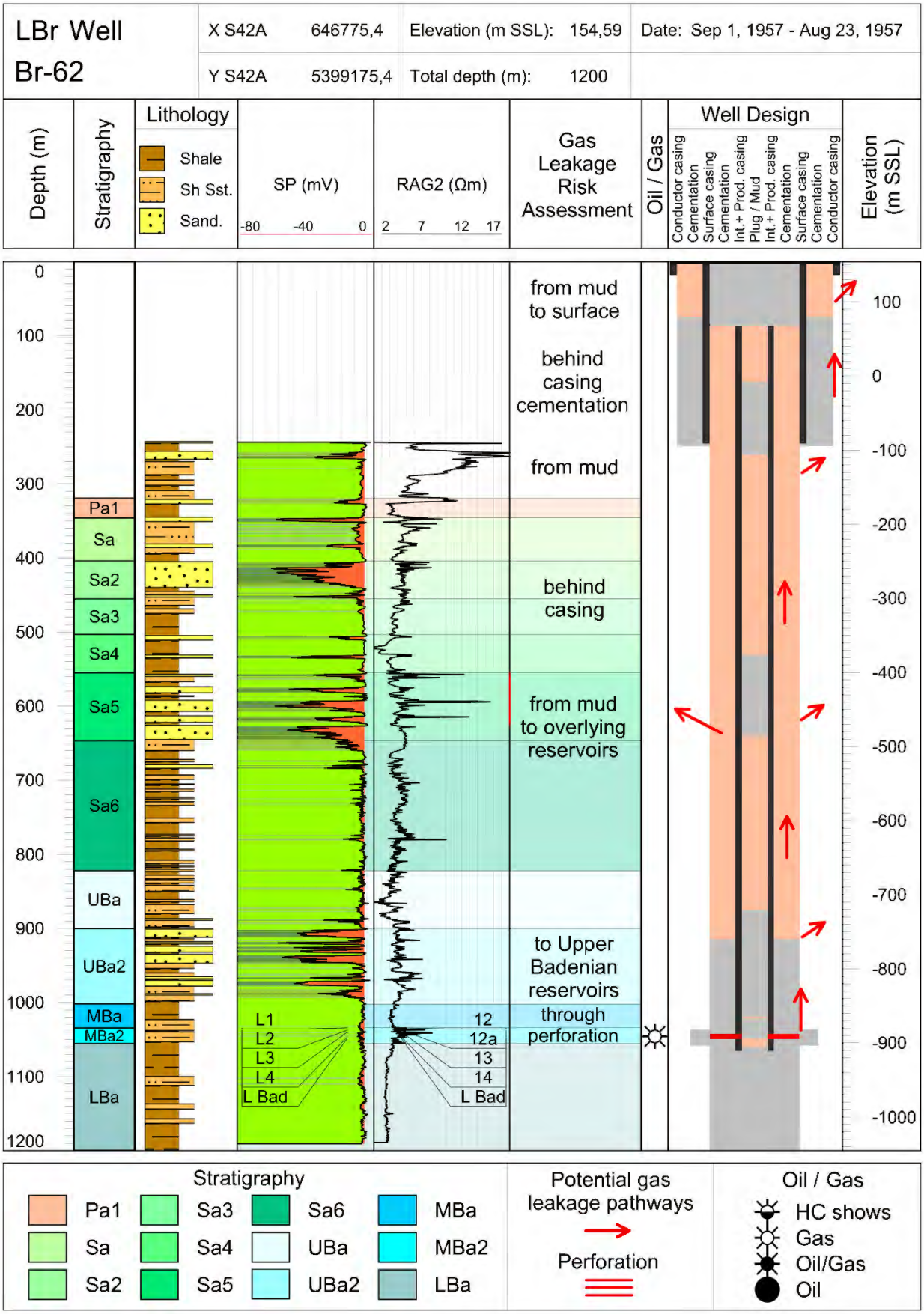
LBr Well
Br-62
X S42A 646775,4
Y S42A 5399175,4
Elevation (m SSL): 154,59
Total depth (m): 1200
Date: Sep 1, 1957 - Aug 23, 1957
Depth (m)
Stratigraphy
Lithology
Shale
Sh Sst.
Sand.
SP (mV)
-80 -40 0
RAG2 (Ωm)
2 7 12 17
Gas Leakage Risk Assessment
Oil / Gas
Well Design
Conductor casing
Cementation
Surface casing
Cementation
Int.+ Prod. casing
Plug / Mud
Int.+ Prod. casing
Cementation
Surface casing
Cementation
Conductor casing
Elevation (m SSL)
0
100
200
300
400
500
600
700
800
900
1000
1100
1200
Pa1
Sa
Sa2
Sa3
Sa4
Sa5
Sa6
UBa
UBa2
MBa
MBa2
LBa
L1
L2
L3
L4
L Bad
12
12a
13
14
L Bad
from mud to surface
behind casing cementation
from mud
behind casing
from mud to overlying reservoirs
to Upper Badenian reservoirs through perforation
100
0
-100
-200
-300
-400
-500
-600
-700
-800
-900
-1000
Stratigraphy
Pa1
Sa
Sa2
Sa3
Sa4
Sa5
Sa6
UBa
UBa2
MBa
MBa2
LBa
Potential gas leakage pathways
Perforation
Oil / Gas
HC shows
Gas
Oil/Gas
Oil

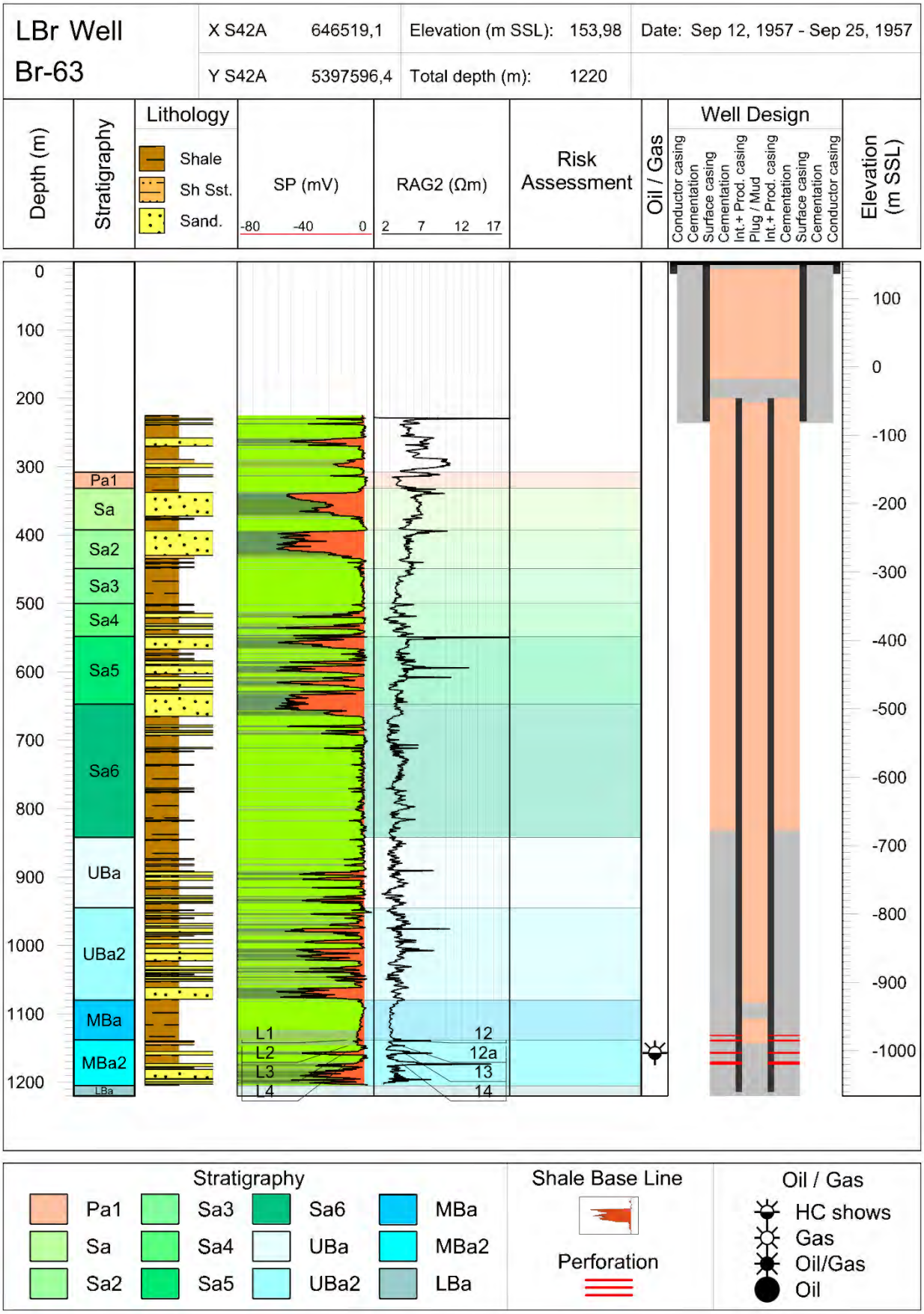
LBr Well
Br-63
X S42A 646519,1
Y S42A 5397596,4
Elevation (m SSL): 153,98
Total depth (m): 1220
Date: Sep 12, 1957 - Sep 25, 1957
Depth (m)
Stratigraphy
Lithology
Shale
Sh Sst.
Sand.
SP (mV)
-80 -40 0
RAG2 (Ωm)
2 7 12 17
Risk Assessment
Oil / Gas
Well Design
Conductor casing
Cementation
Surface casing
Cementation
Int.+ Prod. casing
Plug / Mud
Int.+ Prod. casing
Cementation
Surface casing
Cementation
Conductor casing
Elevation (m SSL)
0
100
200
300
400
500
600
700
800
900
1000
1100
1200
Pa1
Sa
Sa2
Sa3
Sa4
Sa5
Sa6
UBa
UBa2
MBa
MBa2
LBa
L1
L2
L3
L4
12
12a
13
14
100
0
-100
-200
-300
-400
-500
-600
-700
-800
-900
-1000
Stratigraphy
Pa1
Sa
Sa2
Sa3
Sa4
Sa5
Sa6
UBa
UBa2
MBa
MBa2
LBa
Shale Base Line
Perforation
Oil / Gas
HC shows
Gas
Oil/Gas
Oil

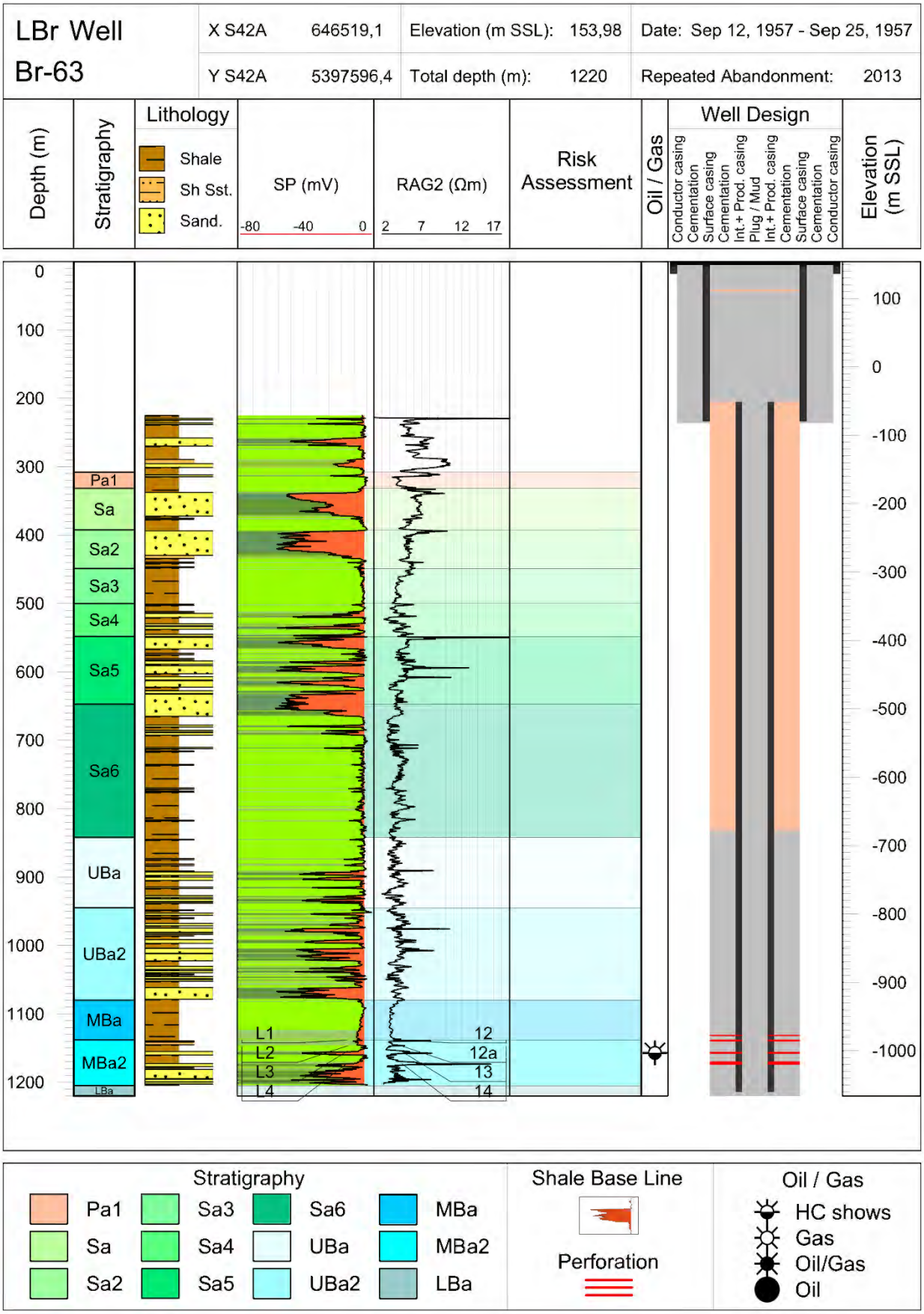
LBr Well
Br-63
X S42A 646519,1
Y S42A 5397596,4
Elevation (m SSL): 153,98
Total depth (m): 1220
Date: Sep 12, 1957 - Sep 25, 1957
Repeated Abandonment: 2013
Depth (m)
Stratigraphy
Lithology
Shale
Sh Sst.
Sand.
SP (mV)
-80 -40 0
RAG2 (Ωm)
2 7 12 17
Risk Assessment
Oil / Gas
Well Design
Conductor casing
Cementation
Surface casing
Cementation
Int.+ Prod. casing
Plug / Mud
Int.+ Prod. casing
Cementation
Surface casing
Cementation
Conductor casing
Elevation (m SSL)
0
100
200
300
400
500
600
700
800
900
1000
1100
1200
Pa1
Sa
Sa2
Sa3
Sa4
Sa5
Sa6
UBa
UBa2
MBa
MBa2
LBa
L1
L2
L3
L4
12
12a
13
14
100
0
-100
-200
-300
-400
-500
-600
-700
-800
-900
-1000
Stratigraphy
Pa1
Sa
Sa2
Sa3
Sa4
Sa5
Sa6
UBa
UBa2
MBa
MBa2
LBa
Shale Base Line
Perforation
Oil / Gas
HC shows
Gas
Oil/Gas
Oil

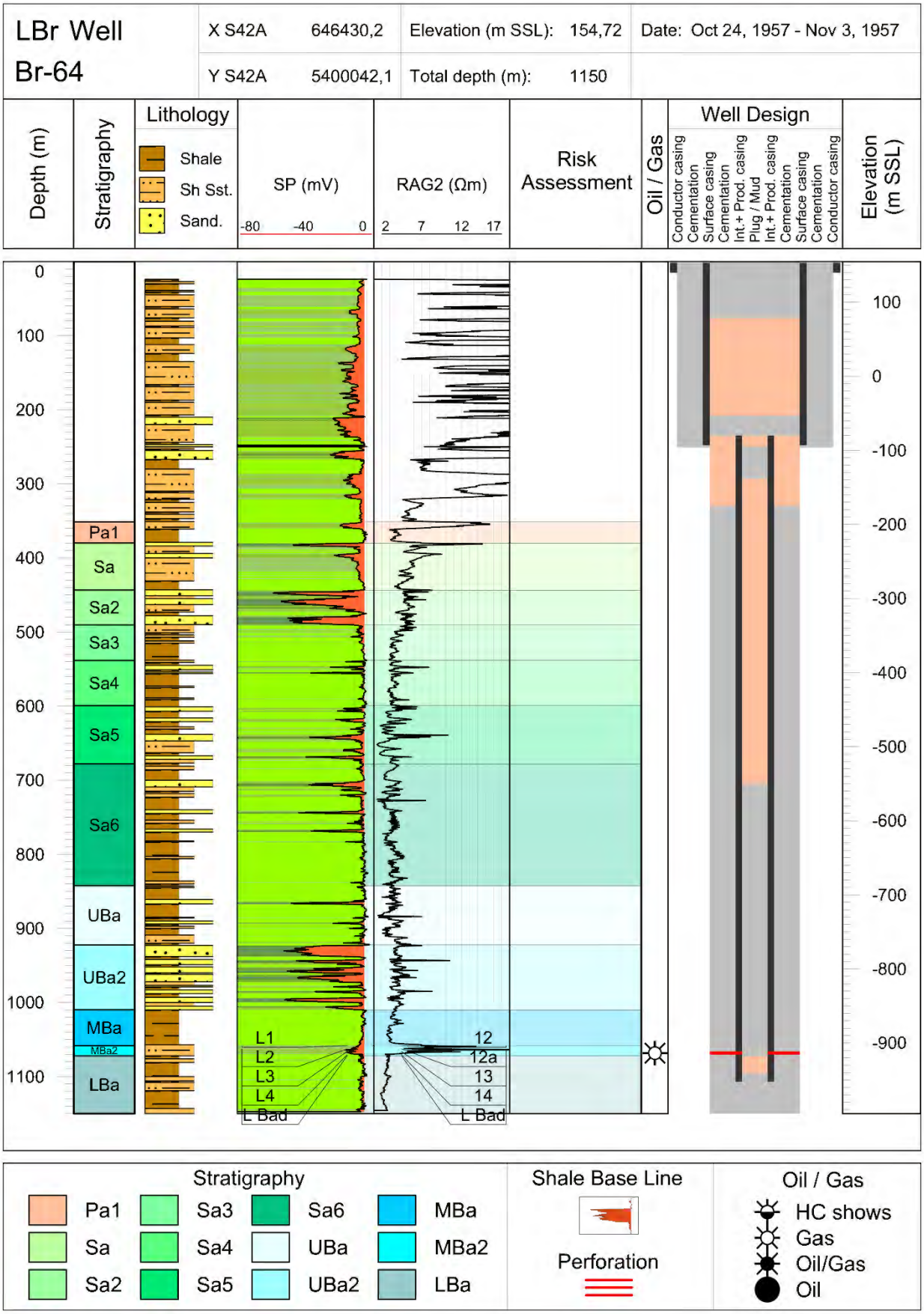
LBr Well
Br-64
X S42A 646430,2
Y S42A 5400042,1
Elevation (m SSL): 154,72
Total depth (m): 1150
Date: Oct 24, 1957 - Nov 3, 1957
Depth (m)
Stratigraphy
Lithology
Shale
Sh Sst.
Sand.
SP (mV)
-80 -40 0
RAG2 (Ωm)
2 7 12 17
Risk Assessment
Oil / Gas
Well Design
Conductor casing
Cementation
Surface casing
Cementation
Int.+ Prod. casing
Plug / Mud
Int.+ Prod. casing
Cementation
Surface casing
Cementation
Conductor casing
Elevation (m SSL)
0
100
200
300
400
500
600
700
800
900
1000
1100
Pa1
Sa
Sa2
Sa3
Sa4
Sa5
Sa6
UBa
UBa2
MBa
MBa2
LBa
L1
L2
L3
L4
L Bad
12
12a
13
14
L Bad
100
0
-100
-200
-300
-400
-500
-600
-700
-800
-900
Stratigraphy
Pa1
Sa
Sa2
Sa3
Sa4
Sa5
Sa6
UBa
UBa2
MBa
MBa2
LBa
Shale Base Line
Perforation
Oil / Gas
HC shows
Gas
Oil/Gas
Oil

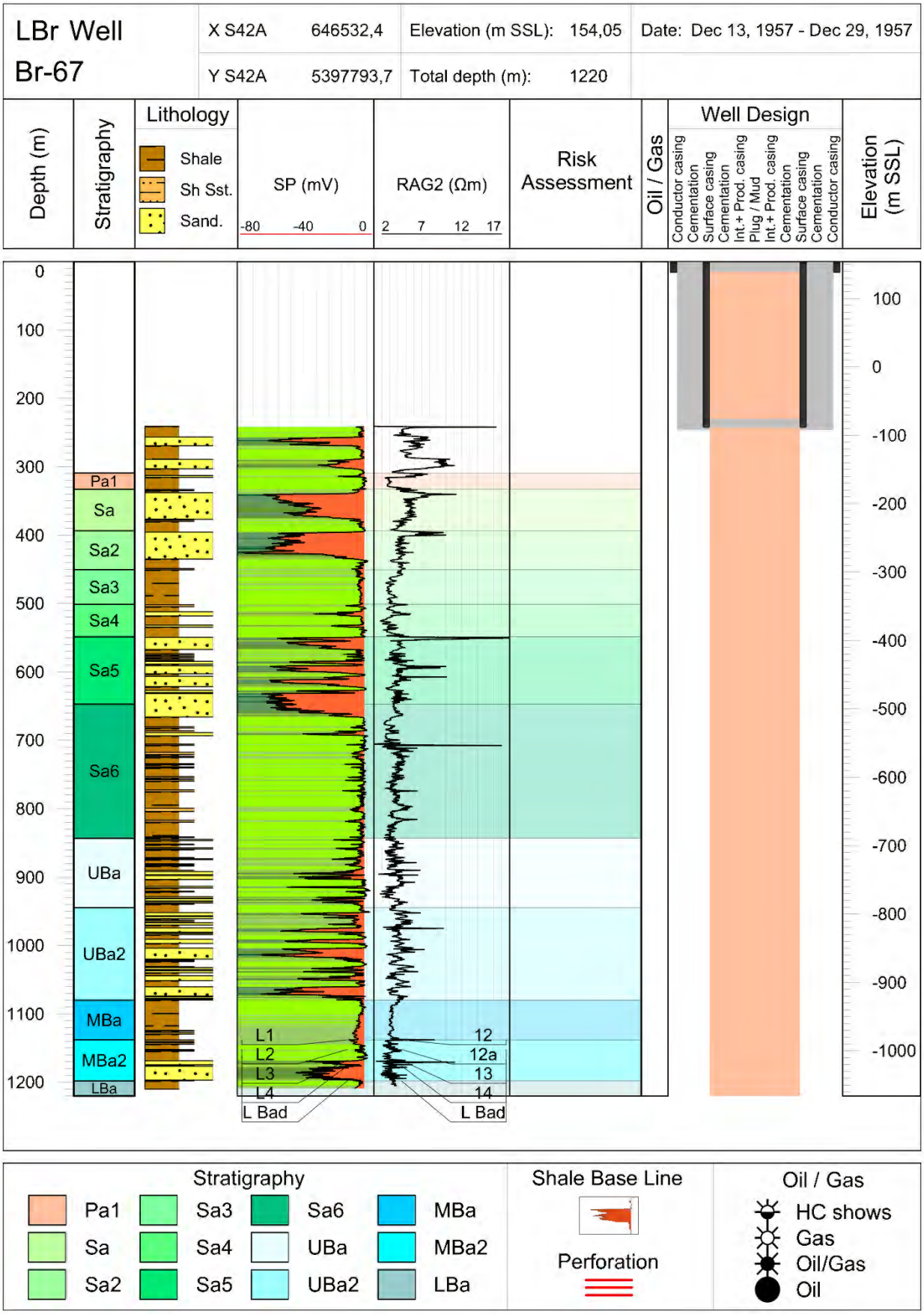
LBr Well
Br-67
X S42A 646532,4
Y S42A 5397793,7
Elevation (m SSL): 154,05
Total depth (m): 1220
Date: Dec 13, 1957 - Dec 29, 1957
Depth (m)
Stratigraphy
Lithology
Shale
Sh Sst.
Sand.
SP (mV)
-80 -40 0
RAG2 (Ωm)
2 7 12 17
Risk Assessment
Oil / Gas
Well Design
Conductor casing
Cementation
Surface casing
Cementation
Int.+ Prod. casing
Plug / Mud
Int.+ Prod. casing
Cementation
Surface casing
Cementation
Conductor casing
Elevation (m SSL)
0
100
200
300
400
500
600
700
800
900
1000
1100
1200
Pa1
Sa
Sa2
Sa3
Sa4
Sa5
Sa6
UBa
UBa2
MBa
MBa2
LBa
L1
L2
L3
L4
L Bad
12
12a
13
14
L Bad
100
0
-100
-200
-300
-400
-500
-600
-700
-800
-900
-1000
Stratigraphy
Pa1
Sa
Sa2
Sa3
Sa4
Sa5
Sa6
UBa
UBa2
MBa
MBa2
LBa
Shale Base Line
Perforation
Oil / Gas
HC shows
Gas
Oil/Gas
Oil

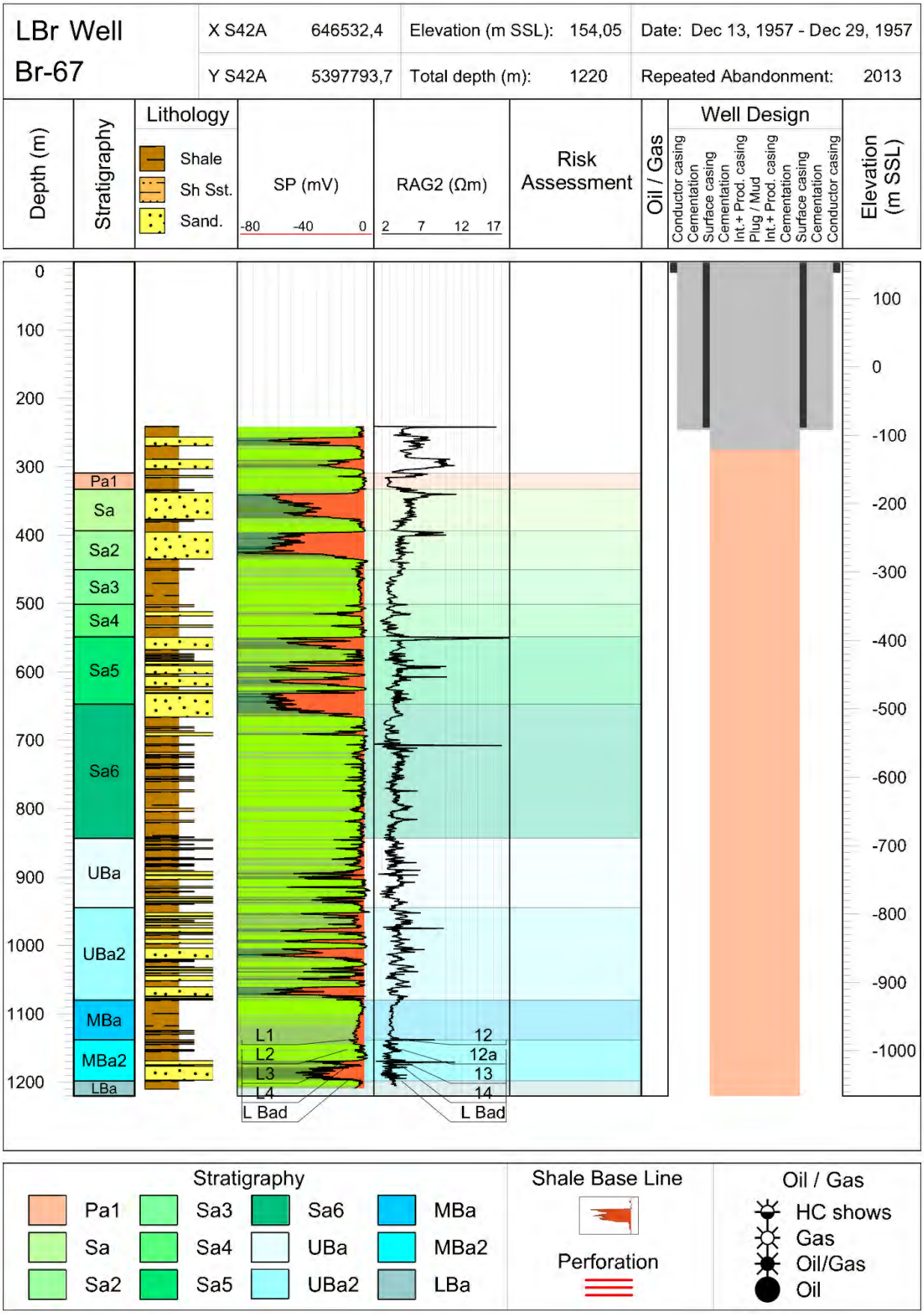
LBr Well
Br-67
X S42A 646532,4
Y S42A 5397793,7
Elevation (m SSL): 154,05
Total depth (m): 1220
Date: Dec 13, 1957 - Dec 29, 1957
Repeated Abandonment: 2013
Depth (m)
Stratigraphy
Lithology
Shale
Sh Sst.
Sand.
SP (mV)
-80 -40 0
RAG2 (Ωm)
2 7 12 17
Risk Assessment
Oil / Gas
Well Design
Conductor casing
Cementation
Surface casing
Cementation
Int.+ Prod. casing
Plug / Mud
Int.+ Prod. casing
Cementation
Surface casing
Cementation
Conductor casing
Elevation (m SSL)
0
100
200
300
400
500
600
700
800
900
1000
1100
1200
Pa1
Sa
Sa2
Sa3
Sa4
Sa5
Sa6
UBa
UBa2
MBa
MBa2
LBa
L1
L2
L3
L4
L Bad
12
12a
13
14
L Bad
100
0
-100
-200
-300
-400
-500
-600
-700
-800
-900
-1000
Stratigraphy
Pa1
Sa
Sa2
Sa3
Sa4
Sa5
Sa6
UBa
UBa2
MBa
MBa2
LBa
Shale Base Line
Perforation
Oil / Gas
HC shows
Gas
Oil/Gas
Oil

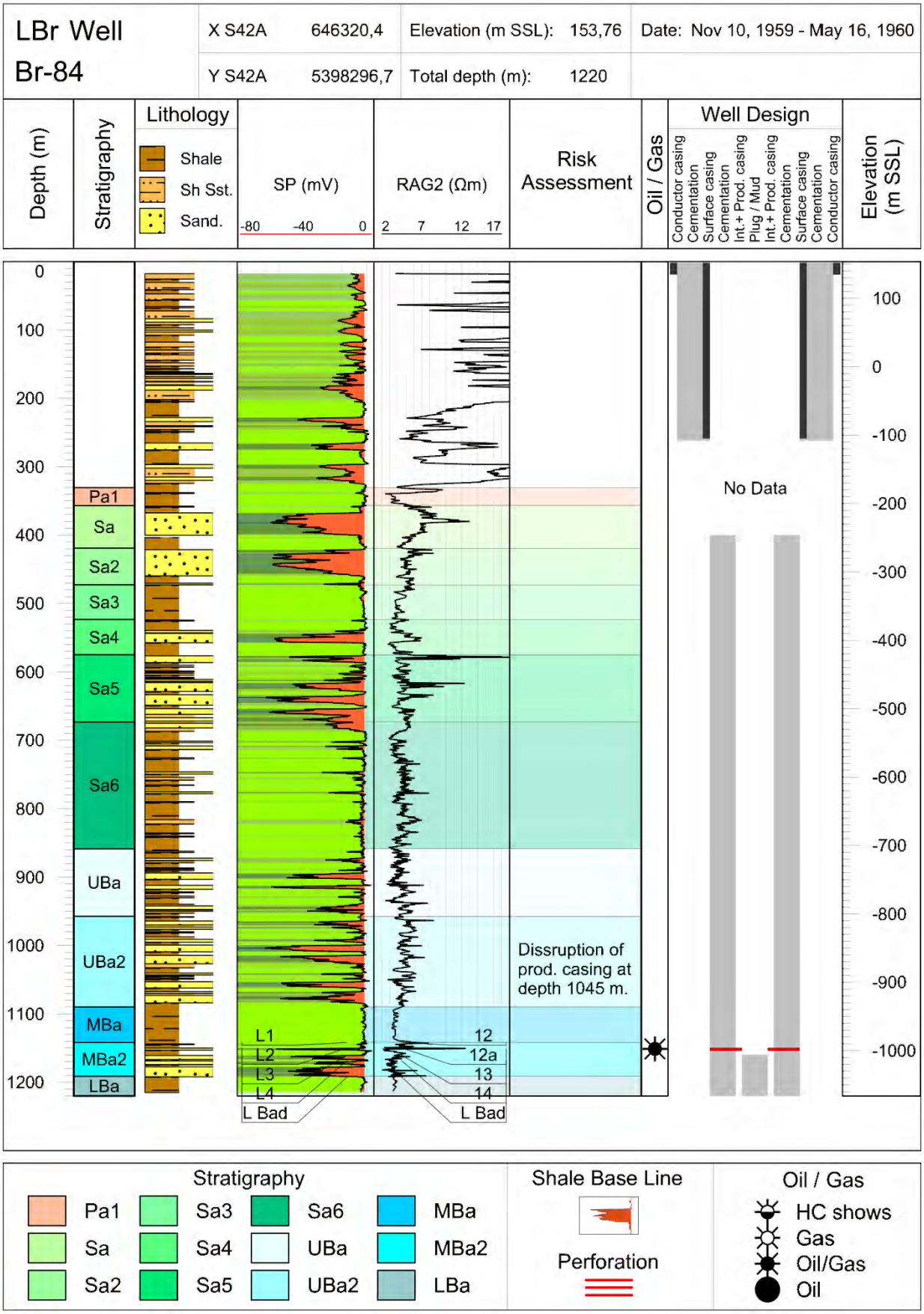
LBr Well
Br-84
X S42A 646320,4
Y S42A 5398296,7
Elevation (m SSL): 153,76
Total depth (m): 1220
Date: Nov 10, 1959 - May 16, 1960
Depth (m)
Stratigraphy
Lithology
Shale
Sh Sst.
Sand.
SP (mV)
-80 -40 0
RAG2 (Ωm)
2 7 12 17
Risk Assessment
Oil / Gas
Well Design
Conductor casing
Cementation
Surface casing
Cementation
Int.+ Prod. casing
Plug / Mud
Int.+ Prod. casing
Cementation
Surface casing
Cementation
Conductor casing
Elevation (m SSL)
0
100
200
300
400
500
600
700
800
900
1000
1100
1200
Pa1
Sa
Sa2
Sa3
Sa4
Sa5
Sa6
UBa
UBa2
MBa
MBa2
LBa
L1
L2
L3
L4
L Bad
12
12a
13
14
L Bad
Dissruption of prod. casing at depth 1045 m.
No Data
100
0
-100
-200
-300
-400
-500
-600
-700
-800
-900
-1000
Stratigraphy
Pa1
Sa
Sa2
Sa3
Sa4
Sa5
Sa6
UBa
UBa2
MBa
MBa2
LBa
Shale Base Line
Perforation
Oil / Gas
HC shows
Gas
Oil/Gas
Oil

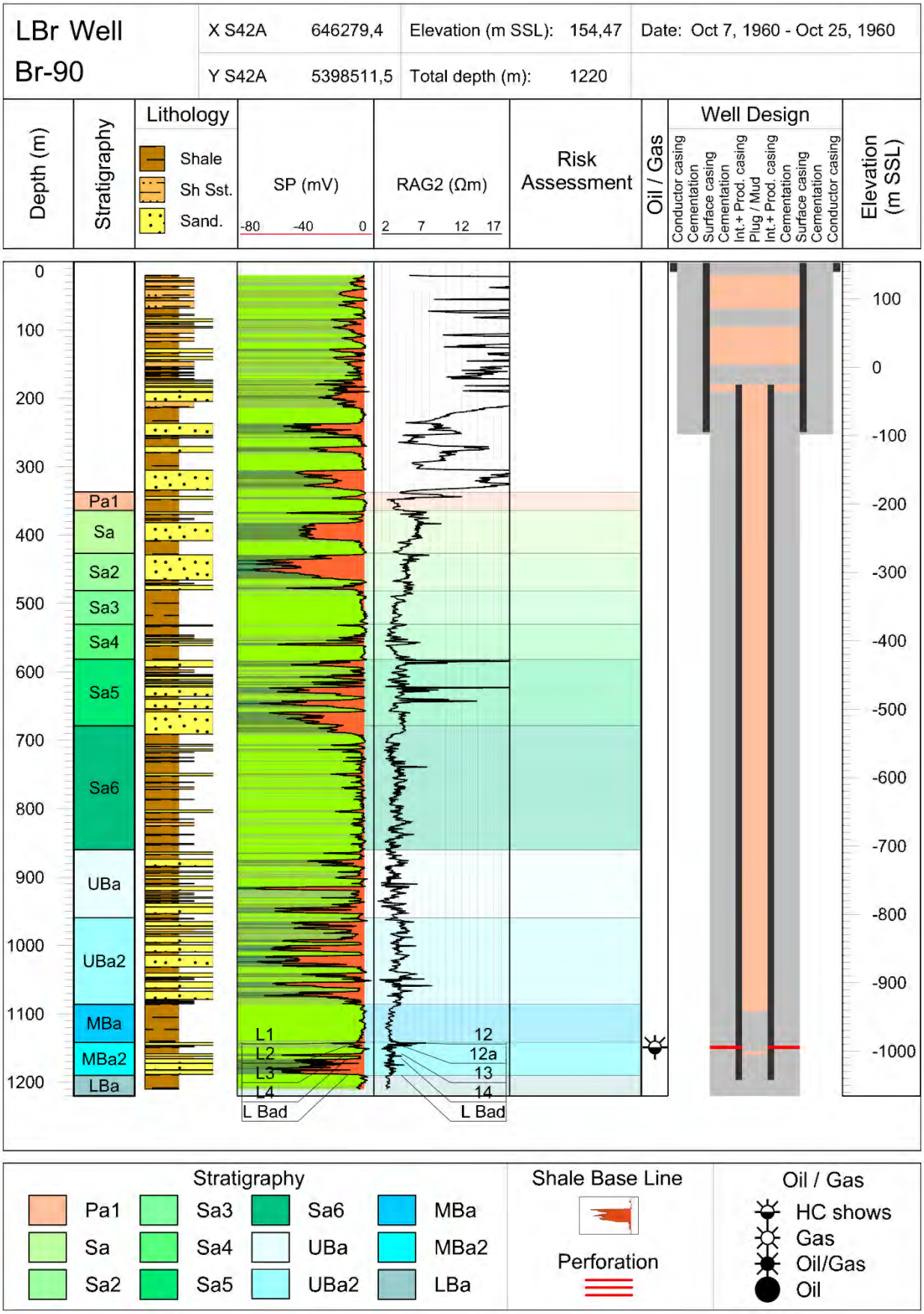
LBr Well
Br-90
X S42A 646279,4
Y S42A 5398511,5
Elevation (m SSL): 154,47
Total depth (m): 1220
Date: Oct 7, 1960 - Oct 25, 1960
Depth (m)
Stratigraphy
Lithology
Shale
Sh Sst.
Sand.
SP (mV)
-80 -40 0
RAG2 (Ωm)
2 7 12 17
Risk Assessment
Oil / Gas
Well Design
Conductor casing
Cementation
Surface casing
Cementation
Int.+ Prod. casing
Plug / Mud
Int.+ Prod. casing
Cementation
Surface casing
Cementation
Conductor casing
Elevation (m SSL)
0
100
200
300
400
500
600
700
800
900
1000
1100
1200
Pa1
Sa
Sa2
Sa3
Sa4
Sa5
Sa6
UBa
UBa2
MBa
MBa2
LBa
L1
L2
L3
L4
L Bad
12
12a
13
14
L Bad
100
0
-100
-200
-300
-400
-500
-600
-700
-800
-900
-1000
Stratigraphy
Pa1
Sa
Sa2
Sa3
Sa4
Sa5
Sa6
UBa
UBa2
MBa
MBa2
LBa
Shale Base Line
Perforation
Oil / Gas
HC shows
Gas
Oil/Gas
Oil

This deliverable is prepared as a part of ENOS project
More information about the project can be found at http://www.enos-project.eu

Be nice to the world!
Please consider using and distributing this document electronically.

The project leading to this application has received funding from the European Union's Horizon 2020 research and innovation programme under grant agreement No 653718